Molecular characterisation of PHA synthase and the *in vivo* synthesis of functionalised PHA beads with surface immobilised proteins

A thesis presented in partial fulfilment of the
requirements of the degree of
Master of Science
in
Microbiology
at Massey University, Palmerston North,
New Zealand.

Jason Wong Lee

2011

Abstract

Polyhydroxyalkanoates (PHAs) are naturally occurring biopolyesters, synthesized by a large range of bacteria and deposited as small spherical water-insoluble cytoplasmic inclusion bodies containing hydrophobic polyester core surrounded by a phospholipid monolayer and associated embedded proteins. The most common form of PHA identified in bacteria is polyhydroxybutyrate (PHB).

Formation of PHA beads requires three important enzymes with PHA synthase (PhaC) being the most important, catalysing the final stereo-selective conversion of (*R*)-3-hydroxyacyl-CoA thioesters into PHA. Increasingly beads are used as microbeads, which display surface immobilised proteins for a range of applications in biotechnology and medicine.

However, functionalised PHA beads are largely produced in Gram-negative bacteria which contain endotoxins that are known to co-purify with the beads and are considered undesirable in medical applications. In addition, despite extensive research towards understanding PHA synthases, to date no structural data is currently available.

Here it was shown that functionalised PHB beads can be produced *in vivo* for both the purification of antibodies and the display of medically relevant antigens (e.g. Hepatitis C) on the surface of PHB beads from the Gram-positive bacterium *L.lactis*. In addition, it was shown that PHA synthase from *R.eutropha* can be highly overproduced, remains largely soluble and can be purified to greater than 90 % purity.

The results demonstrated and supported the use of PHB beads as a platform for the production of functionalised PHA beads suitable for a large range of biotechnological or medical applications. Although no structural data for PHA synthases are currently available, our results demonstrate progress towards obtaining a three-dimensional protein structure for PHA synthase (PhaC).

Acknowledgement

"Success, 100 % persistence and a bit of luck"

Table of contents

VI

Abbreviations

°C	Degree Celsius
$3HA_{MCL}$	Medium chain length (R)-3-hydroxy fatty acids
$3HA_{SCL}$	Short chain length (R)-3-hydroxy fatty acids
3HB	3-hydroxybutyrate
AGE	Agarose Gel Electrophoresis
BSA	Bovine serum albumin
DMSO	Dimethyl sulfoxide
FM	Fluorescent Microscopy
GAP	Bead Associated Proteins
GC/MS	Gas chromatography mass spectrometry
HRP	Horse radish peroxidise
IgG	Immunoglobulin G
IMAC	Immobilised Metal Affinity Chromatography
kDa	Kilo Daltons
LDH	Lactate dehydrogenase
Maldi-TOF\MS	Matrix-assisted laser desorption ionisation time-of-flight mass spectrometry
PBS	Phosphate buffered saline
PHA	Polyhydroxyalkanoate
phaCAB	PHA operon
PhaC	PHA synthase
PhaE	Type II PHA synthase subunit
PhaP	Phasin regulatory protein
PhaZ	PHA intracellular depolymerase
PHB	Polyhydroxybutyrate
RBS	Ribosome binding site
RE	Restriction endonuclease
SDS-PAGE	Sodium dodecyl sulfate gel electrophoresis
TEM	Transmission Electron Microscopy
TEV	Tobacco Etch Virus protease
WT	Wildtype

List of Figures

List of tables

Chapter 1: Introduction

1.1 Polyhydroxyalkanoates (PHAs): Bacterial polyesters

Polyhydroxyalkanoates (PHAs) are naturally occurring biopolyesters composed of (*R*)-3-hydroxy fatty acids. PHAs are synthesized and deposited as spherical water-insoluble cytoplasmic inclusion bodies containing an amorphous hydrophobic polyester core surrounded by a phospholipid monolayer and associated attached or embedded proteins involved in various structural or regulatory functions e.g. depolymerases and phasins (Rehm, 2007; Atwood & Rehm, 2009; Grage *et al.*, 2009). PHAs are naturally synthesized by a large range of Gram-negative and Gram-positive bacteria, and some Archaea species (Rehm, 2007). PHA beads primarily serve as carbon and energy reserves, with synthesis favoured during unfavourable growth conditions due to nutrient limitation (e.g. nitrogen) in the presence of available excess carbon (Rehm, 2003; Koller *et al.*, 2010). Poly(3-hydroxybutyric acid) (PHB), a form of PHA synthesized from the precursor molecule 3-hydroxybutyrate (3-HB), was the first bacterial PHA polymer identified; this was in *Bacillus megaterium* and was published in 1956 by Lemoigne (Lutke-Eversloh *et al.*, 2002). Since their discovery, PHAs have been extensively studied. There are currently greater than 150 different known hydroxyalkanoic acids found to be incorporated in these polyesters and to date, PHB is still the most commonly found and isolated form of PHA from bacteria (Qi *et al.*, 2000; Normi *et al.*, 2005; Keshavarz & Roy, 2010; Rehm, 2010).

Bacteria are capable of accumulating greater than 80% of their cellular dry weight in PHA (Gerngross & Martin, 1995; Rey *et al.*, 2010), with typically 5 - 10 PHA inclusion bodies on average per cell and ranging between 100 - 500 nm in diameter depending on organism (Madison & Huisman, 1999; Zinn *et al.*, 2001; Lee & Lee, 2003; Grage *et al.*, 2009; Koller *et al.*, 2010).

PHAs are known to have a range of attractive properties making them potentially useful for a large range of applications in the industrial and medical fields. These properties include biocompatibility, biodegradability, modifiable physical and thermal properties, and production from renewable resources, (Rehm, 2006; Legat *et al.*, 2010). Examples of possible PHA applications include protein purification and use as biological

microbeads for the immobilisation of proteins or enzymes. Currently, a large range of proteins and molecules have already been successfully immobilised to the surface of these PHA beads, but none are commercially available (Grage *et al.*, 2009).

There are currently two models described for bead formation *in vivo*: (i) the micelle model and (ii) the budding model. *In vitro* synthesis of PHA and self assembly of beads was first demonstrated in 1995 by Gerngross and Martin by using purified PHA synthase and substrate (Rehm, 2006).

Formation of PHA requires three important enzymes, β-ketothiolase, acetoacetyl-CoA reductase, and PHA synthase (PhaA, PhaB, and PhaC respectively) involved in the formation of pre-cursor molecules (*R*)-3-hydroxyacyl-CoA) and subsequent enzymatic conversion into PHA (Satoh *et al.*, 2003; Normi *et al.*, 2005; Rehm, 2007; Grage *et al.*, 2009; Rehm, 2010). The PHA synthase (PhaC encoded by *phaC*) is the most important of these enzymes, as it is the only enzyme required for the polymerisation of PHA. PHA synthase catalyse the final stereo-selective conversion of (*R*)-3-hydroxyacyl-CoA thioesters into PHA with the concurrent release of CoA (Potter & Steinbuchel, 2005; Rehm, 2003). In addition, the PHA synthase (also called polyester synthase) has been shown to remain covalently attached to its growing polyester chain and therefore, has been seen as a primary target involving protein fusions to bead associated proteins (GAPs) (Jahns *et al.*, 2008; Grage *et al.*, 2009).

The primary amino acid sequences of 88 known PHA synthases from at least 68 different bacteria have so far been obtained and the identification of putative PHA synthases is steadily increasing (Rehm, 2003; Rehm, 2007; Grage *et al.*, 2009). PHA synthases can been divided into 4 major classes, designated I – IV, based on primary structure, substrate specificity and subunit composition. Currently there is no structural data available about PHA synthases. However, several threading models of their structure have been predicted and available for classes I to IV (Rehm, 2007).

1.2 PHA synthases

PHA synthases catalyse the final stereo-selective conversion of different (*R*)-hydroxyacyl-CoA thioester monomers into PHA, with the concurrent release of CoA (Qi *et al.*, 2000; Rehm, 2003; Grage *et al.*, 2009). Since their discovery and increasing importance as potential biological tools, extensive research has been done to try and understand how these synthases function in relation to synthesis and structure. Currently, there are greater than 88 PHA synthase genes which have been identified and assigned from at least 68 different bacteria. This number has significantly increased from the previously known 30 synthase genes from 26 different organisms almost a decade ago (Rehm & Steinbuchel, 1999; Rehm, 2003; Rehm, 2007).

1.2.1 Classification of PHA synthases

The current classification of PHA synthases consist of four major classes (class I to IV) based on their primary structure, substrate specificity and subunit composition (Table 1) (Rehm, 2003; Rehm, 2007).

Table 1. The four Classes of PHA synthase (Reproduced from Rehm, 2007)

Class	Subunits	Species	Substrate
I	PhaC ~60-73 kDa	*Cupriavidus necator*	$3HA_{SCL}$-CoA (~C3-C5) $4HA_{SCL}$-CoA, $5HA_{SCL}$-CoA, $3MA_{SCL}$-CoA
II	PhaC ~60-65 kDa	*Pseudomonas aeruginosa*	$3HA_{MCL}$-CoA (~≥C5)
III	PhaC PhaE ~40 kDa ~40 kDa	*Allochromatium vinosum*	$3HA_{SCL}$-CoA ($3HA_{MCL}$-CoA [~C6-C8], 4HA-CoA, 5HA-CoA)
IV	PhaC PhaR ~40 kDa ~22 kDa	*Bacillus megaterium*	$3HA_{SCL}$-CoA

The class I PHA synthase (e.g. *Cupriavidus necator* formally known *as Wautersia eutropha* or *Ralstonia eutropha*) consists of only one subunit (PhaC), with a molecular mass of around 61 - 73 kDa and primarily utilises short chain length (*R*)-3-hydroxy fatty acids ($3HA_{SCL}$) comprising of 3 to 5 carbon atoms. Class II synthases (e.g. *P. aeruginosa*) primarily utilises medium chain length (R)-3-hydroxy fatty acids ($3HA_{MCL}$) comprising of 6 to 14 carbon atoms (Qi *et al.*, 2000; Rehm, 2003; Philip *et al.*, 2007; Rehm, 2007). Class III PHA synthases (e.g. *A. vinosum*) consists of enzymes made up of two subunits (PhaC and PhaE). PhaC has a molecular weight of around 40kDa and shows $21 - 28\%$ amino acid sequence similarity to class I and II PhaC, while PhaE with a similar molecular mass shows no amino acid sequence similarity to PhaC. Synthases of this class primarily utilises both short chain length (*R*)-3-hydroxy fatty acids ($3HA_{SCL}$) and medium chain length (*R*)-3-hydroxy fatty acids ($3HA_{MCL}$) (Qi *et al.*, 2000; Rehm, 2003; Rehm, 2007). Class IV synthases (e.g. *B. megaterium*) have a similar subunit composition to class III PHA synthases. The only difference however, is that PhaE is replaced with PhaR (molecular weight of around 20kDa) and synthases of this class primarily utilises medium chain length (*R*)-3-hydroxy fatty acids ($3HA_{MCL}$) (Rehm, 2003; Rehm, 2007). No hydrophobic C-terminus is present in class III and IV PhaC in comparison to class I and II synthases. However, PhaE and PhaR from Class III and IV respectively have been suggested to functionally replace the hydrophobic C-terminus of PhaC and the C-terminus may have a functional importance in mediating contact with the hydrophobic polyester core (Rehm, 2003; Jahns & Rehm, 2009).

Extensive comparison of the primary amino acid sequences of 88 known PHA synthases from different bacteria has revealed sequence similarity, which ranged from 8 - 96 % identical amino acids. In particular, the identification of six conserved amino acid blocks showing strong similarity, and 8 conserved amino acids among all 88 PHA synthases suggests these regions may be important in enzyme function (Figure 1) (Rehm, 2007; Grage *et al.*, 2009).

The first 100 amino acids of the N-terminus in class I and II synthases has been identified to be highly variable and has experimentally been demonstrated to be dispensable by mutational analysis (Rehm, 2003; Jahns & Rehm, 2009). For example, PHA synthase from *C. necator* lacking 36 to 100 amino acids of the N-terminus still retained functionality (Rehm, 2003). Although this region has no conserved amino

acids, it has been suggested to play a role in PHA synthase production (Grage *et al.*, 2009). In contrast, the C-terminus has been identified to be highly conserved and as previously mentioned, is hydrophobic in all classes and has been suggested to function as the binding domain facilitating attachment to the hydrophobic polyester core (Rehm, 2003). In addition, comparison of the primary amino acid sequences has suggested the presence of a lipase box (GX[S/C]XG) containing the *α/β*-hydrolase fold domain where the catalytic site serine is replaced by a cysteine at the C-terminal region of PHA synthase (Figure 1) (Grage *et al.*, 2009). Identification of this lipase box has led to the current proposed catalytic mechanism for chain elongation based on that of lipases. Although no structural data is yet available about PHA synthases, secondary structure predictions and several threading models have been proposed based on homology to lipase (Rehm, 2007; Valappil *et al.*, 2007).
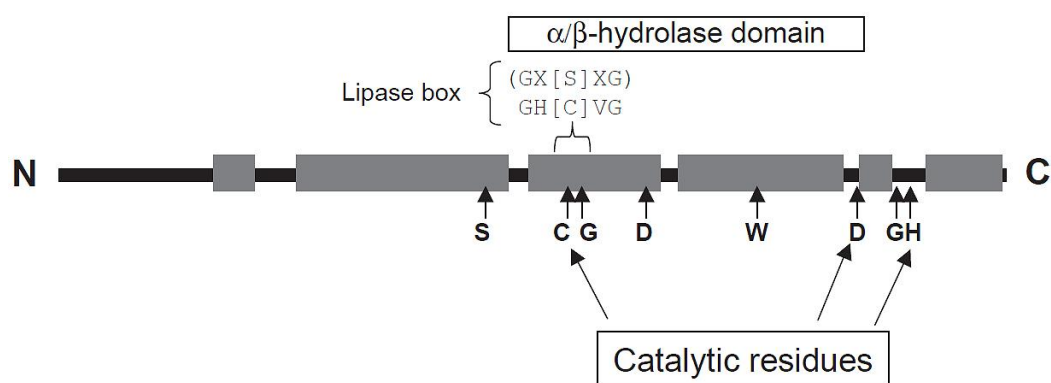
Figure 1. Primary structure of the PHA synthase from *C. necator*. Primary amino acid sequence comparison of PHA PHA synthases revealed 6 conserved blocks (solid grey blocks), 8 conserved amino acids (indicated by arrows), and a conserved α/β-hydrolase domain (GX[S]XG) (Reproduced from Rehm, 2007).

1.2.2 Catalytic mechanism

A mechanism of chain elongation based on the reaction mechanism of fatty acid synthases which involves two thiol groups during the catalytic cycle was proposed in 1968 by Griebel *et al*. (Rehm, 2003). Several conserved residues cysteine-319, aspartate-480, and histidine-508 of the class I PHA synthase were identified by multiple sequence alignments to be conserved in all PHA synthases (Rehm, 2003). However, the second thiol group was not successfully identified. Cysteine-459 and serine-260 were identified as potential candidates from multiple sequence alignment data. Mutational analysis of the cysteine-459 indicated this residue was not essential for catalytic activity, while mutation analysis involving serine-260 was shown to be essential for catalytic activity (Rehm, 2003). In addition, no sequence similarities to fatty acid synthases (β-ketoacyl acyl-carrier protein synthases, or chalcone synthases) were found. Therefore, a new catalytic mechanism model has been proposed from recently emerging data employing a reaction mechanism based on lipases belonging to the α/β-hydrolase superfamily and active PHA synthase involves the formation of homodimers in class I and II PHA synthases, while class III PHA synthases form multimeric heterodimer (Figure 2) (Rehm, 2003; Valappil *et al.*, 2007).

Purified PHA synthase has been shown to exist in an equilibrium of monomeric and dimeric forms. The presence of substrate was found to significantly induce a shift towards the dimeric form, and has been demonstrated to be significantly more active in comparison to its monomer form (Rehm, 2007). Therefore, this dimer formation between PhaC subunits has been suggested to provide the second cysteine thiol group required for catalysis to occur and serves as the site for priming and elongation (Rehm, 2007). The three conserved amino acids previously identified - cysteine-319, Aspartate-480, and histidine-508 of the class I PHA synthase are thought to form the catalytic triad (Grage *et al.,* 2009). In addition, the presence of a α/β-hydrolase fold and conserved residues next to the core structure have also been identified for class II and III PHA synthases (Valappil *et al.*, 2007).
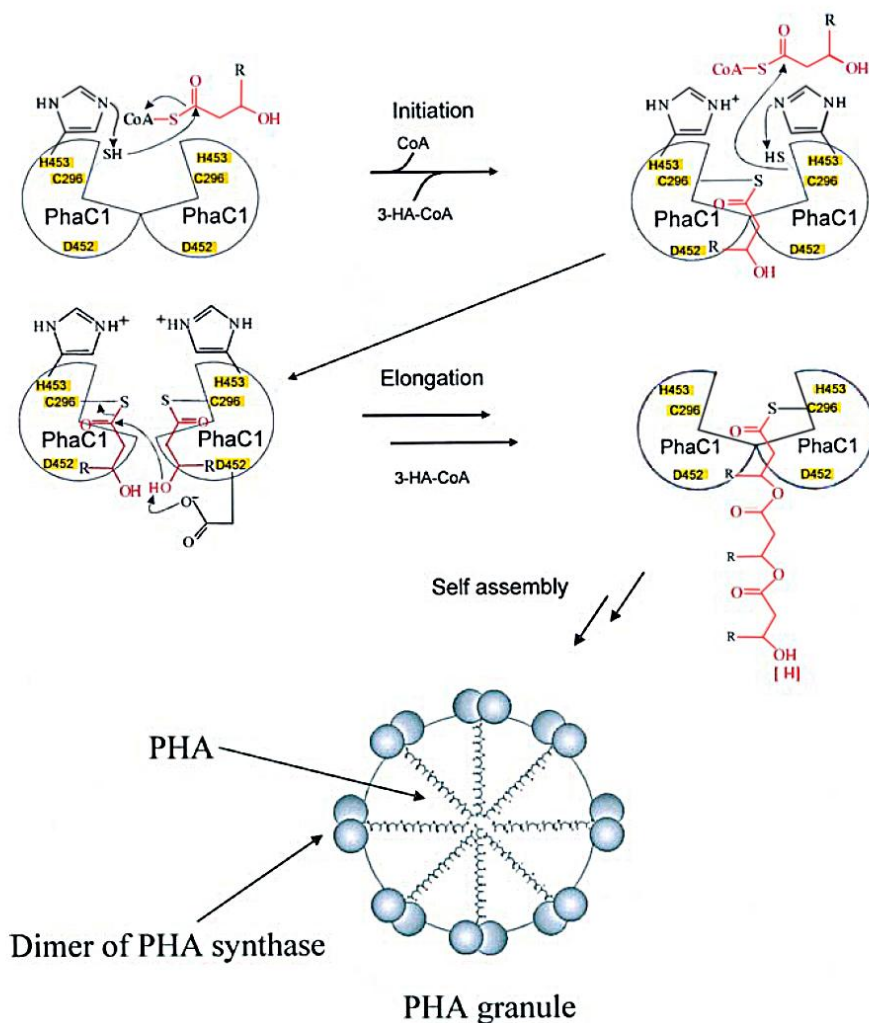
Figure 2. Proposed chain elongation mechanism based on the α/β-hydrolase catalytic mechanism of the *P. aeruginosa* class II PHA synthase (Reproduced from Rehm., 2003)

1.3 α/β-hydrolase superfamily

Lipases, esterases and proteases are examples of enzymes that belong to the large α/β-hydrolase superfamily of proteins. The *α/β*-hydrolase fold was first identified in by comparing several hydrolytic enzymes and currently the structure of over 50 enzymes belonging to this superfamily have been resolved (Ollis *et al.*, 1992). Enzymes belonging to this super family tend to show marked differences between each other such as substrate usage, nucleophile usage, and have poor sequence similarity. They all however show surprisingly conserved structural similarities. In particular the arrangement of the catalytic residues which form the α/β-hydrolase hydrolytic fold (Nardini & Dijkstra, 1999).
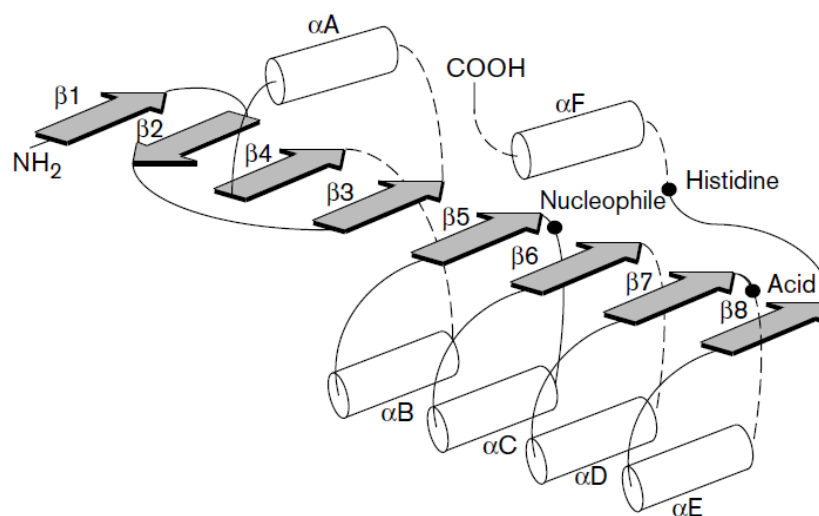
Figure 3. Secondary structure representation of a typical α/β-hydrolase fold. The α helixes are represented by the white cylinders and the β strands by the gray arrows. Black dots indicate the location of the catalytic triad (Reproduced from Nardini & Dijkstra, 1999).

A typical α/β-hydrolase hydrolytic fold, seen in Figure 3, is made up of eight parallel *β*-sheets (with every second *β* sheet being antiparallel) with a left-handed superhelical twist, surrounded on both sides by α helices (Nardini & Dijkstra, 1999; Carr & Ollis, 2009). Although the α/β-hydrolase is highly conserved, analysis of the enzymes' structures within the superfamily suggests this fold is highly adaptive and versatile and is capable of tolerating small or large insertions while still remaining functional. For example, lipase from *Streptomyces exfoliatus* shows many of the β-sheets and α helices of the typical α/β-hydrolase hydrolytic fold except an additional antiparallel strand located on the C-terminus, short α helix at the N-terminus and αF replaced by two α helices (Wei *et al.*, 1998; Nardini & Dijkstra, 1999). Other examples which show more dramatic changes include lipase from *P. aeruginosa* and Acetylxylan esterase from *P. purpurogenum* (Ghosh *et al.*, 1999; Nardini & Dijkstra, 1999).

One particular helix (αC), located between *β*-sheets *β*5 and *β*6, is highly conserved among all enzymes and has been suggested to play a key role in the correct positioning of the nucleophilic residue in the active site (Nardini & Dijkstra, 1999). The active site residues of the α/β-hydrolases form a highly conserved catalytic triad which is

composed of a nucleophile (serine, cysteine, or aspartate), acid (aspartate or glutamate), and histidine residue typically located at the C-terminus (Rehm, 2003; Carr & Ollis, 2009; Grage *et al.*, 2009). The nucleophile is always located in the so called 'nucleophile elbow' of a highly conserved tight strand-elbow-helix motif and can be identified by the consensus sequence Sm-x-Nu-x-Sm (where "Sm" represents any small residue, "x" for any residue and "Nu" for the nucleophile) (Rehm, 2007; Nardini & Dijkstra, 1999). Due to the tightness of the Strand-turn-helix motif, the nucleophile assumes atypical torsion angles which are energetically unfavourable (Nardini & Dijkstra, 1999; Carr & Ollis, 2009). The geometry of the nucleophile elbow has been suggested to help form the 'oxyanion hole' required to stabilise oxyanion intermediates generated during hydrolysis (Carr & Ollis, 2009). The residues which help form the oxyanion hole also contributes to part of a movable lid found in lipases (Nardini & Dijkstra, 1999).

Lipases are characterised by interfacial activation at the lipid-water interface and consists of a movable lid formed over the active site cavity (Rehm, 2003). The presence of a movable 'lid' over the catalytic cavity is a distinguishing feature of lipases and functions to regulate substrate entering and product leaving the active site (Nardini & Dijkstra, 1999). A PHA synthase model for class I PHA synthase (*C.* necator) was generated based on the structure of the *Burkholderia glumae* lipase (Figure 4) (Rehm, 2007). This revealed a 'lid' structure (helical segment) which covered the active site and is shown to be consistent with the polymerisation of PHA at the polyester-water interface by PHA synthase. Opening and closing of the 'lid' is due to interfacial activation at the lipid-water interface and requires conformational changes (Vantilbeurgh *et al.*, 1993; Rehm, 2003).

Several structural studies involving substrate analogue inhibitors confirmed the opening of the lid when substrate was bound, suggesting opening of the lid is essential (Rehm, 2003). In contrast, mutational studies conducted by Taguchi *et al.* (2001) on the PHA synthase showed that the 'lid' structure may not be essential for enzyme function. In addition to providing access to the active site by exposing large hydrophobic surface, structural rearrangements can also change the surface property of the enzyme resulting in an amphipathic molecule (Rehm, 2003). This is consistent with the current proposed model in which the initially soluble PHA synthase becomes amphipathic upon substrate availability and catalyses the synthesis of hydrophobic polyester chain, eventually

forming a PHA bead displaying the PHA synthase on its surface. It has been demonstrated that PHA synthase from *R. eutropha* displayed a significant increase in activity compared to soluble enzyme and suggests interfacial activation (Vantilbeurgh *et al.*, 1993; Rehm, 2003; Rehm, 2007).
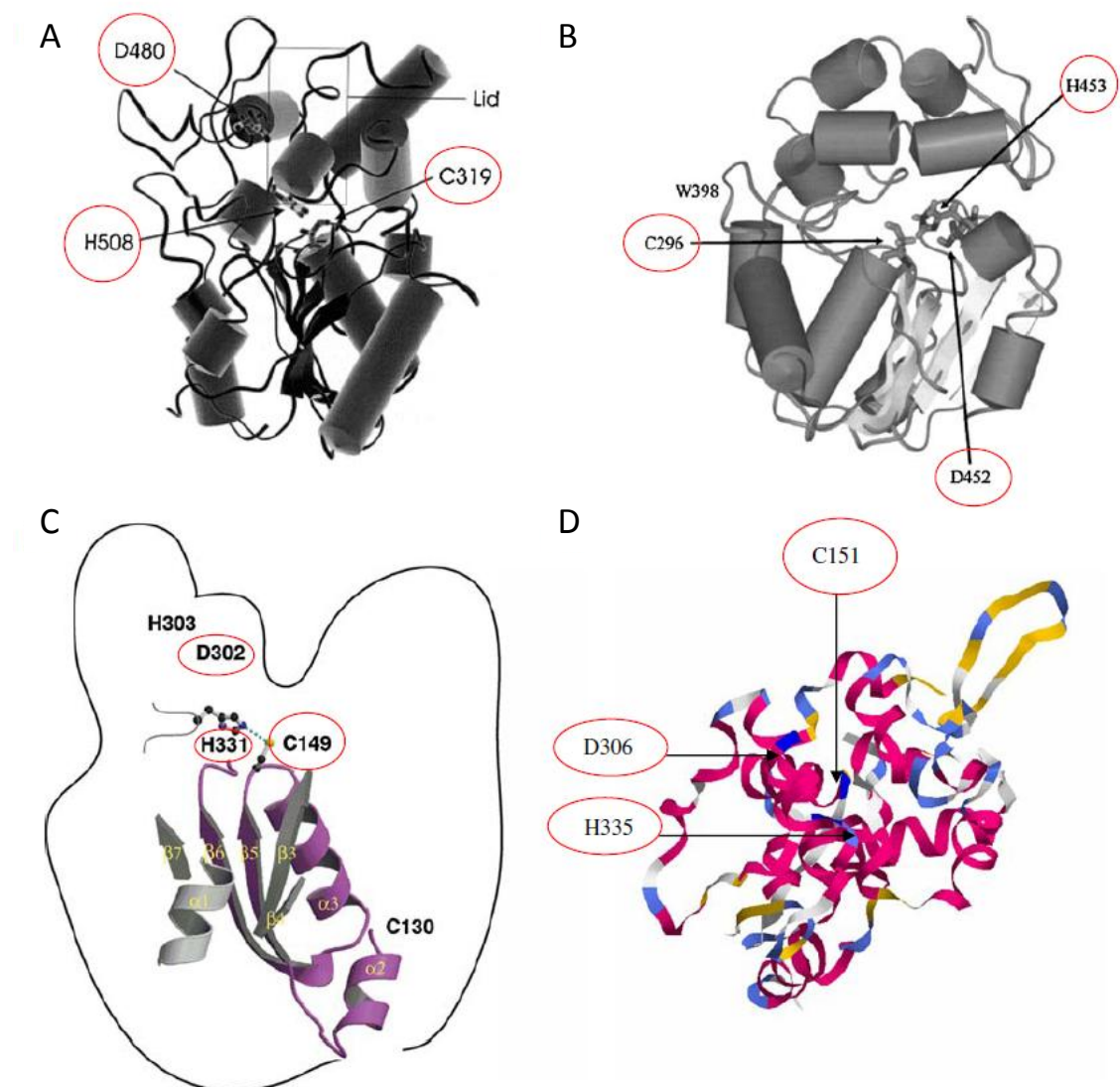
Figure 4. Threading models for PHA synthases. (A) Class I PhaC of *R. eutropha*, (B) Class II PhaC of *Pseudomonas aeruginosa*, (C) Class III PhaC of *Allochromatium vinosum* and (D) Class IV PhaC of *Bacillus cereus* SPV. Catalytic triad residues (cysteine–aspartate–histidine) are encircled (Modified from Valappil *et al*., 2007).

1.4 *Lactococcus lactis* as a production host

Recombinant Gram-negative bacteria such as *E. coli* and *Pseudomonas aeruginosa* are typically used as the host for the biogenesis of functionalised PHA beads (Jo *et al.*, 2006; Valappil *et al.*, 2007). However, Gram-negative bacteria are known to contain lipopolysaccharide (LPS) endotoxins, which constitute a major component of their outer membrane and has been demonstrated to induce strong immune responses in both humans and animals.

Lipopolysaccharides are composed of a hydrophilic polysaccharide moiety (O-antigen region, a core oligosaccharide) which is covalently linked to a hydrophobic lipid moiety (Lipid A) (Magalhaes *et al.*, 2007). Lipid A is responsible for most of the biological activity of endotoxins. Endotoxins are known to elicit a wide variety of pathophysiological effects such as systemic inflammation, fever, coagulopathy, shock and even death (Magalhaes *et al.*, 2007; Yu *et al.*, 2010).

LPS endotoxins are known to co-purify with functionalised beads derived from Gram-negative bacteria and this is seen as undesirable in certain applications (Bermudez-Humaran *et al.*, 2003; Valappil *et al.*, 2007). This is particularly important in the development of functionalised beads related to medical applications, for example, vaccine or drug delivery agents, as all products derived from Gram-negative bacteria need to meet strict guidelines for approval by the U.S. Food and Drug Administration (FDA). FDA guidelines for medical devices derived from Gram-negative bacteria are only allowed a maximum endotoxin level of 20 EU per medical device (Furrer *et al.*, 2007). Laborious purification steps are normally required for the removal of endotoxins to a level approved by the FDA and commonly used methods, such as ion-exchange chromatography, ultrafiltration, and oxidising agents may be ineffective or considered too harsh (Magalhaes *et al.*, 2007; Mifune *et al.*, 2009; Yu *et al.*, 2010).

Therefore, alternative production organisms which make endotoxin-free functionalised beads are advantageous. In particular, Gram-positive bacteria are becoming favourable alternatives to Gram-negative bacteria as they do not contain LPS and therefore obviate the need for laborious methods for the removal of LPS from the production process (Bermudez-Humaran *et al.*, 2003; Valappil *et al.*, 2007; Mifune *et al.*, 2009; Yu *et al.*,

2010). Only a very few Gram-positive PHA producing bacteria, in particular *Bacillus,* have been studied extensively for PHA production. However productivity still remains low in comparison to Gram-negative bacteria. The use of Gram-positive bacteria for the production of functionalised beads was first exploited by Jo *et al.* who established a PHB biosynthetic pathway in *Corynebacterium glutamicum* by introducing the *phaCAB* operon derived from *C. necator* (Jo *et al.*, 2006). More recently, Mifune *et al.* similarly established a PHB biosynthetic pathway in *Lactococcus lactis* which was engineered to produced functionalised PHB beads displaying surface immobilised IgG binding domains (Mifune *et al.*, 2009).

L. lactis is a Gram-positive homofermentative bacterium which belongs to a heterogeneous group of microorganisms called lactic acid bacteria (LAB), which are traditionally and currently used in the production of fermented food products. *L. lactis* is non-pathogenic, has a long history of safety and has been given the status 'Generally Regarded as Safe' (GRAS) organism and holds tremendous industrial importance (Loir *et al.*, 2005; van Hylckama Vlieg *et al.*, 2006)

The whole genomes of several LAB strains, including *L. lactis*, have been sequenced, for example *L. lactis* IL1403 (Bolotin *et al.*, 2001). *L. lactis* does not naturally produce PHA, however, as previously mentioned, Mifune *et al.* established a recombinant PHB production pathway in *L. lactis* by introducing and expressing codon optimised PHA biosynthesis genes (*phaABC*) from *C. necator* under a nisin inducible promoter (Mierau & Kleerebezem, 2005; Mifune *et al.*, 2009). Mifune and co-workers were able to demonstrate and display recombinant proteins on the surface of the PHA beads. PHA beads were engineered to display recombinant IgG (ZZ) binding domains of protein A on the beads surface and isolated beads were assessed by ELISA and IgG affinity purification. Results were encouraging, as the functional beads isolated from *L. lactis* performed equally as well as ZZ beads isolated from Gram-negative *E. coli* (Brockelbank *et al.*, 2006; Mifune *et al.*, 2009).

However, PHB accumulation in *L. lactis* was much lower (6% wt/wt) in comparison to PHB accumulation in recombinant *E. coli* (80% wt/wt) and *C. necator*, as well as other Gram-positive recombinant organisms such as *C. glutamicum* (22% wt/wt) (Jo *et al.*, 2006; Mifune *et al.*, 2009; Rey *et al.*, 2010). It has been suggested PHB yield in both

Gram-positive *L. lactis* and *C. glutamicum* can be improved by monitoring and modulating metabolic flux. For example, redistribution of the pyruvate pool/flux in favour of PHB production using LDH (lactate dehydrogenase) deficient mutant strains (Jo *et al.*, 2006; Mifune *et al.*, 2009). As metabolism of glucose in *L. lactis* is converted to pyruvate, from which 97% of the flux is directed towards production of lactic acid and is unfavourable for PHB biosynthesis, LDH deficient mutants will help shift metabolism towards PHB biogenesis (Figure 5) (Bolotin *et al.*, 2001; Hoefnagel *et al.*, 2002).

Figure 5. Schematic representation of the metabolism of glucose in *L. lactis*. Numbers in circles indicate the following enzymes or steps: 1, 'lumped' glycolysis; 2, LDH; 3, pyruvate dehydrogenase; 4, phosphotransacetylase; 5, acetate kinase; 6, acetaldehyde dehydrogenase; 7, alcohol dehydrogenase; 8, ALS; 9, acetolactate decarboxylase; 10, acetoin efflux; 11, acetoin dehydrogenase; 12, ATPase; 13, NOX; 14, non-enzymic acetolactate decarboxylation; 15, pyruvate formate lyase, not to be active under aerobic conditions. The red dashed arrow and box indicate the PHB biosynthesis pathway from *C. necator* and the solid red arrow indicades the LDH pathway which is knocked out in LDH deficient mutants NZ9010 and NZ9020 (modified from Hoefnagel *et al*, 2002).

Hoefnagel and co-workers in 2002 created a LDH deficient strain of *L. lactis* NZ9000 using a double cross-over event, designated NZ9010. *L. lactis* NZ9010 was created by knocking out the lactate dehydrogenase (*Ldh*) gene in the *las* operon, which also encodes for glycolytic enzymes phosphofructokinase and pyruvate kinase for lactic acid production (Hoefnagel *et al.*, 2002; Bongers *et al.*, 2003). This abolished all production of lactic acid as an end product of aerobic fermentation and allowed the redistribution of the pyruvate pool towards other products, mainly acetoin (Hoefnagel *et al.*, 2002; Bongers *et al.*, 2003). However, not long after the creation of NZ9010, a second lactate dehydrogenase mutant designated NZ9020 was created by Bongers and co-workers (2003). It was observed that LDH mutant NZ9010 reverted back to its wildtype phenotype under repeated anaerobic subculturing and this was discovered to be due to a second silent *Ldh* gene *LdhB* (Bongers *et al.*, 2003).

In regards to their use as recombinant hosts for heterologous protein production and more recently PHB, production for use in medical or therapeutic applications (i.e. vaccine delivery agent), *L. lactis* is becoming increasingly recognized.

1.5 Biogenesis and structure of PHA inclusions

The type of PHA synthesised by bacteria is primarily dependent on the carbon source utilised and type of organism (Rasiah *et al.*, 2010). There are three well-known metabolic pathways towards PHA biosynthesis (Figure 6). Pathways I is the most well characterised and studied pathway (Philip *et al.*, 2007; Rasiah *et al.*, 2010). This pathway is utilized by bacteria which synthesize short chain length PHAs, such as *C. necator*, while Pathways II and III are utilized by bacteria which synthesize medium chain length PHAs, such as *P. aeruginosa* (Philip *et al.*, 2007).
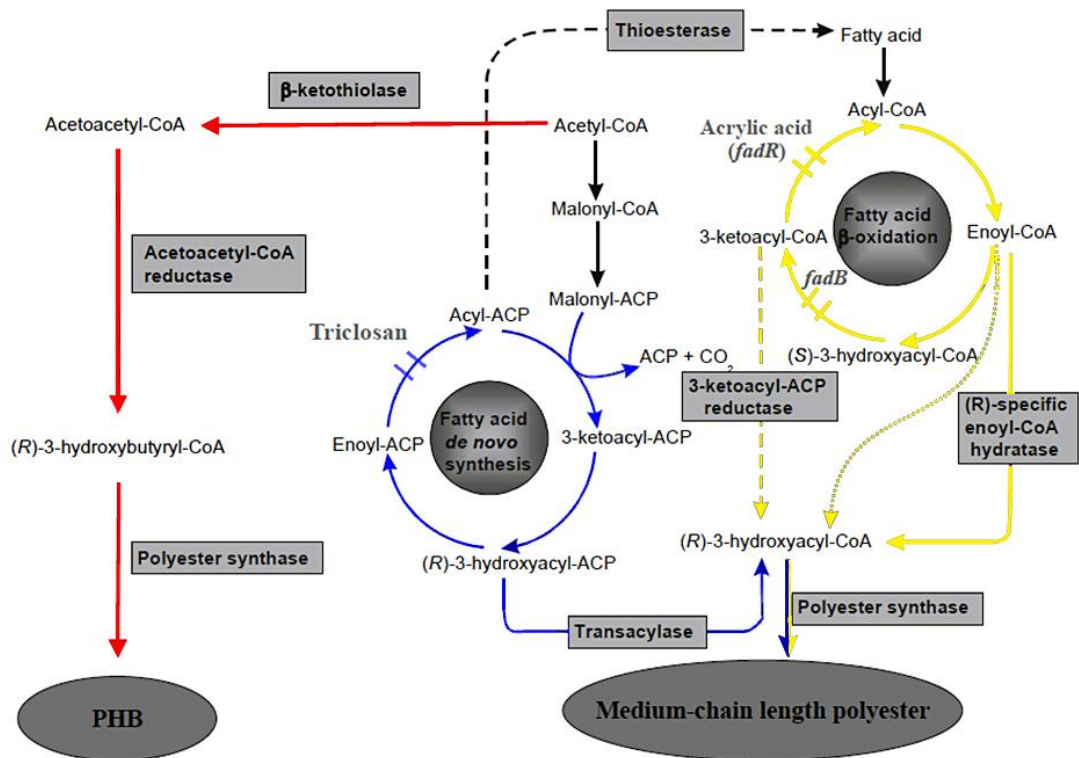
Figure 6. Metabolic routes towards PHA biogenesis. There are 3 well known metabolic pathways towards PHB biogenesis depending on carbon source and type of organism. Pathway I (solid red lines), Pathway II (solid yellow lines) and Pathway III (solid blue lines) (Reproduced from Rehm., 2007).

The PHB biosynthesis pathway in *C. necator* relies on three key enzymes, the polyester synthase, *β*-ketothiolase, and acetoacetyl-CoA reductase (encoded by the genes *phaC*, *phaA*, and *phaB* respectively). These PHB biosynthesis encoding genes are arranged in a single *phaCAB* operon and are involved in the sequential enzymatic conversion of acetyl-CoA to PHB (Lee & Lee, 2003; Rehm, 2007; Grage *et al.*, 2009). The pre-cursor (*R*)-3-hydroxybutyryl-CoA is synthesised by *β*-ketothiolase (PhaA) and acetoacetyl-CoA reductase (PhaB). *β*-ketothiolase (PhaA) condenses two acetyl-CoA molecule to give acetoacetyl-CoA, followed by the subsequent reduction to (*R*)-3-hydroxybutyryl-CoA by NADH-dependent acetoacetyl-CoA reductase (PhaB) (Grage *et al.*, 2009; Normi *et al.*, 2005; Rehm, 2007; Rehm, 2010; Satoh *et al.*, 2003). In the final step, PhaC catalyses the formation of PHB using (*R*)-3-hydroxybutyryl-CoA monomers as substrate, with the concurrent release of CoA (Rehm, 2003; Potter & Steinbuchel, 2005).

Pathway II bacteria, such as *P. aeruginosa* are known to utilize intermediates generated from the fatty acid *β*-oxidation pathway and from related carbon sources. In this pathway various *β*-oxidation pathway intermediates (alkanes, alkenes and alkanoates) are converted into (*R*)-3-hydroxyacyl-CoA thioesters, while non-related sources like sucrose, glucose or gluconate are metabolized to acetyl-CoA which enter the fatty acid de novo biosynthesis pathway (Pathway III) (Philip *et al.*, 2007; Rehm, 2007; Lu *et al.*, 2009).

In pathways I, II and III PhaC is the only enzyme involved in the stereo-selective conversion of (*R*)-hydroxyacyl-CoA thioesters into PHA with the concurrent release of CoA, confirmed by *in vitro* PHA bead formation using only purified PHA synthase and its respective thioesters (Rehm, 2003; Gerngross & Martin, 1995).

Formation of PHA inclusions *in vivo* and *in vitro* is mediated by the presence of (*R*)-3-hydroxyacyl-CoA thioesters and PHA synthase starts to catalyse the formation of PHA inclusions upon availability of these substrates. During the polymerisation process the PHA synthase remains covalently attached to the growing polyester chain (Jahns *et al.* 2008; Grage *et al.*, 2009) while more substrate is being continually incorporated until metabolic or spatial constraints terminate polymerisation. Although the exact mechanism of PHA inclusion biosynthesis is unknown, there are currently two models for the biogenesis of *in vivo* PHA inclusions: (i) Micelle model and (ii) Budding model (Figure 7).

The "micelle" model is based on the assumption that the initially soluble enzyme is thought to dimerise when polymerisation is initiated by the presence of substrate and becomes an amphipathic molecule which undergoes a self-assembly process whereby the growing hydrophobic PHA chains aggregate into a micelle-like structure (Grage *et al.*, 2009; Rehm, 2007). Phospholipids and other bead associated proteins (GAP) then become gradually incorporated with the growing micelle-like structure (Grage *et al.*, 2009). However, this model is currently only supported by PHA inclusion formation *in vitro* (Rehm, 2006).
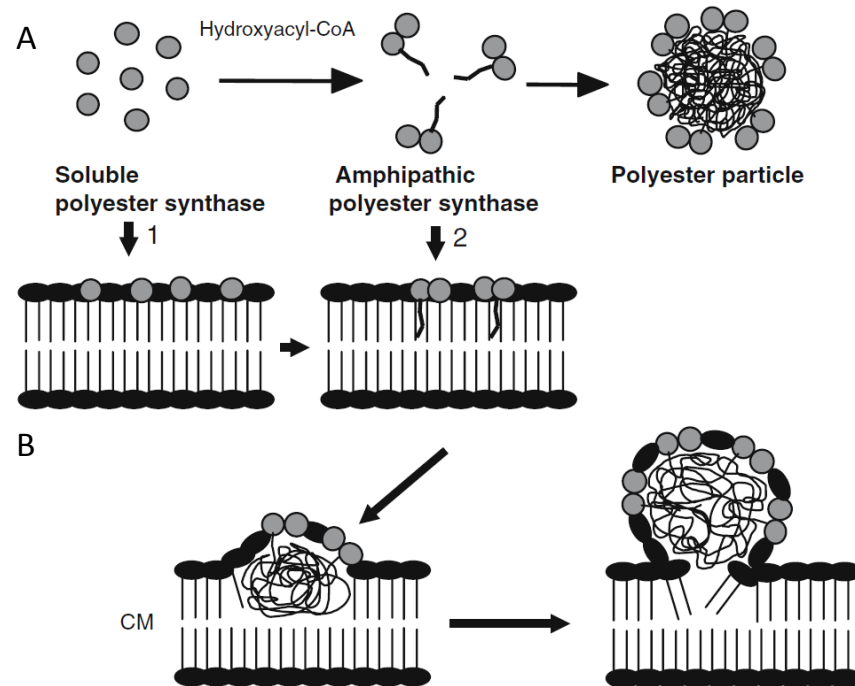
Figure 7. Models for polyester bead self-assembly. (a) Micelle model and (b) Budding model of PHA bead formation. 1 and 2 indicate possible routes during *in vivo* assembly (Reproduced from Rehm., 2006)

The "budding" model on the other hand suggests that soluble enzyme localises to the inner face of the cytoplasmic membrane either inherently or as soon as PHA chains emerges from the enzyme (Thomson *et al.*, 2010). In this case, the growing polyester chain is synthesised into the inner membrane space where it will continue to grow into a PHA inclusion surrounded with a monophospholipid layer (Rehm, 2007). GAPs are also thought to incorporate into the phopholipid monolayer of the growing PHA inclusion until it eventually buds off the membrane into the cytoplasm (Rehm, 2007; Thomson *et al.*, 2010). Recently emerging evidence is in favour of the budding model of PHA inclusion formation (Rehm, 2006; Rehm, 2007).

Studies done by Jendorssek *et al.* using confocal laser scanning fluorescence microscopy (CLSM), and by Peters and Rehm using fluorescence microscopy (FM), demonstrated newly emerging PHA bead in young cultures were not randomly distributed but located predominately at the cell poles and centre of the cell (Jendrossek, 2005; Peters & Rehm, 2005). Peters and Rehm also demonstrated bead formation was

dependent on nucleoid structure, and observed newly emerging beads oscillating rapidly between the poles and suggested this might play a role in equal distribution (Peter and Rehm, 2005).

A third model has been suggested from studies done by Tian *et al.* based on PHB inclusion formation in *C. necator* (Tian *et al.*, 2005). Interestingly they found newly emerging beads arose only from the centre of the cell at unknown dark staining mediation elements. The newly emerging beads were seen to be localised at the mediation element and therefore were not randomly distributed, correlating with the two models mentioned above. These mediation elements were suggested to act as scaffolds and provide a site for initiation of bead formation. However, this proposed model is currently not well supported (Rehm, 2007).

1.5.1 *In vitro* PHA bead formation

In vitro PHA bead formation for class I PHA synthase from *C. necator* was first described by Gerngross and Martin in 1995 and they established the minimal requirements for PHB inclusion body formation *in vitro* to be soluble purified PHA synthase and its corresponding CoA-thioester (Gerngross & Martin, 1995). A number of PHA synthases (class I, II and III) have since been isolated and purified from a large array of organisms (Rehm, 2007).

PHA inclusions formed *in vitro* were found to be spherical, but showed significant increase in diameter ($> 3\mu m$) and molecular weight ($> 10x10^6$) in comparison to inclusions formed *in vivo* (Jossek *et al.*, 1998; Rehm, 2007; Han *et al.*, 2009). It has been suggested that lack of phasins and phospholipids results in coalescence of the individual PHA beads (Thomson *et al.*, 2009). The size of the *in vitro* synthesized beads was found to be proportional to the substrate:enzyme ratio (Jossek *et al.*, 1998).

High levels of free CoA released from polymerisation was also shown to have inhibitory effects on the activity of PHA synthases; this has also been confirmed by *in vitro* studies by other researchers (Jossek *et al.*, 1998; Jossek & Steinbuchel, 1998). Several *in vitro* PHA production systems which recycle CoA have been described, with the most recent being published by Han *et al* based on a water-organic solvent two-phase reaction system (TPRS) (Han *et al.*, 2009). *In vitro* PHA production systems offer

several advantages to *in vivo* PHA bead formation such as easily controllable reaction conditions, resulting in PHA beads of uniform size, properties and free of contamination i.e. endotoxins (Han *et al.*, 2009). In addition, *in vitro* PHA bead formation studies have been important in aiding our understanding of substrate specificity and reaction mechanisms, which are applicable to PHA bead formation *in vivo* (Thomson *et al.*, 2009).

1.5.2 Structure of PHA beads and their bead associated proteins
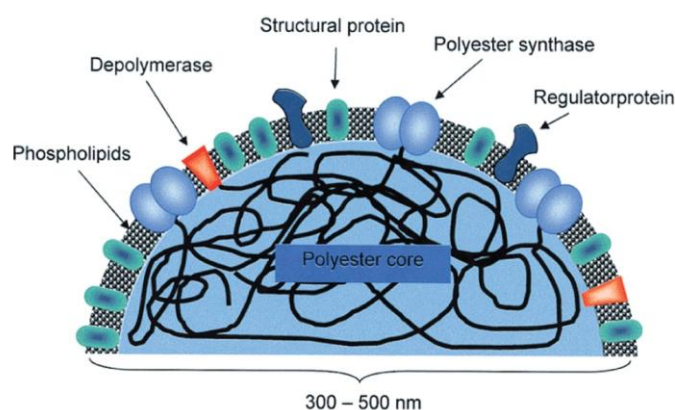
Figure 8. Schematic representation of a PHA bead and its associated proteins. (Reproduced from Rehm, 2003)

Bead-Associated Proteins (GAP) is a term given to proteins which are associated and embedded into the phospholipid surface of the bead (Figure 8). These proteins play a major role in PHA synthesis and degradation and in bead formation and have been designated into four major classes: PHA synthases, depolymerases, regulatory proteins, and phasins. *C. necator* for example: PHA synthase (PhaC), depolymerase (PhaZ), regulatory protein (PhaR), and phasins (PhaP). For discussion on PHA synthase, please refer to section 1.2.

Depolymerases

PHA depolymerases (encoded by *phaZ*) are only present in their native host and are important for both the degradation of extracellular PHA derived from dead bacteria and intracellular PHA mobilisation by thiolysis. Extracellular PHA depolymerases have been shown to be widely spread but are not limited to PHA-producing bacteria (Potter & Steinbuchel, 2005; Grage *et al.*, 2009). Extracellular PHA depolymerases can be secreted into the environment, and mediated by an N-terminal signal peptide to degrade PHA released from dead bacteria. Intracellular depolymerases, on the other hand, are not as extensively studied as extracellular depolymerases and function to mobilize intracellular PHA. Saegusa and co-workers in 2001, were first to publish the sequence of intracellular PHA depolymerase from *C. necator*, designated PhaZ1 (Saegusa *et al.*, 2001). Western blot experiments employing polyclonal antibodies raised against PhaZ1 demonstrated PHA depolymerases are found to be associated with the surface of PHA beads in native hosts (Potter & Steinbuchel, 2005).

Regulatory proteins

Both PHA bead synthesis and Phasin (PhaP) production are tightly regulated by the transcriptional regulator PhaR, as demonstrated by mutagenesis studies performed in *C. nectator* (Grage *et al.*, 2009).

An autoregulation model for PhaP/PhaR has been proposed based on evidence from *C. necator* and *P. denitrificans* (Grage *et al.*, 2009; Potter *et al.*, 2002). Under non-permissive PHA accumulating conditions, PhaR binds to the *phaP* promoter and inhibits its transcriptions. While under PHA accumulating conditions, PhaR starts to interact and bind to the hydrophobic surfaces of newly forming PHA beads lowering the cytoplasmic concentration of available PhaR leading to active transcription of PhaP which binds to PHA beads. After the beads have reached maximum size, the bead surface is completely covered with Phasins, preventing additional binding of PhaR, resulting in the increase of cytoplasmic PhaR. Once again PhaR binds to the PhaP promoter region and prevents transcription (Potter *et al.*, 2002; Potter & Steinbuchel, 2005; Grage *et al.*, 2009).

PhaR and other regulatory proteins bind non-covalently to the PHA beads (Rehm, 2006). It has been recently suggested that PhaR might also play a role in other

metabolic pathways acting as a global PHA-repressor (Grage *et al.*, 2009). Other bead-associated proteins with regulatory function have been reported, for example PhaF from pseudomonads (Rehm, 2006).

Phasins

Phasins, encoded by the *phaP* gene, are low-molecular-weight proteins ranging from 11 - 25kDa and are the most abundantly produced bead-associated protein and can represent as much as 5% of the total protein (Wieczorek *et al.*, 1995; Hanley *et al.*, 1999). Phasins are non-catalytic amphipathic protein molecules and like most GAPs are non-covelently associated with the hydrophobic core of the PHA bead (Grage *et al.*, 2009). It has been shown that phasins have a structural role acting to stabilise PHA beads and prevent separate proteins from coalescing, thereby influencing the size and number of PHA beads (Wieczorek *et al.*, 1995; Rehm, 2006; Grage *et al.*, 2009). In *C. necator*, four phasin gene homologs have been identified and confirmed, designated *phaP1* to *phaP4* (Potter & Steinbuchel, 2005). Phasins have been shown not to be essential for PHA accumulation but cells defective in phasin production leads to the form a single large bead which occupies most of the cell rather than many small beads seen in the presence of phasin production (Hanley *et al.*, 1999).

1.6 Applications of PHA granules as bio-beads

Traditional plastics are derived from crude oil, which is a non-renewable resource (Keshavarz & Roy, 2010). In addition, petroleum-based plastics are non-biodegradable and pose a major environmental problem. Due to the increasing costs and public awareness of these problems, there has been a push for research into the development of environmentally friendly and sustainable technologies (Philip *et al.*, 2007; Keshavarz & Roy, 2010).

A range of environmentally friendly alternatives to traditional plastics are currently available, such as starch-based plastics and chemically synthesised plastics. However, most of these alternatives lack versatility and material properties. Polyhydroxalkanoates (PHAs) are highly versatile, biodegradable biopolymers with a range of material properties similar to traditional plastics, making them a suitable alternative to traditional plastics (Keshavarz & Roy, 2010). Properties of PHA are influenced by the length and

composition of hydroxyl fatty acids. PHAs can be homopolymers or copolymers of alternating or blocks of different hydroxyl fatty acids and they can be grouped into either short chain length PHAs or medium chain length PHAs. Short chain length PHAs are considered hard or brittle, with a high degree of crystallinity, whereas medium chain length PHAs tend to be more elastomeric, with less tensile strength and lower melting temperatures (Hazer & Steinbuchel, 2007; Philip *et al.*, 2007). The large variety of PHAs with varying physical and chemical characteristics is due to their monomer composition and currently greater than 150 different hydroxyalkanoic acids are known as constituents of these PHAs (Rehm, 2010). Many factors can influence monomer content including strain, cultivation conditions, and carbon sources (Keshavarz & Roy, 2010). In addition, PHAs can also be subjected to chemical modification. Many research groups have targeted the PHA synthase for altering substrate specificity, resulting in various tailor-made polyesters. Various random and rational approaches have been successfully used in changing substrate specificity (Rehm, 2003).

The cost of PHA production is currently more expensive in comparison to traditional plastics, making them commercially non-feasible and therefore current use is limited to high value applications (Zinn *et al.*, 2001; Rehm, 2010). To make PHAs more commercially viable, it is necessary to develop more cost effective PHA production strategies.

Currently, PHAs are produced mainly by recombinant Gram-negative bacteria such as *E. coli*. However, Gram-positive organisms are becoming an attractive alternative for the production of LPS free products for medical applications (Jo *et al.*, 2006; Valappil *et al.*, 2007; Mifune *et al.*, 2009). Non-prokayotic organisms, such as transgenic plants have recently been explored. Plants offer several major advantages over 'microbial cell factories'. These advantages include increased biomass in comparison to bacteria, sterile conditions growth conditions are not required, and also significant cost reductions have been proposed, as plants are able to obtain their carbon directly from carbon dioxide (CO_2) (Mullaney & Rehm, 2010). Currently, PHA has been successfully synthesised in *Arabidopsis,* cotton, switchgrass, and tobacco only to name a few. However, PHA is produced only at low levels in these (Bornke & Broer, 2010; Mullaney & Rehm, 2010).

A lot of research has gone into modifying PHAs physical, thermal and elastic properties, substrate specificity and functional groups and side chains, leading to

biopolymers with specialised material properties. In the last 10 years there has been a lot of interest surrounding the use of PHA in their native form as microbeads with surface attached proteins as their material, biodegradable and biocompatible properties and small size makes them suitable for a wide range of applications in biotechnology and medicine (Grage *et al.*, 2009).

Protein purification is the ability to purify a high yield of a single protein from a complex mixture which is free of contaminants while maintaining functionality. Affinity-based purification methods are typically used in protein purification and they rely on the interaction of protein of interest with its corresponding immobilised matrix (Arnau *et al.*, 2006). This interaction typically requires the fusion of affinity tags to the protein of interest. Affinity tags are designed to simplify protein purification and allow for the purification of a range of different proteins using a common method, without any prior knowledge of its biochemical properties (Arnau *et al.*, 2006). In addition, affinity tags may also contribute to a range of positive effects such as solubility and improved protein production. However, negative effects of affinity tags include altering protein conformation and/or lower protein production (Waugh, 2005; Arnau *et al.*, 2006). A range of commonly used affinity tags include polyHis-tag, polyarg-tag, c-myc, and Strep-tag II (Terpe, 2003).

However, protein purification using affinity-based methods can be costly and time consuming requiring multiple separation steps and expensive affinity resins to get the desired purity (Grage *et al.*, 2009). In addition, expensive proteolytic enzymes are commonly employed to enzymatically cleave the affinity tag from the protein of interest and cleavage can also result in soluble protein becoming insoluble (Esposito & Chatterjee, 2006).

Recently, several PHA-based protein purification strategies have been developed as a low-cost means of protein purification by taking advantage of the bead associated proteins and large-molecular-weight (Grage *et al*, 2009).

Banki *et al.* developed a strategy which exploits the hydrophobic property of PhaP, involving the use of an intein-mediated self-cleaving affinity tag and PhaP from *C. necator* (Banki *et al.*, 2005). The protein of interest is fused to the C terminus of PhaP and acts as the affinity tag which binds to the PHA beads (matrix). Both fusion protein and PHA beads are co-produced in *E. coli* resulting in protein bound PHA beads which

can be recovered by cell disruption and centrifugation, followed by subsequent mild washing steps and self-cleaving of intein. Maltose binding protein (MBP) and *β-galactosidase* (LacZ) were a few of the proteins successfully purified by this method. A similar strategy was demonstrated in *C. necator* by Barnard *et al.* (Barnard *et al.*, 2005) and another slightly different approach was described by Wang *et al.* whereby protein production and PHA bead production steps were separated (Wang *et al.*, 2008).

Other similar approaches have been described, although all PHA-based protein purification methods described so far are based on fusions to PhaP. However, Zhang *et al.* have just recently described a strategy which is a combination from Banki *et al.* and Wang *et al.*, involving the use of repressor protein PhaR as an affinity tag for *in vitro* protein purification (Zhang *et al.*, 2010).

Overall PHA-based protein purification strategies provide a low-cost alternative to currently used affinity-based purification strategies and is particularly suitable for preparative protein purification.

It has been recognised only recently that PHA beads in their natural form have great potential as microbeads in a long and growing list of diagnostic and therapeutic applications. This 'proof of principle' was first demonstrated in 2005 by Peters and Rehm by fusing a functional protein (GFP) to the N-terminus of PHA synthase from *C. necator* (Peters & Rehm, 2005). Follow up studies were done whereby more complicated proteins such as enzyme *β-galactosidase* were immobilised onto the beads surface (Grage *et al.*, 2009).

In both cases the protein remained functional and did not affect bead formation and eventually paving the way for further studies involving protein fusions to GAP proteins. The PhaC is commonly targeted for protein immobilisation, but other GAP proteins such as phasins (PhaP) and the substrate binding domain of the depolymerase enzyme from *Alcaligenes faecalis* have been successfully used (Lee & Lee, 2003; Brockelbank *et al.*, 2006; Wang *et al.*, 2008; Atwood & Rehm, 2009). However, protein fusions to PhaC offer two distinct advantages to its counterparts. Firstly PHA synthases remain covalently attached to the polyester core and secondly it allows for a simpler recombinant production system, removing the need for extra proteins (Jahns *et al.*, 2008; Grage *et al.*, 2009).

A large number of proteins and enzymes have already been successfully immobilised on the surface of these PHA beads to produce functionalised micro beads (Figure 9). For example, immunoglobulin G binding ZZ domain of protein A from *Staphylococcus aureus* was N-terminally fused to the PHA synthase which mediated the production of ZZ domain displaying PHA beads in recombinant *E. coli* (Brockelbank *et al.*, 2006; Lewis & Rehm, 2009). These functionalised beads showed IgG purification similar to that of commercially available protein A beads and also successful purification of monoclonal antibodies from mouse hybridoma supernatants (Brockelbank *et al.*, 2006; Lewis & Rehm, 2009). Also the immobilisation of enzymes has been demonstrated, such as α-amylase to the surface of PHA beads in a one-step process in recombinant *E. coli* by fusion of α-amylase from *Bacillus licheniformis* N-terminally to the PHA synthase (Rasiah & Rehm, 2009). Immobilisation of enzymes to the PHA beads offers several advantages compared to non-immobilised enzymes such as increased stability resulting in increased activity, recovery and reusability (Steinmann *et al.*, 2010).

In addition, bifunctional beads displaying targeted protein immobilised on the PHA beads surface are possible. Jahns *et al.* successfully produced multifunctional beads in recombinant *E. coli* which displayed a binding peptide for an inorganic material (Au) and IgG binding domain ZZ of protein A N-terminally fused to the PHA synthase from *C. necator* (Jahns *et al.*, 2008). Atwood and Rehm successfully produced multifunctional beads in recombinant *E. coli* displaying Green fluorescent protein (GFP) and myelin oligodendrocyte glycoprotein (MOG) by fusing the respective proteins to the N-terminus of the phasin and synthase or fusing both to the N- and C-terminus of the Phasin (Atwood & Rehm, 2009).
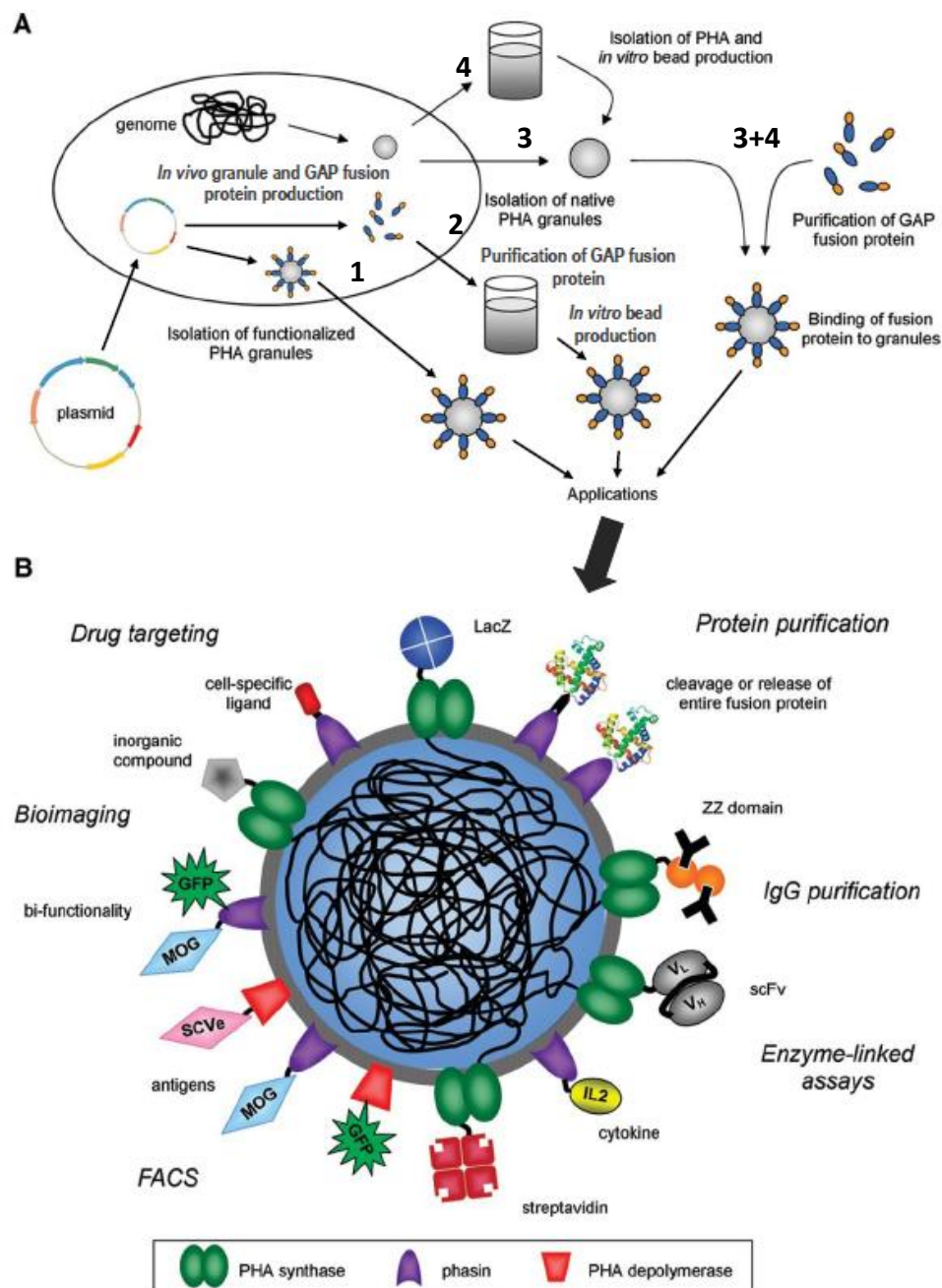
Figure 9. Potential applications of PHA beads produced *in vivo* and *in vitro*. (A) Different approaches for the generation of PHA beads. Plasmid encoding target protein fusion to GAP is expressed in recombinant host, either in the presence of genes encoding substrate formation, producing beads displaying surface immobilised proteins (1) or in the absence, leading to overproduction of recombinant protein which can be purified and used to produce PHA beads *in vitro* (2). PHA beads can be produced and isolated in their natural form (3) or by chemical extraction and subsequently produced *in vitro* (4). These beads can then be fused with GAP fusion protein *in vitro* (3+4). (B) Schematic overview of proteins and enzymes which have currently been immobilised successfully on the surface of PHA beads (Modified from Grage *et al.,* 2009)

Most of the early studies involving PHA synthase from *C. necator* (class I) involved fusions to the highly variable N-terminus. However, the highly conserved and hydrophobic C-terminus of the class I PHA synthase has recently been demonstrated to tolerate fusions to the C-terminus while still remaining functional (Peters & Rehm, 2008; Jahns & Rehm, 2009). This has opened up a whole new avenue for protein immobilisation.

In addition to protein purification and enzyme immobilisation, microbeads can also be used as a versatile platform for a range of medical and therapeutic applications due mainly to their highly biocompatible properties (Zinn *et al.*, 2001). Parlane and co-workers successfully demonstrated immunogenicity in mice when injected with functionised PHA beads which were engineered to display antigens (Ag85A) and (ESAT-6) from *Mycobacterium tuberculosis* on its surface (Parlane *et al.*, 2009). Kim *et al.* demonstrate that *in vitro* synthesised PHA beads displaying an N-terminal or C-terminal fusion to a tumour-targeting ligand could be used as a nanocarrier for targeting hydrophobic drugs to cancers (Kim *et al.*, 2009).

The above examples demonstrate the versatility and applicability of PHAs as microbeads for a large list of current and emerging applications, although currently only economically feasible for high value biotechnological and biomedical applications i.e. bioseparation, medical implants, and drug delivery. Because of their potential, there is considerable interest in improving PHA properties, production and synthesis of tailor-made polymers suggests a promising future.

1.7 Aim and objectives of study

My research project can be divided into three main sections focusing on: (I) Molecular characterisation of the class I PHA synthase, (II) production of functionalised PHA beads *in vivo* in recombinant *E. coli*, and (III) production of functionalised PHA beads *in vivo* in recombinant *L. lactis* and characterisation of lactate dehydrogenase (LDH) deficient *L. lactis* mutants under PHB accumulating conditions.

Part (I): This section of the study focuses on molecular characterisation of class I PHA synthase from *C. necator* (PhaC) in recombinant *E. coli.* The aim of this study was to purify and concentrate PHA synthase (PhaC) to a level suitable for protein crystallisation and ultimately x-ray diffraction studies. As currently, there is no structural data available for any class of PHA synthase (Rehm., 2003).

Part (II): The main focus and aim of *in vivo* formation of PHA beads was to demonstrate functional activity of the PHA synthase in regards to the polyHis-tag /IgG (ZZ and GB1) binding domain fusion to the N-terminus of the PHA synthase plasmids used in Part 1. In addition, functionality of the IgG binding domain and differences between truncated and full length forms of the PHA synthase were to be determined.

Part (III): Gram-positive organisms provide an alternative means for the production of endotoxin-free functionalised beads. The aim here was the production of functionalised PHB beads displaying medically relevant (HA and HepC) antigens immobilised on the surface of *Lactococcus lactis*. However, PHB production in *L. lactis* is relatively poor in comparison to its Gram-negative counterparts. The second aim here is to characterise PHB biogenesis in the LDH deficient *L. lactis* mutants NZ9010 and NZ9020.

Objectives - I

Part I   Molecular characterisation of class I PHA synthase from *C. necator*

- **Cloning of relevant plasmids** – plasmids encoding a polyHis-tagged and solubility tag fused to the PHA synthase (pET16b-His$_{10}$ZZC, pET14b-His$_{10}$GB1Δ1-93C and pET14b-His$_9$ZZTEVΔ1-93C) for the expression in recombinant *E. coli*.

- **Protein production** – protein production and optimisation for soluble recombinant protein.

- **Purification** – immobilized metal ion affinity chromatography (IMAC) and gel filtration chromatography.

- **Crystal screening studies** – using commercially available crystal screening buffers and vapour diffusion techniques (done in collaboration with Andrew Sutherland Smith, Massey University).

Objectives - II

Part II   *In vivo* **polyhydroxyalkanoate inclusions**

- **Cloning of relevant plasmids** – plasmids pET16b-His$_{10}$C and pET14b-ZZTEVΔ1-93C, in addition to plasmids from part I for the expression in recombinant *E. coli.*

- **PHA bead biogenesis** – plasmids were expressed under PHB accumulating conditions for the biogenesis of functionalised PHB beads displaying surface immobilised proteins.

- **Cell disruption and isolation** – using mechanical or detergent based methods for cell lysis and ultracentrifugation with 2 step glycerol gradient for bead isolation.

- **Functional assessment** – Enzyme-linked immunosorbent assay (ELISA) and IgG purification.

Objectives - III

Part III   **Antigen displaying beads from *L. lactis***

- **Cloning of relevant plasmids – plasmids** pNZ-HA*CAB* and pNZ-HepC*CAB* for expression in recombinant *L. lactis.*

- **PHA bead biogenesis –** plasmids were expressed under PHB accumulating conditions for the biogenesis of functionalised PHB beads displaying surface immobilised antigens.

- **Cell disruption and isolation –** using mechanical based methods of cell disruption and bead isolation by ultracentrifugation with 2 step glycerol gradient.

- **Functional assessment** – using a mouse model to assess immunogenicity of the surface displaying antigen beads (done in collaboration with Natalie Parlane (Hopkirk Research Institute, AgResearch).

Characterisation of *L. lactis* lactate dehydrogenase (LDH) mutants

- **Transformation of *L. lactis* strains** – *L. lactis* NZ9000, NZ9010 and NZ9020 strains were transformed with plasmids pNZ-*CAB* and pNZ-8148.

- **PHA bead biogenesis and characterisation –** under PHB accumulating conditions and characterisation by OD_{600}, pH, lactate production, acetate production, and GC/MS analysis.

Chapter 2: Materials and Methods

Unless stated, all reagents were purchased from Sigma-Aldrich, Ajax Finechem, or Merck.

2.1 Strains and Plasmids

In the tables below, lists the strains and plasmids used in this study

2.1.1 Strains

Table 2. Bacterial strains used in this study

Strain	Relevant characteristics[a]	References
For *E.coli*		
BL21 (DE3)	F$^-$ *dcm ompT hsdS*(r$_B^-$ m$_B^-$) gal λ(DE3)	Stratagene
BL21 (DE3) pLysS	F$^-$ *dcm ompT hsdS*(r$_B^-$ m$_B^-$) gal λ(DE3) [pLysS Cm^r]	Stratagene
TOP10	F$^-$ *mcr*A Δ(*mrr-hsd*RMS-*mcr*BC) Φ80*lac*ZΔM15 Δ*lac*X74 *rec*A1 *ara*D139 Δ(*ara-leu)*7697 *gal*U *gal*K *rps*L (Str^r) *end*A1 *nup*G	Invitrogen
XL1-Blue	*recA1 endA1 gyrA96 thi-1 hsdR17 supE44 RelA1 lac* [F' *proAB lacI^{q}Z*ΔM15 Tn*10* (Tet^r)]	Stratagene
For *L. Lactis*		
NZ9000	MG1363 derivative, *pepN*::*nisRK*	Hoefnagel *et al*., 2002
NZ9010	NZ9000 derivative, *ldh*::*ery*	Hoefnagel *et al*., 2002
NZ9020	NZ9010 derivative, *ldh*::*ery*, *ldhB*::*tet*	Bongers *et al*., 2003
[a] Phenotypic characteristics: Cm^r, chloramphenicol resistance; Tet^r, tetracycline resistance; Ery^r, erythromycin resistance		

2.1.2 Plasmids

The following plasmids listed below in tables 3 (plasmids for *E. coli*) and 4 (Plasmids for *L. lactis*) have been used in this study

Table 3. *E. coli* plasmids used in this study.

Plasmid name	Characteristics[a]	References
pGemT-Easy	Ap^r, T7 & SP6 RNA promoter, *lac*Z	Promega
pET14b-ZZ(-)phaC	Ap^r; T7 promoter, pET14b vector containing *Xba*I/*Bam*HI fragment gene ZZ-*phaC* without signal sequence-encoding region	(Brockelbank *et al.* 2006)
pET14b-His$_6$ZZTEVΔ1-93C	Ap^r; T7 promoter, pET14b vector containing *Xba*I/*Bam*HI fragment gene ZZ-Δ*phaC* with N-terminal His$_6$-tag	Jane Mullaney (former name Atwood)
PJ201_GB1	GB1 gene optimised by DNA2.0 from Strep for *E.coli*, a solubility tag fused with an N-terminus His$_{10}$-tag	Jane Mullaney (former name Atwood)
pET14b	Ap^r; T7 promoter; His$_6$-tag	Novagen
pET16b	Ap^r; T7 promoter; His$_{10}$-tag	Novagen
pET14b-His$_9$ZZTEVΔ1-93C	Ap^r; T7 promoter, pET14b vector containing *Xba*I/*Bam*HI fragment gene ZZ-TEV-Δ*phaC* with an N-terminal His$_9$-tag	This study
pET6b-His$_{10}$C	Ap^r; T7 promoter, pET16b vector containing *Nde*I/*Bam*HI fragment gene *phaC* with an N-terminal His$_{10}$-tag	This study
pET16b-His$_{10}$ZZC	Ap^r; T7 promoter, pET16b vector containing *Nde*I/*Bam*HI fragment gene ZZ-*phaC* with an N-terminal His$_{10}$-tag	This study
pET14b-His$_{10}$GB1Δ1-93C	Ap^r; T7 promoter, pET14b vector containing *Xba*I/*Bam*HI fragment gene GB1-TEV-Δ*phaC* with an N-terminal His$_{10}$-tag	This study
pMCS69	Cm^r; T7 promoter; pBBR1MCS derivative containing codon optimised genes *phaA* and *phaB* from *C. necator*	(Amara & Rehm, 2003)
[a] Phenotypic characteristics: Cm^r, chloramphenicol resistance; Ap^r, Ampicillin resistance		

Table 4. *L. lactis* plasmids used in this study.

Plasmid name	Characteristics[a]	References
pNZ-8148	Cm[r]; pSH71 origin, P*nisA*	(Mifune *et al*., 2009)
pNZ-CAB	Cm[r]; P*nisA*-*phaCAB*	(Mifune *et al*., 2009)
pUC57-HA	Cloning vector, ColE1 origin, Ap[r], Codon-optimized *HA* antigen	This study
pUC57-HepC	Cloning vector, ColE1 origin, Ap[r], Codon-optimized *Hep C* core antigen	This study
pNZ-HACAB	Cm[r]; P*nisA*-*HAphaCAB*	This study
pNZ-HepCCAB	Cm[r]; P*nisA*-*HepCphaCAB*	This study
[a] Phenotypic characteristics: Cm[r], chloramphenicol resistance; Ap[r], Ampicillin resistance		

2.2 Primers

The following primers were used in this study

Table 5. Primers used in this study

Primer name	Description/sequence 5' to 3'	References
Sequencing primers		
T7	Forward primer, amplification of N-terminal region	Allan Wilson Centre
	TAA TAC GAC TCA CTA TAG GG	
SP6	Reverse primer, amplification of C-terminal region	Allan Wilson Centre
	ATT TAG GTG ACA CTA TAG	
Pnis1	Forwards primer, amplification of N-terminal region downstream of NisA promoter	(Mifune *et al*., 2009)
	CTA CCC ATT ATT ACA GCA GG	
pET14b-His₉ZZTEVΔ1-93C PCR primers		
10xHis	Forward primer, amplification of N-terminal region encoding *Xba*I, His-tag, & start of ZZ domain	Jane Mullaney (former name Atwood)
	ATG GTG ATG GTG ATG ATG ATG GTG ATG GTG CAT GTA TAT CTC CTT CTA GAG GG	
revTEV_*Age*I	Reverse primer, amplification of C-terminal region encoding *Age*I and end of *pha*C	Jane Mullaney (former name Atwood)
	TTT ACC GGT AGA TTG AAA ATA TAA ATT TTC GGG TAC CGA GCT CGA ATT CGC GTC TAC TTT CGG CG	

pET14b-ZZTEVΔ1-93C PCR primers		
fwd_*Xba*I_ZZ	Forward primer, amplification of N-terminal region encoding *Xba*I & start of ZZ domain	This study
	GTT GTT CTT TGT TGA ATT TGT TGT CTA CGG CTT CAT CGT GTT GCG CCA TGT ATA TCT CCT TCT AGA TAT	
rev_*pha*C	Reverse primer, amplification of C-terminal region encoding *Age*I & end of *pha*C	This study
	GTC GCC GGC GAA GCG CCG GTC GTG CAG CGG	

2.3 Liquid media

Below shows a list of liquid media used during this study. All mediums were autoclaved at 121°C for 20 minutes. Unless stated, all supplements were sterilised either by autoclaving or filtration through a 0.22μm filter before being added to sterile autoclaved medium.

2.3.1 Luria-Bertani (LB)-Medium

Luria-Bertani (LB)-medium (Invitrogen) was prepared according to manufacturers instructions, by adding 20g per litre of Milli-Q water.

2.3.2 M17 and GM17 medium

GM17 medium consists of 1 x M17 media supplemented with 0.5% (w/v) glucose. For preparing GM17 medium, M17 medium (Merck, Germany) was prepared according to manufacturers instructions, by adding 42.5g per litre of Milli-Q water and supplementing with 0.5% (w/v) glucose.

2.4 Solid media

For preparing solid media, 1.5% (w/v) agar (Oxoid) was added to the liquid media and autoclaved at 121°C for 20 minutes.

2.4.1 X-Gal Medium

The following supplements were added to sterile LB-agar medium:

	Stock solution	Final concentration
IPTG	1M dissolved in Milli-Q water	1mM
X-Gal	4% (w/v) dissolved in DMSO	4×10^{-3} %

If necessary, the relevant antibiotics were added (2.5). All solutions were sterilised by filtration through a 0.22 µm filter.

2.4.2 Nile-red Medium (Spiekermann *et al*., 1999)

In addition to the X-Gal medium (2.4.1) the following supplements were added:

	Stock solution	Final concentration
Glucose	20 % (w/v) dissolved in Milli-Q water	1 %
Nile-red	0.25 mg/ml dissolved in DMSO	0.5 µg/ml

If necessary, the relevant antibiotics were added (2.5).

2.5 Antibiotic stock solutions and final concentrations

Antibiotics solutions were prepared as listed in Table 6. Sterilisation was achieved by filtration through a 0.22 µm filter and then subsequently stored at -20°C for further use. Autoclaved nutrient media was cooled to approximately 50°C before the addition of antibiotics.

Table 6. Antibiotic stocks and final concentrations.

Antibiotic	Stock solution (mg ml^{-1})	Final concentration (µg ml^{-1})
For *E.coli*		
Ampicillin (Na-salt)	75 in Milli-Q water	75
Chloramphenicol	30 in absolute EtOH	30
Tetracycline (hydrochloride)	12.5 in 70% EtOH	12.5
Kanamycin (-sulfate)	25 in Milli-Q water	25
Erythromycin	5 in Milli-Q water	5
For *L.lactis*		
Chloramphenicol	10 in absolute EtOH	10
Erythromycin	10 in Milli-Q water	10
Nisin	0.25 in 0.05 % acetic acid	0.01

2.6 Cultivation conditions

Cultivation of bacterial strains in liquid cultures was performed in Erlenmeyer flasks, with all *E. coli* cultures grown at 37°C and *L. lactis* cultures grown at 30°C with shaking at 200 x rpm unless stated. To maximise aeration, the ratio of flask volume to liquid medium was kept high ($\geq$ 6:1). Cultivation was performed in either LB or M17 medium for *E. coli* or *L. lactis* respectively, containing the appropriate antibiotic(s), supplement(s), and carbon source.

2.6.1 PHA accumulating conditions

PHA bead production in *E. coli*

Recombinant pET expression vectors were transformed into *E. coli* (2.10.1) strain BL21 (DE3) (Stratagene) harbouring plasmid pMCS69. BL21 (DE3) main cultures were inoculated with 1 % (v/v) of fully grown overnight culture and cultivation was performed at 37 °C in LB medium containing 75 µg/ml ampicillin, 30 µg/ml chloramphenicol and 1 % glucose. Once cultures had reached OD_{600} 0.4 – 0.5 (approximately 3 hours) they were induced by the addition of IPTG at a final concentration of 1 mM and cultures were subsequently grown at 25 °C for 72 hours.

PHA bead production in *L. lactis*

Recombinant pNZ plasmids were transformed into *L. lactis* strains NZ9000, NZ9010 or NZ9020 by electroporation (2.10). *L. lactis* main cultures were inoculated with 1% (v/v) of fully grown overnight culture and cultivation of large cultures was performed at 30 °C in M17 medium containing 1 % (w/v) glucose, 0.3 % (w/v) L-arginine and appropriate antibiotics. Induction was performed by the addition of nisin (Sigma-aldrich, USA) to a final concentration of 10 ng/ml when OD_{600} reached 0.4 – 0.5, cultures were subsequently grown at 30 °C for 24 - 48 hours.

2.6.2 Protein production

Recombinant plasmids using the pET expression system were transformed into *E. coli* (2.10.1) BL21 (DE3) or *E. coli* BL21 (DE3) pLysS protein production strains in the absence of plasmid pMCS69. The main cultures were inoculated with 1 % (v/v) of overnight culture and cultivation was performed at 37 °C in plain LB media. Induction of the large culture was performed by the addition of IPTG to a final concentration of 1 mM when OD_{600} reached 0.3 and cultures were subsequently grown at 25 °C.

2.7 Selection on solid media

2.7.1 Blue/white selection

Blue/white selection is a method used for the detection of successful ligation between pGEM –T Easy vector and A-tailed blunt end PCR products (2.11.8). After ligation (2.11.8), the ligation mixture was then transformed into *E. coli* (2.10.1) XL1-Blue (Invitrogen) and plated on to solid X-Gal medium in the presence of 75 µg/µl ampicillin and incubated at 37 °C. White colonies indicate insertional inactivation of the β-galactosidase, therefore, single white colonies were selected and replated on to fresh solid X-Gal medium (2.4.1) to confirm loss of β-galactosidase activity.

2.7.2 Nile-red selection (Spiekermann *et al*., 1999)

For the routine screening of PHA accumulating colonies, *E. coli* BL21 (DE3) transformants harbouring pMCS69 plasmid were plated on LB-agar plates containing lipophilic stain Nile-red (2.4.2). Plates were wrapped in foil and incubated at 37 °C for 24 hours, followed by additional incubation at room temperature for 24 – 48 hours for PHA production and red colour development. Plates were viewed under ultraviolet light $\lambda = 312$ nm for detection of PHA accumulating colonies. Single colonies were selected based on intensity of Nile-red florescence for further studies.

2.8 Long term storage of bacterial strains

Storage of *E. coli* strains

To maintain the viability of recombinant *E. coli* strains for long term storage, 1ml of overnight culture, grown in the presence of antibiotics at 37 °C with aeration on a thermoline orbital shaker TLM510 (N.S.W, Australia), was mixed with 70 µl of sterile dimethylsulfoxide (DMSO) to give a final concentration of 6.5 % (v/v) in a 2 ml cryovial tube and subsequently stored at -80 °C.

Storage of *L. lactis* strains

For maintain the viability of recombinant *L. lactis* strains for long term storage, 1.2 ml of overnight culture grown in the presence of antibiotics at 30 °C with aeration on a gyratory shaker G-25 (New Brunswick Scientific, USA) was mixed with 200 µl of sterile 80 % glycerol to give a final concentration of 11.4 % (v/v) in a 2 ml cryovial tube and subsequently stored at -80 °C.

2.8.1 Strain revival

The revival of *E. coli* and *L. lactis* strain(s) was achieved by removing a small chip of frozen stock using a sterile pipette tip, which was then used to inoculate liquid media containing the appropriate antibiotic. Inoculated medium with recombinant *E. coli* was incubated overnight at 37°C with aeration on a thermoline orbital shaker TLM510 (N.S.W, Australia) (2.6), while recombinant *L. lactis* was incubated overnight at 30°C with aeration on a gyratory shaker G-25 (New Brunswick Scientific, USA) (2.6).

2.9 Preparation of competent cells

2.9.1 Competent *E. coli*

50 ml LB media was inoculated with 1 % inoculum of overnight culture and cultivated at 37 °C until OD_{600} reached 0.3 - 0.4. Cell culture was subsequently stored on ice for 10 – 15 mins and harvested by centrifugation at 8,000 x *g* (Heraeus multifuge1 S-R, Sorvall). Cell sediment was re-suspended in 16 ml of RF1 solution and further stored on ice for 30 min. Cells were then harvested again by centrifugation at 8,000 x *g* for 15 min and re-suspended in 4 ml of RF2 solution. 200µl aliquots of competent cells were distributed into sterile 1.5 ml microfuge tubes, flash frozen in liquid nitrogen and stored at -80 °C for future use.

RF1 solution

100 mM	RbCl
50 mM	$MnCl_2$
30 mM	Potassium acetate
10 mM	$CaCl_2.6H_2O$

Adjust to pH 5.8 using acetic acid

RF2 solution

10 mM	RbCl
10 mM	MOPS
75 mM	$CaCl_2.6H_2O$
15 % (v/v)	Glycerol

Adjust to pH 5.8 using NaOH

Solutions were sterilised by filtration (0.22 µm) and stored at -20 °C.

2.9.2 Electro-competent *L. lactis* (NISO food research, Netherlands)

100 ml of SGM17, GM17 (2.3.2) supplemented with 0.2 M sucrose and 1 % glycine, was inoculated with 5 % inoculum of overnight culture and incubated at 30 °C with shaking on a gyratory shaker G-25 (New Brunswick Scientific, USA) shaker until OD_{600} of 0.4 – 0.5. The culture was split into 2x 50 ml falcon tubes (Greiner Bio-One), cells harvested by centrifugation at 4,000 x *g* for 15 min (Heraeus multifuge1 S-R, Sorvall) and supernatant discarded. Each sediment was re-suspended and washed with 50 ml of ice cold 0.5 M sucrose containing 10 % glycerol, before harvesting by centrifugation as stated previously. The sediment was resuspended in 25 ml ice cold 0.5 M sucrose containing 10 % glycerol and 0.05 % EDTA and re-suspended cells combined for a total of 50 ml. Storage on ice for 15 min was followed by centrifuging at 4000 x *g* for 15 min (Heraeus multifuge1 S-R, Sorvall), supernatant discarded and sediment washed a second time with 25 ml ice cold 0.5 M sucrose containing 10 % glycerol. After another centrifugation as before, supernatant was discarded and resuspended in ice cold 0.5 M sucrose containing 10 % glycerol. The resulting cells were distributed in 40 µl aliquots into 1.5 ml microfuge tubes, flash frozen with liquid nitrogen and stored at -80 °C for future use.

2.10 Transformation and electroporation

2.10.1 Transformation of plasmid into *E. coli*

200 µl aliquots of frozen *E. coli* competent cells were thawed on ice for 40 mins before the addition of 1 - 3 µl of purified plasmid DNA or 10 µl ligation mix, followed by incubation on ice for an additional 20 mins. To promote the uptake of plasmid DNA, competent cells were briefly mixed and then heat-shocked at 42 °C for 90 sec, followed by incubation on ice for 5 mins. Cells were regenerated by adding 800 µl of liquid LB media and incubated at 37 °C for one hour. For the selection and isolation of recombinant clones, 100 µl of cells was plated on solid LB-agar medium containing the appropriate antibiotics and the remaining cells were sedimented by centrifugation at 16,200 x *g* on a Heraeus Pico 17 (Thermo Scientific) for 1min, re-suspended in 100 µl of fresh LB media and also plated on to fresh solid LB-agar medium.

2.10.2 Electroporation of plasmid into *L. lactis*

40 µl aliquots of frozen *L. lactis* electro-competent cells were thawed on ice for 40 mins before being transferred to an ice chilled 0.2 cm electroporation cuvette (Bio-Rad Laboratories, USA). 1 µl of plasmid DNA or 9 µl of ligation mix was then added and mixed with cells. Electroporation was achieved by increasing cell permeability of the plasma membrane using a BIORAD MicroPulser (Bio-Rad Laboratories, USA) set at 2 kv, 1 pulse, and at 5.8 ms. 1 ml of sterile recovery medium (GM17 medium supplemented with 20 mM $MgCl_2$ and 2 mM $CaCl_2$) was added immediately after electroporation and cells were transferred to a 1.5 ml microfuge tube and incubated on ice for 10 mins. After incubation on ice, cells were further incubated for 1.5 – 2 hours with shaking at 30 °C on an gyratory shaker G-25 (New Brunswick Scientific, USA) (2.6). For the selection and isolation of recombinant clones, 100 µl of cells was plated on solid GM17-agar medium (2.3.2) containing the appropriate antibiotics. The remaining cells were sedimented by centrifugation at 16,200 x *g* (Heraeus Pico 17, Thermo Scientific) for 1 min, re-suspended in 100 µl GM17 and also plated on solid GM17-agar medium and incubated at 30 °C with the appropriate antibiotics.

2.11 DNA manipulation

2.11.1 Plasmid isolation and concentration

Plasmid isolation from recombinant *E. coli* was done by at least one of two methods described below:

2.11.1.1 Alkaline lysis

1 - 3 ml of overnight culture harbouring the respective plasmid was sedimented in a 1.5 ml microfuge tube by centrifugation at 16,200 x *g* for 2 mins (Heraeus Pico 17, Thermo Scientific). Supernatant was discarded and sediment was re-suspended in 100 µl of chilled GET solution. 200 µl of freshly prepared SDS-NaOH lysis solution was added, followed by gently mixing by inversion and then the tubes left to stand at room temperature for 5 mins. Clear solution was indicative of complete lysis. Proteins were then precipitated by the addition of 150 µl of HSS buffer and incubation on ice for 10 mins. Precipitated protein was removed by centrifugation at 16,200 x *g* for 30 min (Heraeus Pico 17, Thermo Scientific). Supernatant was transferred to a new 1.5 ml microfuge tube and centrifuged again at 16,200 x *g* for 15 min to remove remaining precipitate. Supernatant was transferred to a new 1.5 ml microfuge tube, and 300 µl of

ice-chilled isopropanol was added, followed by gentle mixing by inversion and centrifugation at 16,200 x g for 30 mins. Supernatant was discarded and 300 µl of 70% ice-chilled ethanol was added. Sediment was re-suspended by vortexing briefly and centrifuged at 16,200 x g for 10 mins. Supernatant was removed and the sediment left to dry at room temperature before dissolving in 30 µl of TER buffer. Plasmids were stored at -20 °C for future use.

GET solution

25 mM	Tris/HCl (pH 8.0)
10 mM	EDTA
50 mM	Glucose

SDS-NaOH solution

200 mM	NaOH
1 %	SDS

HSS buffer

3 M	Potassium acetate
1.8 M	Formic acid (pH 4.8)

TER buffer

990 µl	TE-buffer (pH 8.0)
10 µl	RNase-A (20 mg/ml)

2.11.1.2 High Pure Plasmid isolation kit

Plasmid isolation using the High Pure Plasmid isolation kit (Roche, Switzerland) was used according to manufacturer'sinstructions.

2.11.1.3 Plasmid isolation from *L. lactis*

For the successful isolation of plasmids from Gram-positive *L. lactis*, a heavily modified version of the plasmid isolation protocol from NIZO (NISO food research, Netherlands) was used in conjunction with a modified version of the High Pure Plasmid isolation kit (Roche, Switzerland) (2.11.1.2). Total volume of 5 - 10 ml of overnight culture was sedimented in a microfuge tube at 16,200 x g for 1 min (Heraeus Pico 17, Thermo Scientific). The sediment was re-suspended in 250 µl of THMS-buffer

containing 10 mg/ml lysozyme and incubated for 10 - 15 mins at 37 °C. Cells were then lysed by the addition of 500 µl of freshly made lysis buffer (0.2 N NaOH + 3 % SDS) and incubated on ice for a maximum of 5 mins. Following cell lysis, isolation of plasmid from crude cell lysate was done using a modified version of the High Pure Plasmid isolation kit. Proteins were precipitated by the addition of 350 µl of chilled binding buffer and incubated on ice for a further 5 mins. The white precipitate was removed by centrifugation at 16,200 x g for 10 mins (Heraeus Pico 17, Thermo Scientific). Supernatant was then transferred to a new high pure filter tube and centrifuged at 16,200 x g for 1 min. 500 µl wash buffer I was added, centrifuged for 1 min at 16,200 x g and then repeated with 700 µl of wash buffer II, with supernatant being discarded. To elute the plasmid DNA, the high pure filter tube was transferred to a sterile microfuge tube, 80 - 100 µl of elution buffer was added and incubated for 5 mins at room temperature before being centrifuged at 16,200 x g for 1 min to maximise recovery of plasmid DNA.

THMS-buffer

30 mM	Tris/HCL (pH 8.0)
3 mM	$MgCl_2$
25 % (w/v)	Sucrose

2.11.1.4 Clean and concentrator kit (Zymo)

The Clean and concentrator kit (Zymo Research, USA) was used following plasmid isolation methods for low concentration or dirty plasmid preparations required for cloning or DNA sequencing.

2.11.2 Polymerase Chain Reaction (PCR)

PCR was employed for the amplification of DNA fragments for subcloning and diagnostics. *Pfx* DNA polymerase (Invitrogen Corporation, USA) was used when high fidelity was required. A typical PCR reaction mixture is described below:

***Pfx*-DNA-polymerase reaction mix**

10.0 µl	10 X *Pfx* reaction buffer
5.0 µl	$MgSO_4$ (50mM)
5.0 µl	DMSO

10.0 µl	Primer 1 (10 pmoles/µl)
10.0 µl	Primer 2 (10 pmoles/µl)
10.0 µl	dNTPs (10mM each)
~1 - 10 ng	Template DNA
0.5 µl	*Pfx*-DNA-polymerase (2.5 U/µl)
to 100 µl	H_2O

PCR reactions were performed in a Biometra Tpersonal thermocycler (Whatman Biometra, Germany). A typical reaction conditions are listed below:

Pfx-DNA-polymerase reaction conditions

1. Denature	94 °C for 120 sec
2. Denature	94 °C for 15 sec
3. Anneal	~5 °C below the lowest T_m of the primer pair for 30s
4. Extend	68 °C for 60 sec per 1 kb
5. Cycle	Repeat steps 2 – 4 for 33 cycles
6. Hold	10 °C

2.11.3 Determination of DNA concentration

The Qubit^{TM} fluorometer (Invitrogen, USA) was used in conjunction with Quant-iT DNA BR assay kit (Invitrogen, USA) for the accurate determination of DNA concentrations between 2 – 1000 ng, and was used according to manufacturer'sinstructions.

2.11.4 DNA hydrolysis with restriction endonucleases

DNA hydrolysis with restriction endonucleases (RE) was used for cloning and restriction analysis of plasmid DNA. Various restriction enzymes were used depending on available restriction sites. All restriction enzymes used were purchased commercially from Invitrogen, Roche, or New England Biolabs and were used according to manufacturer'sinstructions. For restriction analysis of plasmid DNA using a single RE, a typical 10 µl reaction mixture contained the following: 7µl Plasmid DNA, 1µl RE buffer (10x), 1µl RE, and 1µl Milli-Q water.

For DNA hydrolysis with two RE using incompatible RE buffers, an intermediate isopropanol precipitation step was required (2.11.4.1). RE with compatible buffers were combined into one single reaction.

2.11.4.1 Isopropanol precipitation of DNA

DNA was precipitated by adding 3 volumes of room temperature isopropanol and incubating on ice for 5 mins. Precipitated DNA was sedimented by centrifugation at 16,200 x g for 30 mins (Heraeus Pico 17, Thermo Scientific) and supernatant carefully removed by pipetting. Sediment was then washed once with 3 volumes of 70 % ethanol to removed traces of isopropanol and air dried.

2.11.5 Agarose gel electrophoresis (AGE)

Separation of DNA fragments was performed using agarose gel electrophoresis with a horizontal gel setup. Typically 1 – 2 % agarose gels were made in 1x TBE Buffer depending on fragment sizes being separated (1 % for DNA fragments >1000 bp and 2 % for DNA fragments <1000 bp). 3x loading dye was added to DNA samples before loading into the wells of the gel. A suitable molecular size standard was also loaded along with samples. Gel electrophoresis was run in 1x TBE buffer at 100 - 120 V for 35 - 60 mins depending on the gel electrophoresis chamber and degree of separation required. Analytical gels were stained for at least 20 min in ethidium bromide solution and destained for at least 1 min in distilled H_2O. Visualisation of the gel was performed using a UV transilluminator at $\lambda = 254$ nm (Bio-Rad, Gel Doc 2000). For separation of DNA fragments required for cloning, SYBR safe DNA gel stain was used according to manufacturer'sinstructions and visualised using blue light screen (Invitrogen, USA).

10x TBE

500 mM	Tris-HCl
500 mM	Boric acid
25 mM	EDTA
Adjust to pH 8.0 using HCl	

3x Loading dye

60 mM	Tris-HCl
60 mM	EDTA

60 % (v/v)	Glycerol
0.2 % (w/v)	Orange G
0.05 % (w/v)	Xylen Cyanol FF

2.11.5.1 DNA molecular size standards

λ-DNA molecular size standard

This consists of λ-DNA (Invitrogen, USA) digested with *Pst*I restriction endonuclease (2.11.4) to give the fragment showed below (Table 7). Digested DNA was mixed with 3x loading dye and stored at -20 °C for future use.

Table 7. λ-DNA molecular size standard

Enzyme	Size (bp)
*Pst*I	15, 72, 94, 160, 164, 200, 211, 216, 264, 339, 448, 468, 514, 805, 1093, 1159, 1700, 1986, 2140, 2443, 2449, 2560, 2838, 4507, 4749, 5077, 11490

GeneRuler 100 bp DNA ladder plus

GeneRuler 100 bp DNA ladder plus (Fermentas, Canada) was used according to manufacturer'sinstructions. The fragment sizes are shown in Table 8.

Table 8. GeneRuler 100 bp DNA ladder plus

Ladder	Size (bp)
Generuler 100 bp DNA ladder plus	100, 200, 300, 400, 500, 600, 700, 800, 900, 1000, 1200, 1500, 2000, 3000

2.11.6 Agarose gel DNA fragment recovery

For the recovery of DNA fragments from AGE (2.11.5), QIAquick® Gel Extraction Kit (Qiagen, Germany) or Zymoclean^{TM} Gel DNA Recovery Kit (Zymo Research, USA) was used according to the manufacturer'sinstructions.

2.11.7 Dephosphorylation of 5' ends

To prevent re-ligation of linearized plasmids (2.11.4), Antarctic phosphatase was used according to manufacturer'sinstructions to catalyse the removal of the 5' phosphate group.

2.11.8 DNA A-tailing and ligation (pGEM T-easy system)

To ligate blunt end PCR products effectively into an intermediate cloning vector pGEM –T Easy Vector (Promega, USA), A-tailing of PCR products was required. The A-tailing reaction was performed in a Biometra Tpersonal thermocycler (Whatman Biometra, Germany) at 70 °C for 30 min. A typical 10 µl reaction mixture contained the following:

A-tailing reaction mix

1 µl	dATP (0.2 mM)
1 µl	*Taq*-DNA-polymerase (Invitrogen)
1 µl	10x *Taq* reaction buff (-MgCl$_2$)
1 µl	MgCl$_2$
6 µl	PCR product

An aliquot of A-tailed PCR product was used to set up a 10 µl ligation reaction with pGEM –T Easy Vector. The reaction was incubated at 4 °C in a floating water bath overnight. A typical ligation reaction contains the following:

pGEM –T Easy ligation mix

5 µl	pGEM-T Easy 2x ligase buffer
0.5 µl	pGEM-T Easy vector
1 µl	pGEM-T Easy ligase
3.5 µl	A-tailed PCR product

2.11.9 DNA ligation (T4 DNA ligase)

For the ligation of desired fragments into the appropriate expression vectors, T4 DNA ligase (Invitrogen, USA) was used. DNA fragments and vectors were obtained first by DNA hydrolysis using the appropriate restriction endonucleases (2.11.4), separated by AGE with SBYR safe DNA gel stain (2.11.5), and purified (2.11.6). To increase the efficiency of ligation between insert and vector, a high insert to vector ratio of ≥ 6:1 was used. Reactions were set up in 1.5 ml microfuge tubes according to manufacturer'sinstructions and incubated overnight at 4 ºC in a floating water bath.

2.11.10 DNA sequencing

All DNA sequencing of recombinant plasmids and PCR products were performed in house by Allan Wilson Centre Genome Service using a capillary ABI3730 Genetic Analyzer (Applied Biosystems Inc). Sequencing reactions were set up in sterile 0.2 ml thin walled PCR tubes (Axygen, USA) and contained 250 – 350 ng of DNA and 3.2 pM primer in a 15 µl total reaction volume. Results were provided in ABI format and analysed using Vector NTI version 10.

2.12 PHA extraction, preparation and analysis

2.12.1 Cell disruption

Listed below are various cell disruption methods which were employed to lyse bacterial cells for the isolation of PHA beads or PHA synthase protein. Large cell cultures were harvested by centrifugation at 6,000 x rpm for 20 mins in a Sorvall RC-5B (Du Pont instruments). Cell sediments were re-suspended in 50 mM potassium phosphate buffer (pH 7.5) and transferred to 50 ml falcon tubes. Cells were sedimented by centrifugation at 8,000 x g for 10 min in a Heraeus Multifuge 1 S-R (Sorvall, Germany) and supernatant removed.

50 mM Potassium Phosphate Buffer

50 mM	K_2HPO_4 (Base)
50 mM	KH_2PO_4 (Acid)

The pH of K_2HPO_4 was adjusted to pH 7.5 using KH_2PO_4

2.12.1.1 Bugbuster® Protein Extraction Reagent

Bugbuster® Protein Extraction Reagent (10x) (Merck, Germany) was used only for the purpose of PHA bead isolation. Bugbuster was used according to manufacturer's instructions, 5 ml of 1x Bugbuster solution was used per gram cell wet weight. A small amount (few mg) of lysozyme (Sigma-Aldrich, USA) was added to the re-suspended cells and incubated with shaking at room temp for 10 – 20 mins to help with cell lysis. This was followed by the addition of a small amount (few mg) of DNase (Sigma-Aldrich, USA) and $MgCl_2$ to a final concentration of 5 mM, and the mixture incubated again with shaking at room temp for an additional 20 mins. After incubation, the cell lysate was centrifuged at 8,000 x g for 10 min at 4 °C (Heraeus multifuge1 S-R, Sorvall) to sediment PHA beads, and the supernatant was discarded. To lyse remaining

cells and to remove host cellular material, the sediment was resuspended again in the same volumes of bugbuster and lysozyme as before and incubated at room temperature for 10 mins, before harvesting by centrifugation. The sediment was then washed once with 50 mM potassium phosphate buffer to remove residual bugbuster and re-suspended in a small amount of 50 mM potassium phosphate buffer.

2.12.1.2 Cell disruptor

Cell disruptor method for *E. coli*

The cell disruptor was used for generating the crude cell extracts for both the isolation of PHA beads and for the isolation of PHA synthase protein. Cell sediment was resuspended in 50 mM potassium phosphate buffer. 1 tablet Complete, Mini, EDTA-free protease inhibitor cocktail (Roche, Switzerland) was added to 10 ml buffer when inhibition of protease activity was important. A small amount (few mg) of lysozyme (Sigma-Aldrich, USA) and DNase (Sigma-Aldrich, USA) was added and mixtures incubated on ice for 10 mins to help cell lysis, before being subjected to 2 passes of mechanical cell disruption at 20 kPsi. Crude cell lysate containing PHA beads or PHA synthase protein was centrifuged at 8000 x *g* for 15 min at 4 °C (Heraeus multifuge1 S-R, Sorvall) to sediment beads, unlysed cells and large insoluble cellular debris. For PHA bead isolation, sediment was re-suspended in a small amount of 50 mM potassium phosphate buffer.

Cell disruptor method for *L. lactis*

For the generation of crude cell extracts for PHA bead isolation from *L. lactis* strains, cell sediment was re-suspended in a small volume (< 10 ml total volume for a 1 L culture) of buffer containing 3 mM $MgCl_2$ and 25 % (w/v) sucrose solution and 10 mg/ml lysozyme. The mixture was incubated at 37 °C with shaking for 15 mins and then chilled on ice for 5 − 10 mins. Cells were then lysed by subjecting to 2 passes of mechanical cell disruption at 20 kPsi. Crude cell lysate containing PHA beads was processed similarly to that described for *E. coli*, crude cell lysate was centrifuged to sediment beads and unlysed cells. Sediment was re-suspended in a small amount of buffer plus protease inhibitor (1 Complete, Mini, EDTA-free protease inhibitor cocktail tablet to 10 ml buffer) (Roche, Switzerland).

2.12.1.3 French press

The French press was only used for the isolation of PHA synthase protein. Cell sediment was re-suspended in the 50 mM potassium phosphate buffer containing Complete, Mini, EDTA-free protease inhibitors (Roche, Switzerland) (1 tablet in 10 ml buffer) and small amount of DNase (Sigma). Cell mixture was incubated on ice for 10 mins before being subjected to 2 passes of mechanical cell disruption at 4 kPsi.

2.12.2 Isolation of PHA from crude extracts (Ultracentrifugation)

PHA beads isolated from Bugbuster® (2.12.1.1) or cell disruption (2.12.1.2) methods were purified by ultracentrifugation at 100,000 x g for 2 hours (Sorvall WX Ultra 80, Thermo Scientific) using a 2 step glycerol gradient containing a lower 88 % glycerol layer and a upper 44% glycerol layer. Purified PHA beads were recovered as a layer between the 44 % and 88 % glycerol interface. A schematic representation of the extraction process is shown Figure 10 below:
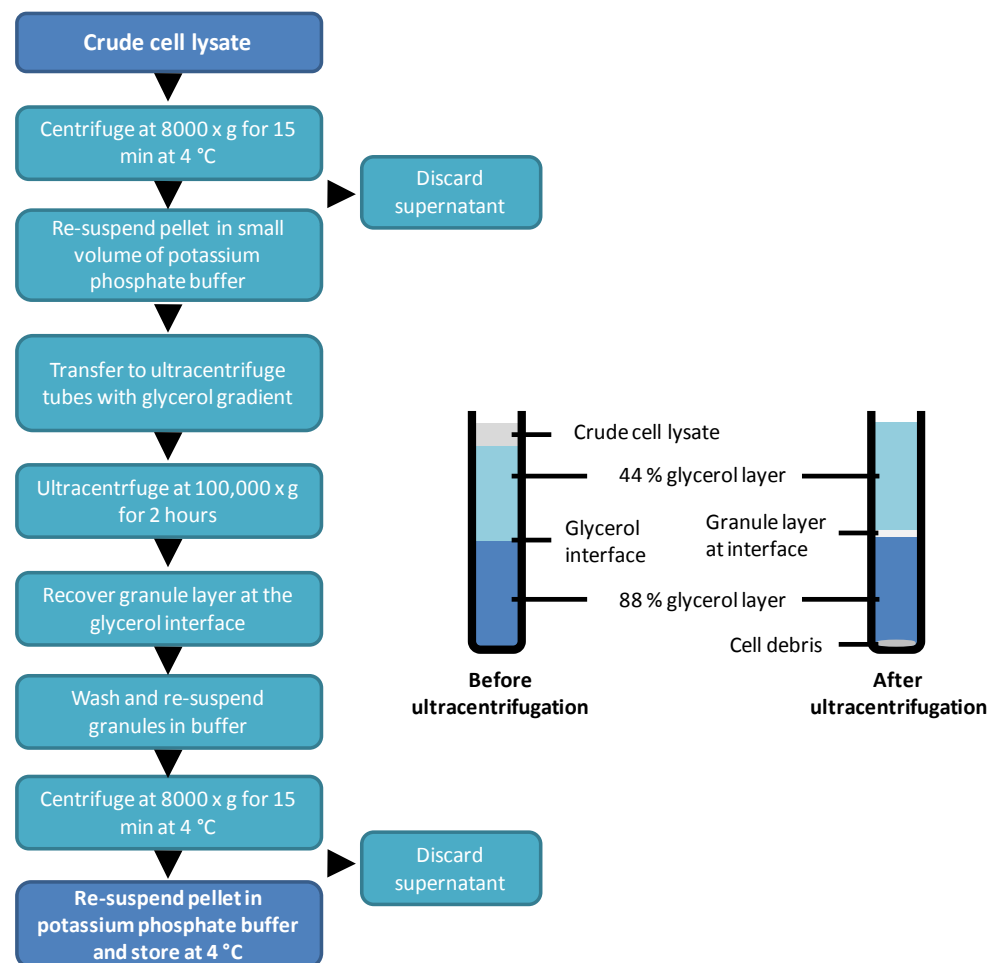
Figure 10. Schematic representation of the PHA bead extraction process. PHA beads were extracted from crude cell lysate using ultracentrifugation with 2 step glycerol gradient.

2.12.3 Nile-red detection (Spiekermann *et al.*, 1999)

For routine analysis of PHA accumulating cells grown in liquid media, 1 ml of culture was harvested by centrifugation (Heraeus Pico 17, Thermo Scientific), 10 µl of Nile-red stock solution (0.25 mg/ml in DMSO) was added to the cell sediment and mixed, followed by addition of 1 ml 50 mM potassium phosphate buffer (pH 7.5) and incubation at room temperature for 15 min. Cells were harvested by centrifugation and washed once with 1 ml of 50 mM potassium phosphate buffer. The cells were then resuspended in 1 ml fresh 50 mM potassium phosphate buffer (pH 7.5) and spotted onto a microscope slide, and a cover slip added. The slide was examined using fluorescent microscopy (Olympus) and Magnafire imaging software was used to capture images digitally.

2.12.4 Gas chromatography-mass spectrometry analysis (GC/MS)

Typically 10 – 20 mg of lyophilised cells was suspended in 2 ml of chloroform and subjected to methanolysis in 2 ml methanol in the presence of 15 % (v/v) sulphuric acid. Methanolysis was performed in a heated oil bath for 5 hour at 100 °C. After methanolysis, tubes were removed and left to cool at room temperature before the addition of 2 ml of H_2O, briefly vortexed to mix and left at room temp for phase separation. The bottom phase containing methyl esters of the corresponding fatty acid constituents was recovered and analysed by Gas chromatography-mass spectrometry (GC/MS) for 3- hydroxyalkanoate methyl esters. All GC/MS analysis was performed at Plant and Food (Palmerston North).

2.12.5 Transmission Electron Microscopy (TEM)

All TEM samples were processed at the Manawatu Microscopy and Imaging Center (Massey University, Palmerston North). Samples for TEM were provided to the MMIC as a small sediment in a microfuge tube and all subsequent sample processing was done by MMIC. Images were taken by the author.

2.12.6 Analysis of lactate and acetate

L. lactis strains were cultivated under PHA accumulating conditions as described in section 2.6.1 for 24 hours, with cell culture samples taken throughout the 24 hour cultivation period at specified time intervals. Samples were centrifuged to remove cells and supernatant analysed. The concentration of lactate and acetate in culture supernatant

was determined using a Lactate assay kit (Eton Bioscience Inc, USA) or acetate assay kit (Megazyme, USA) respectively in a 96 well format as described below:

2.12.6.1 Lactate assay

Quantification of lactate was done using the Lactate Assay Kit (Eton Bioscience Inc, USA) according to manufacturer's instructions.

2.12.6.2 Acetate assay

Quantification of acetate was done using the K-ACETAK Acetic acid assay kit (Megazyme, USA) for use in an auto-analyser and was used according to manufacturer's instructions. 0.29 ml of R1 solution was added to the well along with 5 µl sample, mixed and sample read at $\lambda = 340$ nm (A1) on an ELx808iu ultra microplate reader (BIO-TEK Instruments Inc., USA). After the A1 reading, 20 µl of R2 solution was added to each well to start the reaction. The calibration curve required to calculate the amount of acetic acid in the test samples was made using 100 % acetic acid and Milli-Q water to concentrations ranging from 5 to 30 µg/ml in a 96 well format. All reactions were then conducted at 25 °C for 10 mins and read at $\lambda = 340$ nm (A2). To calculate the change in absorbance, reading A2 is subtracted from A1. The change in absorbance was compared with the calibration curve for known acetic acid concentrations to calculate the concentrate in unknown samples.

2.13 General methods for protein analysis
2.13.1 Protein determination
2.13.1.1 Bradford protein assay (Bio-Rad laboratories, USA)

Bradford protein assay was used for the accurate determination of the concentrations of proteins associated with PHA beads. 10 µl serial dilutions of samples were made in a medium binding flat bottom microtitre plate (Greiner bio-one) along with known BSA (bovine serum albumin) or IgG (immunoglobulin G, GE life sciences) standards. 200 µl of filtered 1x Bradford reagent (Bio-Rad laboratories, USA) was added to each microtitre plate well and incubated at room temperature for 5 min for colour development. The absorbance was measured spectrophotometrically using an ELx808iu ultra microplate reader (BIO-TEK Instruments Inc., USA) at $\lambda = 595$ nm. Protein concentration was determined from a standard curve prepared with known

concentrations of BSA ranging from 0.05 mg/ml to 0.4 mg/ml or IgG ranging from 0.05 mg/ml to 0.8 mg/ml.

2.13.1.2 UV measurement at 280 nm

UV measurement at λ = 280 nm was used for the accurate determination of protein concentration for purified PHA synthase. Absorption of radiation by proteins near UV (280 nm) depends on the presence of aromatic rings and the tyrosine and tryptophan content. Pure protein solutions were added to quartz cuvettes and measured spectrophotometrically at λ = 280 nm. For an accurate reading, protein solutions were diluted to give an absorbance reading between 0.3 – 1. The UV absorbance for the protein solution can be calculated using the equation below. The extinction coefficient was calculated using the primary protein sequence with ProtParam tool (ExPASy.com).

Beer-Lambert law   Protein concentration

$A = \varepsilon \, C \, l$ $C = A \, / \, \varepsilon l$

A = Absorbance

ε = Extinction coefficient

C = concentration of protein

l = Path length (1 cm)

2.13.2 Sodium dodecylsulfate gel electrophoresis (SDS-PAGE)

For characterisation and evaluation of proteins, sodium dodecyl sulfate gel electrophoresis (SDS-PAGE) was performed in a vertical slab gel electrophoresis apparatus. Each Tris-glycine gel consists of a lower separating gel layer (8 – 10 %, w/v, pH 8.9) and an upper stacking gel layer (4 %, w/v, pH 6.8). The stacking gel was prepared between two clean glass plates (16 cm x 19.5 cm) separated by 0.8 mm gap or in a pre-cast cassette (Invitrogen, USA) (8 cm x 8 cm) separated by 1.5 mm gap.

Separating gel

8 % (w/v)	10 % (w/v)	
10.4 ml	10.4 ml	Separating / resolving buffer
11.1 ml	13.9 ml	Acrylamide (30%)
20.1 ml	17.3 ml	Milli-Q water
41.6 ml	41.6 ml	Total volume

The separating gel mixture was prepared and degassed by the addition of a small amount (few mg) of Na_2SO_3 to prevent formation of air bubble. The polymerisation reaction was started by the addition of 20 µl of N, N, N', N'-tetramethylethyl-endiamin (TEMED) and 40 µl of ammonium persulfate (APS) (40 %, w/v). This solution was gently poured between the 2 glass plates or pre-cast cassette (leaving significant space for the stacking gel) and immediately layered with isopropanol. The gels were left to stand for 1 hr to set.

Stacking gel (4%, w/v)

3.12 ml	Stacking gel buffer
1.88 ml	Acrylamide (30%)
7.50 ml	Milli-Q water
12.5 ml	Total volume

Once the gels had set, the isopropanol was removed by washing with distilled H_2O. The stacking gel layer was prepared as indicated above in a similar method to the separating gel layer. A small amount of Na_2SO_3 was added to degas the stacking gel mixture, followed by the addition of 4.4 µl TEMED and 8.8 µl of APS (40 %, w/v) to start the polymerisation reaction. This solution was gently poured between the two glass plates or pre-cast cassette on top of the separating gel layer and a comb was inserted for the formation of the wells and left to stand for 30 min to set.

Separating gel buffer

54.45 g	Tris/HCl
1.2 g	SDS
300 ml	Milli-Q water

Adjust to pH 8.9 with HCl

Stacking gel buffer

18.14 g	Tris/HCl
1.2 g	SDS
300 ml	Milli-Q water

Adjust to pH 6.8 with HCl

Electrode buffer

14.4 g	Glycine
3.0 g	Tris
1 g	SDS

Make up to 1 L with distilled H_2O and adjust to pH 8.5 with HCl

2.13.2.1 Preparation of protein samples and electrophoresis conditions

For preparation of protein samples, generally 1 – 20 µl of protein sample containing between 5 – 25 µg of protein was used. 2 volumes of protein sample was mixed with 1 volume of 3x SDS-denaturing buffer in a 1.5 ml microfuge and incubated on a heating block at 95 °C for 15 min. Denatured protein solution was cooled on ice before loading into wells.

Denaturing buffer (3x)

8.0 g	SDS
37.2 mg	EDTA
40.0 ml	Glycerol
20.0 ml	β-mercaptoethanol
10.0 mg	Bromothymol blue

Make up to 100 ml with Tris/HCl (100 mM, pH 6.8)

Standard running conditions were 15 mA through the stacking gel layer and 25 mA through the separating gel layer until samples had reached the end of the gel.

2.13.2.2 Protein Marker Broad Range

Protein Marker Broad Range (2 – 212 kDa) (New England Biolabs, England) was used as the molecular weight standard for protein size determination on SDS-PAGE (2.13.2).

Table 9. Protein Marker

Protein Marker	Weight (kDa)
Protein Marker Broad Range (NEB, England)	212, 158, 116, 97.2, 66.4, 55.6, 42.7, 34.6, 27.0, 20.0, 14.3, 6.5
Mark 12 (Invitrogen, USA)	200, 116.3, 97.4, 66.3, 55.4, 36.5, 31, 21.5, 14.4, 6, 3.5, 2.5

2.13.2.3 Protein staining with Coomassie brilliant blue

The SDS-PAGE gel was carefully removed from its cast and transferred to Coomassie brilliant blue staining solution and stained for a minimum of 20 min with slow shaking.

Coomassie blue staining solution

4 g	Coomassie blue R-250
450 ml	Ethanol
90 ml	Acetic acid
460 ml	Distilled H_2O

After Staining, the gel was washed thoroughly with distilled H_2O and then destained using destaining solution until protein bands were visible and background colour removed.

Destaining solution

660 ml	Ethanol
200 ml	Acetic acid
1140 ml	Distilled H_2O

2.13.3 Maldi-TOF mass spectrometry (Maldi-TOF/MS)

Protein bands of interest on SDS-PAGE were cut out and subjected to peptide fingerprinting using Maldi tandem Time-of-Flight mass spectrometry. All sample preparation and Maldi-TOF/MS was performed by The Centre for Protein Research (Otago University). A general procedure for identification of proteins using Maldi-TOF/MS is described below. Excised protein bands were subjected to in-gel digestion with trypsin, according to the method of Shevchenko *et al*. (Proc Natl Acad Sci U S A 93, 14440-14445, 1996). Eluted peptides were dried using a centrifugal concentrator. Peptides were re-suspended in 30 % (v/v) ACN (acetonitrile) and 0.1% (v/v) TFA (trifluoroacetic acid) in water. 1 µl of peptide solution was premixed with 2 µl of matrix (10 mg per ml alpha cyano-4-hydroxycinnamic acid (CHCA) dissolved in 65 % (v/v) aqueous acetonitrile containing 0.1 % (v/v) TFA and 10 mM ammonium dihydrogen phosphate). 0.8 µl of sample/matrix mixture were spotted onto a Maldi sample plate (Opti-TOF 384 well plate, Applied Biosystems, MA) and air dried. Samples were

analysed on a 4800 Maldi tandem Time-of-Flight Analyzer (Maldi-TOF/TOF, Applied Biosystems, MA). All MS spectra were acquired in positive-ion mode with 800-1000 laser pulses per sample spot. The 15 - 20 strongest precursor ions of each sample spot were selected for MS/MS collision-induced dissociation (CID) analysis. CID spectra were acquired with 2000-4000 laser pulses per selected precursor using the 2 kV mode and air as the collision gas at a pressure of 1*E-6 torr. For protein identification MS/MS data was searched against the UniProt/SWISS-PROT amino acid sequence database (downloaded in January 2006) using the Mascot search engine (http://www.matrixscience.com). The search was set up for full tryptic peptides with a maximum of 4 missed cleavage sites. Carboxyamidomethyl Cysteine, oxidized methionine, pyroglutamate (E,Q) were included as variable modifications. The precursor mass tolerance threshold was 75 ppm and the max fragment mass error 0.4Da.

2.13.4 Determination of fusion protein activity on PHA beads

2.13.4.1 Enzyme-linked immunosorbent assay (ELISA)

Enzyme-linked immunosorbent assay (ELISA) was used to confirm the activity of the PhaC N-terminal IgG binding domain fusion (ZZ domain of protein A and GB1 domain of protein G). All PHA bead samples were first normalised by diluting PHA beads to a concentration of 100 µg/ml with 1x PBS buffer (pH 7.5) in a 1.5 ml microfuge tube. 100 µl of normalised sample was added to the first column of a high-binding capacity flat bottom microtitre plate (Greiner Bio-one) and then 2x serially titrated across the rows using 1x PBS buffer (pH 7.5). The microtitre plate was incubated at 4 °C overnight to allow PHA bead to adsorb to the surface of the wells. Wells were then washed 3 – 4 times with ELISA buffer (1x PBS and 0.05 % Tween20). To prevent non-specific binding of antibodies to the wells' surface, 150 µl of 3 % (w/v) BSA solution was added to each well and plates left to incubate for 1 hour at room temperature in a dark humidified container. Wells were washed 3 – 4 times using ELISA buffer to remove unbound BSA. 90 µl of 1:5000 dilution of Antimouse-HRP antibody was added to each well and plates incubated for 30 – 40 mins at room temperature in a dark humidified container. OPD (O- pheylenediamine.2HCl reagent (Abbott Laboratories, USA) was prepared according to manufacturer'sinstructions, 100 µl was added to the wells and the plates incubated at room temperature in a dark humidified container for 15 min for colour development. Colour development was stopped by the addition of 50 µl of 1N

H_2SO_4 to the wells and read on an ELx808iu ultra microplate reader (BIO-TEK Instruments Inc., USA).

1x PBS buffer

137 mM	NaCl
2.7 mM	KCl
10.0 mM	Na_2HPO_4
1.76 mM	KH_2PO_4

Adjust pH to 7.5 using HCl

2.13.4.2 IgG Binding assay

The IgG binding assay was used to assess the maximum binding capacity of recombinant PHA beads displaying protein A and protein G IgG binding domains (ZZ and GB1 respectively) on their surface. 50 mg wet weight of PHA beads was weighed out per sample along with appropriate controls (IgG Sepharose 6 fast flow, GE and/or IPA300, Repligen) in a 1.5 ml microfuge tube. GE beads were washed twice with chilled1x PBS buffer (pH 7.5) to remove storage ethanol, discarding supernatant and re-weighing after the 2nd wash. All samples including controls were re-suspended with 500 µl chilled 1x PBS buffer. 3 mg total protein of purified IgG from human serum (Sigma-Aldrich, USA) was added to each sample and tubes were incubated at 25 °C for 30 mins with agitation. After centrifugation at 6000 x g for 4 mins (Heraeus Pico 17, Thermo Scientific), aliquots of supernatant were taken for analysis and the remaining supernatant discarded. The sediment was then washed 3 times to remove unbound IgG by re-suspending in 1 ml of 1x PBS buffer (pH 7.5), centrifuging at 6000 x g for 4 mins and discarding the supernatant. Bound IgG from PHA beads and controls was eluted using low pH elution by re-suspending sediment in 1 ml of 50 mM Glycine (pH 2.7) and incubating at 25 °C. After incubation for 5 mins at room temperature, followed by centrifugation at 16,200 x g for 5 mins, the supernatant containing eluted IgG was transferred to a new tube. The supernatant was immediately adjusted to ~pH 7.0 using 1M K_2HPO_4 and stored at -20 °C for further analysis.

2.13.5 Cleavage of fusion protein

Fusions proteins containing the seven-amino-acid TEV sequence EXXYXQ(G/S) were cleaved by proteolytic digestion using ProTEV Protease (Promega, USA) and was used according to manufacturer's instructions. ProTEV protease reactions were carried out either in a 1.5 ml microfuge tube or affinity resin with immobilised fusion protein. A typical 100 µl ProTEV protease reaction contained the following:

ProTEV protease reaction mixture

5 µl	20X ProTEV buffer (20x)
1 µl	100 mM DTT
20 µg	Fusion protein
1 µl	ProTEV protease (10 U)
Make up to 100 µl	Sterile Milli-Q water

For the microfuge tube based cleavage reaction method, a 100 µl reaction was set up in a sterile 1.5 ml microfuge tube and incubated overnight at 4 °C in a floating water bath. Removal of the affinity tag from cleaved fusion protein was achieved by incubating with His-Affinity Gel (2.13.6.1) for 20 min on ice with regular mixing. The cleaved fusion product was recovered as a flow-through by centrifugation at 16,200 x g for 2 mins (Heraeus Pico 17, Thermo Scientific). For the affinity resin-based cleavage reaction method, fusions proteins were purified from crude cell lysate by His-affinity purification (2.13.6.1) using His-Spin Protein Miniprep (Zymo Research, USA) up to the elution step. The His-affinity Gel with immobilised fusion protein was then directly subjected to proteolytic digestion in a 100 µl reaction was set up as described.

2.13.6 Protein affinity purification

Polyhistidine tagged recombinant proteins from crude cell lysates were recovered by one of the Ni^{2+} -NTA based His-affinity purification methods described below. Crude cell lysates generated from cell disruption (2.12.1) were centrifuged at 8000 x g for 10 mins (Heraeus multifuge1 S-R, Sorvall) to removed unlysed cells and large insoluble cell debris, while smaller insoluble material was removed by ultracentrifugation at 100,000 x g for 2 hr using a Optima TLX ultracentrifuge (Beckman Coulter, USA) and/or filtration through a 0.22 µm filter before affinity purification with one of the methods described below:

2.13.6.1 His-Spin protein Miniprep

For quick and fast purification on a small scale, His-Spin protein Miniprep (Zymo Research, USA) was used for the purification of polyhistidine-tagged proteins. Up to 1 mg can be purified and eluted in a small volume with this kit. When possible, all purification steps were performed in the cold (4°C). In a typical protocol, 300 - 600 µl of crude cell lysate containing His-tagged recombinant protein was mixed and incubated with 250 - 300 µl drained His-Affinity Gel in a Zymo-Spin P1 column inserted into a collection tube. His-Affinity Gel was re-suspended every min during the 5 min incubation to maximise binding of His-tagged proteins to the Nickel-charged agarose. The mixture was then centrifuged at 16,200 x g for 10 sec (Heraeus Pico 17, Thermo Scientific) and the flow-through discarded. To fully utilise the binding capacity of the His-Affinity Gel, the sample loading and binding steps above were repeated 5-10 times. His-Affinity Gel was re-suspended and washed twice using 250 µl of His-Wash Buffer. Drained His-Affinity Gel was then re-suspended in 90 – 150 µl of His-Elution Buffer, incubated for 5 mins and recovered by centrifugation at 16,200 x g for 2 min to maximise recovery.

2.13.6.2 His-Trap HP (5 ml)

For larger scale purification of polyhistidine-tagged recombinant proteins, His-Trap HP (5 ml) affinity columns (Amersham Biosciences) packed with precharged Ni-Sepharose were used. These columns have a maximum binding capacity of 40 mg. To operate HP columns either a peristaltic pump or liquid chromatography system (ÄKTA*explorer* 10S) was used.

2.13.7 Analytical gel filtration chromatography

Affinity purified polyhistidine-tagged recombinant proteins were further purified and analysed by size exclusion gel filtration chromatography. A Superdex 200 10/300 GL (GE life sciences, USA) high performance gel filtration column was typically used and operated on an ÄKTA*explorer* 10S (Amersham Biosciences) liquid chromatography system.

2.13.8 Hanging drop/Sitting drop method

The most commonly used techniques to obtain protein crystals by vapour diffusion are the hanging drop and sitting drop methods (Figure 11). Below describes a general 96 well microtitre plate setup for the screening of 96 different crystallisation conditions by HAMPTON Crystal screen I and II, and/or Molecular Dimensions PACT premier. For the initial setup, 100 µl of room temperature crystallisation solution was aliquoted to each of the microtitre plate wells. A high protein solution concentration of >5 mg/ml is commonly required. A Mosquito® (TTP Lab Tech, UK) was used to setup crystallisation plates, by aliquoting and mixing a few nanolitres (400 nl) of protein solution with the reservoir solution containing the crystallization cocktail in a 1:1 ratio onto a ViewdropII 96-well plate seal for the hanging drop method (TTP Lab Tech, UK) or Intelli-plate 96-2 (ART Robbins Instruments, USA) for a sitting drop method. The viewdropII-well plate seal was then used to seal the reservoirs with its corresponding protein/cocktail mixture for the hanging drop method and a clean viewdropII-well plate seal was used to seal the reservoirs for the sitting drop method. Plates are incubated at 21 °C or 4 °C until protein crystals of ≥ 20 micron appear (Figure 12).
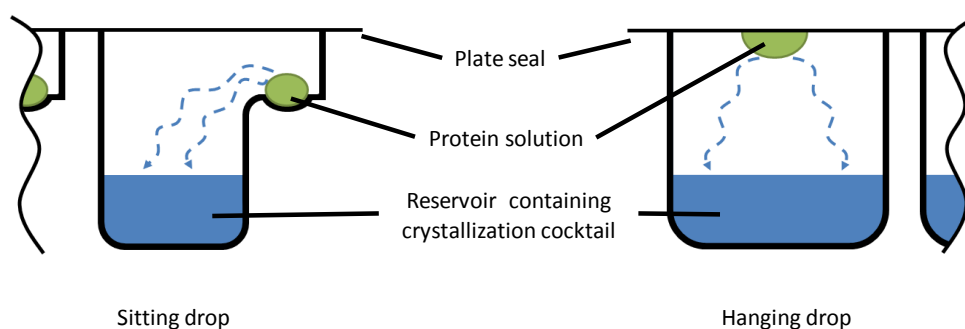
Figure 11. Vapour diffusion. Diagrammatic illustration of both the sitting drop (left) and hanging drop (right).

Chapter 3: Results

3.1 Molecular characterisation of PHA synthase (PhaC)

For the molecular characterisation of class I PHA synthase from *C. necator* (PhaC) in recombinant *E. coli*, the following plasmids were made in this study, pET14b-His$_9$ZZTEVΔ1-93C, pET16b-His$_{10}$ZZC, and pET14b-His$_{10}$GB1TEVΔ1-93C. Molecular cloning of these plasmids are described below, employing the pET expression system. The pET expression system allows for high overexpression of recombinant genes, resulting in the overproduction of protein. These plasmids are designed to produce fusion proteins which have an N-terminal polyhistidine-tag fused to the N-terminus of an IgG binding ZZ domain of protein A from *Staphylococcus aureus* (source commercial vector pEZZ18) or GB1 (NCBI accession CAA27638) domain of protein G from *Streptococcus sp.* which in turn is fused to the N-terminus of a full length or truncated forms of the codon optimised class I PHA synthase from *C. necator*. The polyhistidine-tag allows for affinity purification of the fusion protein using immobilised Ni^{2+}-NTA agarose columns, while the IgG binding domain was used as a tag to enhance solubility of recombinant protein in *E. coli*. The 93 amino acid N-terminal deletion truncated form (Δ1-93C) of the class I PHA synthase was used to primarily help with protein solubility as the probability of obtaining soluble protein has been shown to decrease with larger proteins (Graslund *et al.*, 2008). In addition to increasing solubility of the synthase, the truncated form was also expected to allow easier determination of structure by x-ray diffraction, due to its reduced size.

3.1.1 Construction of pET16b-His$_{10}$ZZC and pET16b-His$_{10}$C

Plasmid pET16b-His$_{10}$ZZC was constructed to encode a 10xHis-tag and IgG binding ZZ domain of protein A N-terminally fused to the full length PhaC from *C. necator*. Plasmid pET16b-His$_{10}$C is an intermediate plasmid in the construction of pET16b-His$_{10}$ZZC and is used as a negative control for the IgG binding ZZ domain in IgG purification experiments.

Construction of pET16b-His$_{10}$ZZC is a multi step process (Figure 12 and 13 for the cloning of pET16b-His$_{10}$C and pET16b-His$_{10}$ZZC respectively). Firstly, the gene

fragment encoding the ZZ domain of protein A and entire *phaC* were isolated from pET14b-ZZ(-)phaC (Table 3) by RE analysis (2.11.4) using restriction enzymes *Nde*I and *Bam*HI. The fragments were then separated using AGE with SYBR safe stain (2.11.5). Complete digestion of pET14b-ZZ(-)phaC produced 3 fragments 4581bp (Vector backbone), 1774bp (*pha*C), and 399bp (ZZ domain). The 1774 bp and 399 bp fragments were isolated and purified using gel purification (2.11.6). Simultaneously, pET16b vector containing the 10xHis-affinity tag and amp^r selectable marker was subjected to RE analysis (2.11.4) using *Nde*I and *Bam*HI, followed by isolation (2.11.5) and purification (2.11.6) of the larger sized vector back bone fragment (5699 bp).

The second step in constructing pET16b-His$_{10}$ZZC involved cloning *phaC* fragment into the *Nde*I and *Bam*HI sites of the linearized pET16b vector mediated by T4 DNA ligase (2.11.9) (Figure 12). After ligation, the product was transformed into *E. coli* (2.10.1) XL1-blue and plated onto LB medium containing 75 µg/ml ampicillin. Single white colonies were selected for plasmid isolation (2.11.1) and RE analysis (2.11.4) using *Bgl*II and *Pvu*I. Three fragments of expected size 4589bp, 2134bp, and 750bp were seen after complete digestion using AGE.

The third step in constructing pET16-His$_{10}$ZZC (Figure 13) involved cloning the DNA encoding fragment IgG binding ZZ domain from protein A into the newly constructed pET16b-His$_{10}$C. Firstly, pET16b-His$_{10}$C was linearised by RE analysis (2.11.4) between the 10xHis tag and and *phaC* using *Nde*I. Following RE analysis, the product was isolated (2.11.5) and purified from agarose gel (2.11.6). The purified linear vector was treated with Antarctic phosphatase (2.11.7) to prevent re-ligation of the vector. The ZZ domain fragment and de-phosphoryted linear pET16b-His$_{10}$C fragments was ligated together using T4 DNA ligase (2.11.9). The ligation product was then transformed into XL1-blue (2.10.1) and plated onto LB medium containing 75 µg/ml ampicillin. Single white colonies were selected for plasmid isolation (2.11.1) and confirmation of plasmid by RE analysis (2.11.4) using *Eco*RI and *Nco*I. Correctly oriented ZZ domain produces fragments of 5317bp, 1838bp, 442bp, and 275bp, while an incorrectly oriented fragment produces fragments of 5317bp, 1838bp, 636bp and 81bp. Plasmids which showed correct "co" restriction patterns were further confirmed by DNA sequencing analysis (2.11.10).
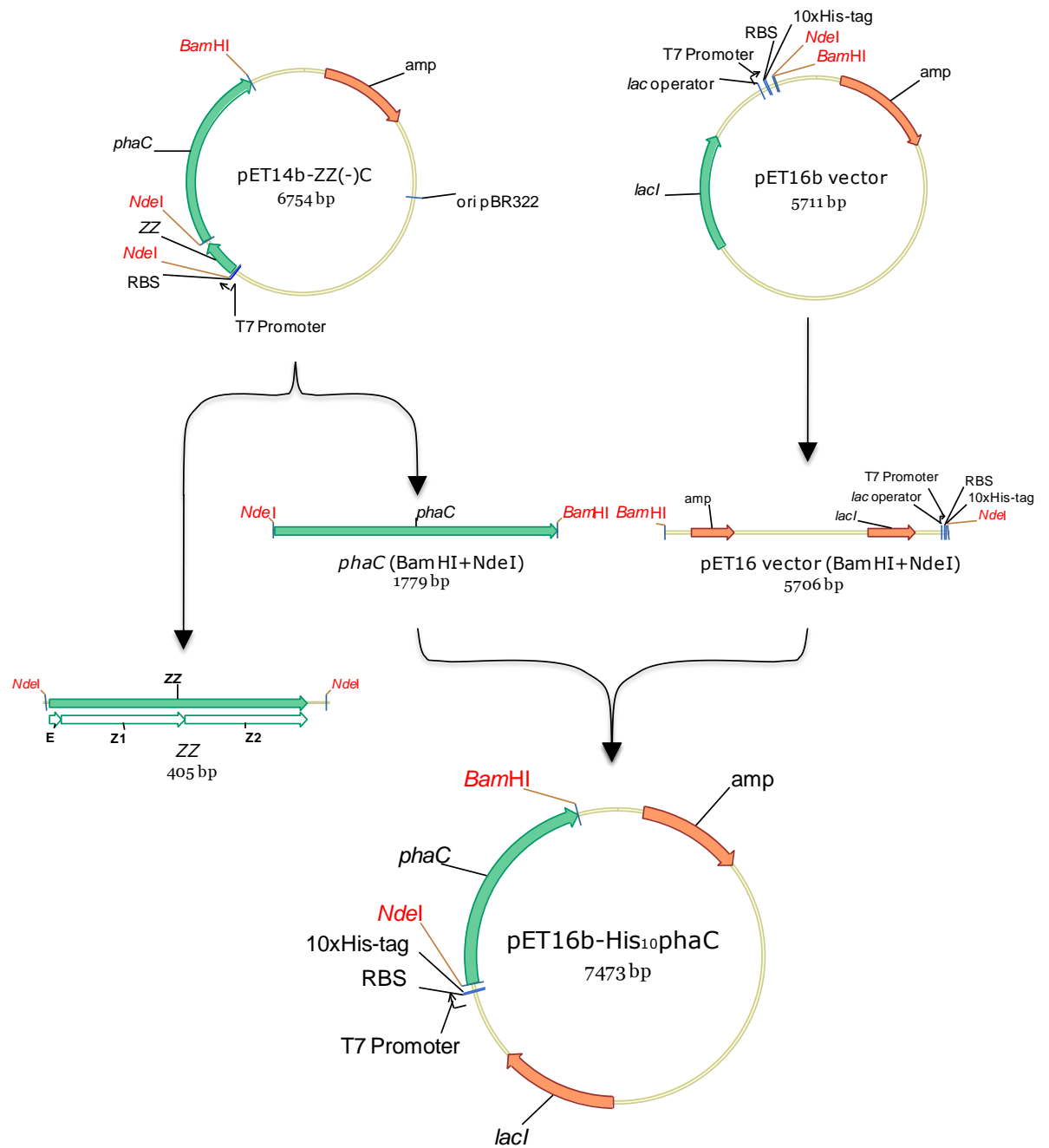
Figure 12. Construction of intermediate cloning plasmid pET16b-His$_{10}$*phaC* for the generation of pET16b-His$_{10}$ZZC. The DNA fragment encoding ZZ domain from protein A and *phaC* were isolated from pET14b-ZZ(-)C by restriction digest using *Nde*I and *Bam*HI followed by separation of DNA fragments by agarose gel electrophoresis and gel extraction. The *phaC* gene was ligated into linearized pET16b vector digested with *Nde*I and *Bam*HI using T4 DNA ligase. The resulting plasmid was designated pET16b-His$_{10}$*phaC*.
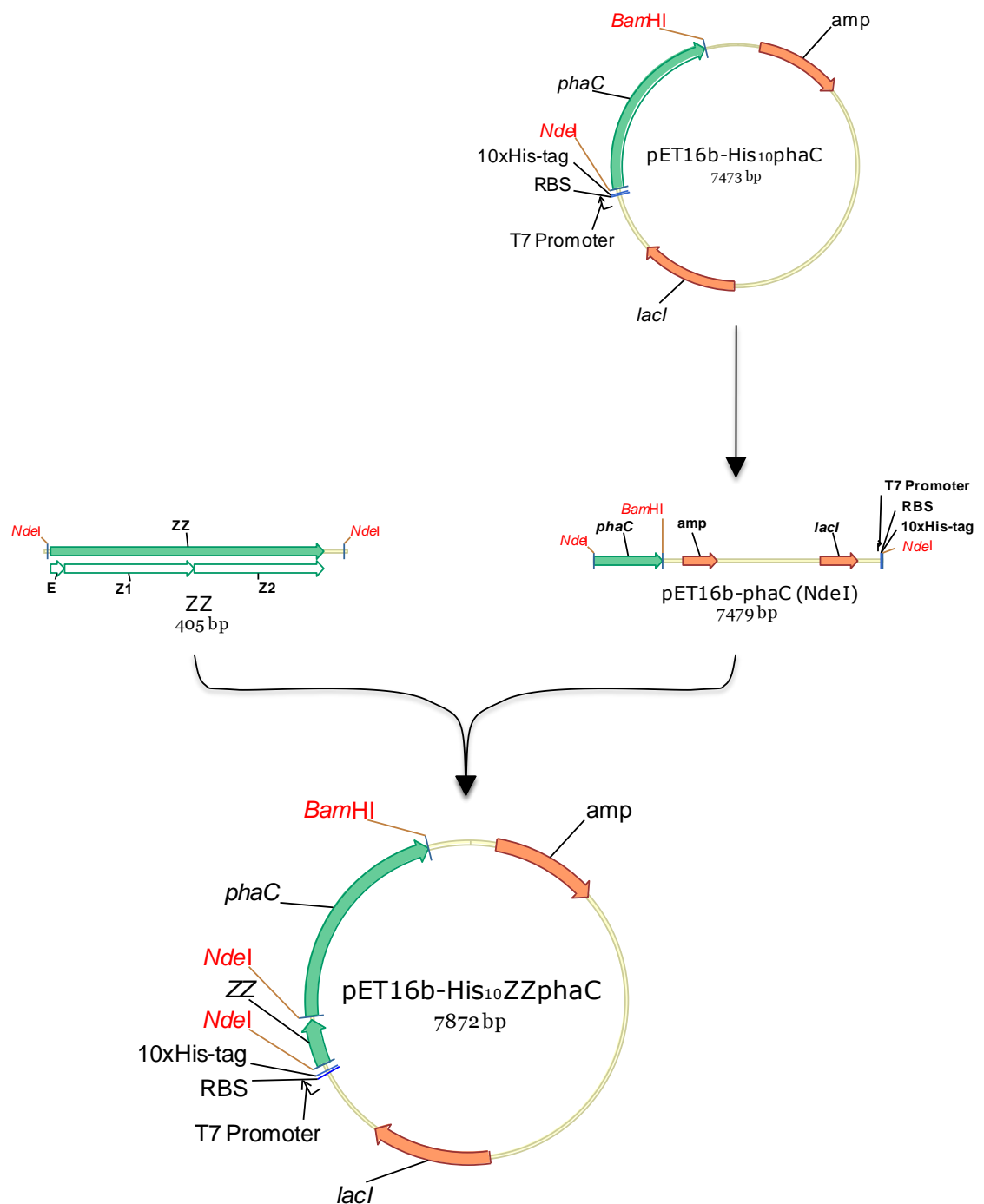
Figure 13. Construction of pET16b-His$_{10}$ZZC. The DNA fragment encoding the ZZ domain from protein A isolated from pET14b-ZZ(-)C by restriction digest using *Nde*I and *Bam*HI as described in Figure 12 was ligated into the linearized pET16b-His$_{10}$*phaC* digested with *Nde*I using T4 DNA ligase. The linearized pET16b-His$_{10}$*phaC* was treated with Antarctic phosphatase to prevent re-ligation and the orientation of the ZZ domain was assessed by restriction analysis using *Eco*RI and *Nco*I.

3.1.2 Construction of pET14b-His$_{10}$GB1TEVΔ1-93C

Construction of 10xHis-tagged IgG binding GB1 domain N-terminally fused to the truncated form of PhaC (pET14b-His$_{10}$GB1TEVΔ1-93C) was done by one step cloning (Figure 14). The His$_{10}$GB1TEV fragment was first excised from pJ201_GB1 by restriction analysis (2.11.4) using *Age*I and *Xba*I. PJ201_GB1 was designed by Jane Atwood and was synthesised by GeneScript with codon optimisation for expression in *E. coli*. Following restriction analysis, the fragment with the correct size (242 bp) was isolated (2.11.5) and purified from agarose gel (2.11.6). To obtain the vector for subcloning of the His$_{10}$GB1TEV fragment, plasmid pET14b-His$_{10}$ZZTEVΔ1-93C (refer to section 3.2.2 for construction) was hydrolysed using restriction enzymes (2.11.4) *Age*I and *Xba*I, giving two fragments of 446 bp and 6059 bp when completely hydrolysed. The larger fragment containing the selectable marker (amp^{r}) and *pha*C was isolated (2.11.5) and purified from agarose gel (2.11.6). Ligation of purified fragment and vector was mediated by using T4 DNA ligase (2.11.9) and subsequently transformed into *E. coli* (2.10.1) XL1-blue and plated on to LB agar plates containing 75 µg/ml ampicillin. Colonies which grew on LB Amp agar plates were selected for plasmid isolation (2.11.1), followed by restriction analysis (2.11.4) using restriction enzymes *Pvu*I and *Xba*I. Transformants which gave the correct restriction pattern on agarose gel electrophoresis were further confirmed by DNA sequencing analysis (2.11.10). Once the plasmid has been confirmed by RE analysis and sequencing, frozen stocks of transformants were made for long term storage (2.8).
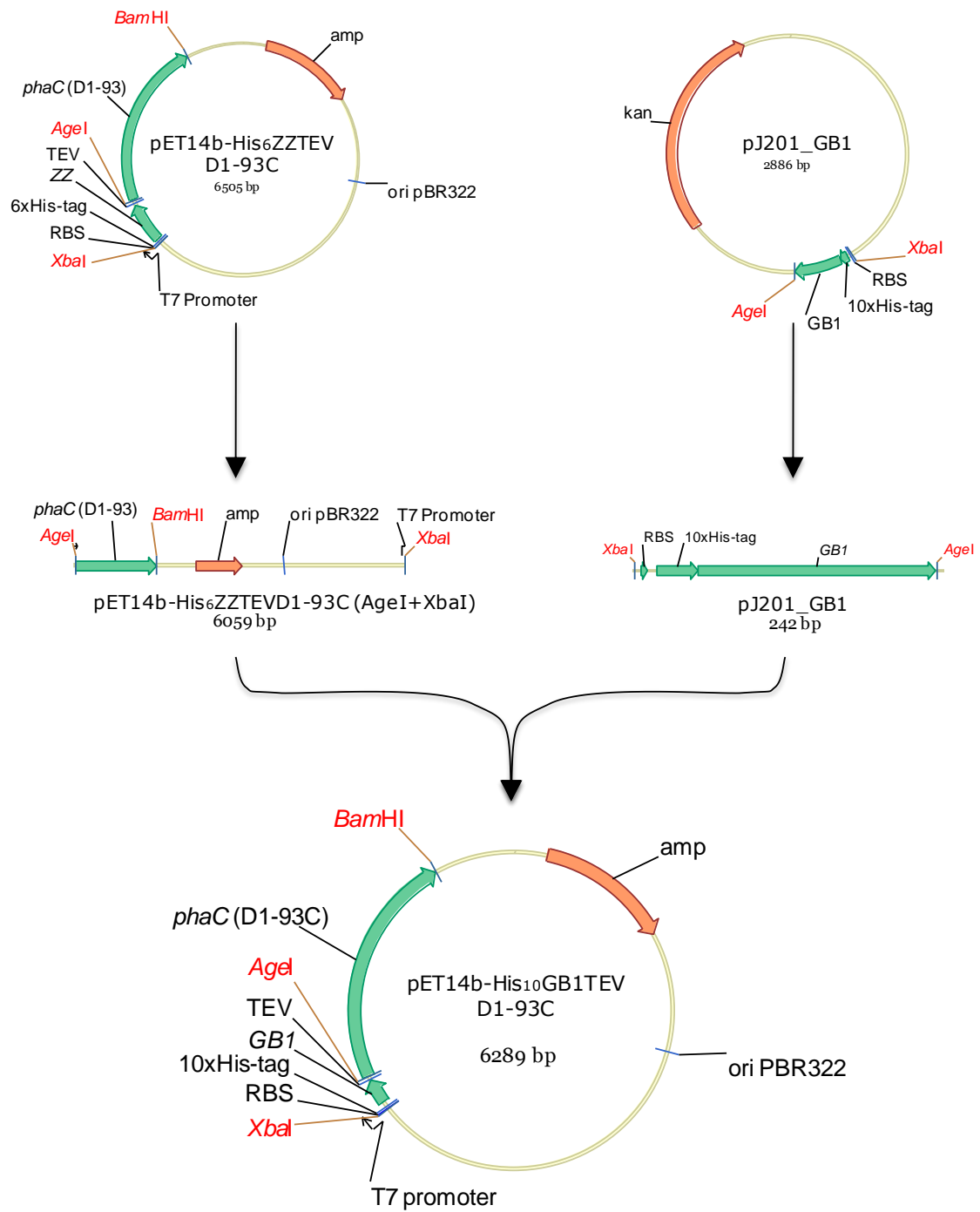
Figure 14. Construction of pET14b-His₁₀GB1TEVΔ1-93C. The *E.coli* codon optimised GB1 fragment with a N-terminal 10xHis-tag was excised from plasmid PJ201_GB1 by restriction analysis using *Age*I and *Xba*I followed by fragment separation on agarose gel electrophoresis and gel purification. The 242bp 10xHis-tag fragment was ligated into linearized pET14b-His₆ZZTEVΔC digested with *Age*I and *Xba*I using T4 DNA ligase.

3.1.3 Construction of pET14b-His$_9$ZZTEVΔ1-93C

Plasmid pET14b-His$_6$ZZTEVΔ1-93C (Table 3) encoding the IgG binding ZZ domain was used as the template for PCR (2.11.2) (Figure 15). The DNA region encoding the ZZ domain and TEV site was amplified using primers 10xHis (forward) and revTEV_*Age*I (reverse) designed by Jane Mullaney (Table 5). The primers were designed to introduce additional histidines to the polyHis-tag and restriction sites *Xba*I and *Age*I corresponding to the N- and C-terminal regions respectively to allow easy subcloning. A small aliquot of the PCR product was then subjected to AGE (2.11.5) for confirmation of size and quality of the PCR product. Following confirmation, the remaining PCR product was purified using AGE (2.11.5) and SYBR safe DNA stain and isolated (2.11.6) from gel. The purified blunt end PCR product was then "A-tailed" using Taq DNA polymerase (2.11.8). The resulting A-tailed PCR was then ligated into the pGEM –T Easy vector (2.11.8). pGEM –T Easy is a high copy number intermediate cloning vector, with a selectable amp^r marker and *lacZα* for blue-white selection (2.7.1). After ligation, the product was transformed into *E. coli* (2.11.1) XL1-blue and plated onto X-Gal medium (2.4.1) agar containing 75 µg/ml ampicillin. Single white colonies were selected for subsequent plasmid isolation (2.11.1) and RE analysis (2.11.4). DNA sequencing analysis (2.11.10) was performed on plasmids which showed the correct restriction patterns with RE analysis.

After confirmation of the PCR product by DNA sequencing, the 467 bp fragment His$_9$ZZTEV (Figure 16) was excised by RE analysis (2.11.4) using *Xba*I and *Age*I. The His$_9$ZZTEV fragment was separated from other fragments using AGE (2.11.5), followed by isolation and purification (2.11.6). The purified His$_{10}$ZZTEV fragment was then cloned into vector pET14b-His$_6$ZZTEVΔ1-93C mediated by T4 DNA ligase (2.11.9). Vector pET14b-His$_6$ZZTEVΔ1-93C was prepared by RE analysis (2.11.4) using *Xba*I and *Age*I. After ligation, the product was transformed into *E. coli* XL1-blue (2.10.1) and plated on LB Amp medium. Single colonies were selected for plasmid isolation (2.11.1) and RE analysis (2.11.4) to confirm successful ligation and transformation of the plasmid.
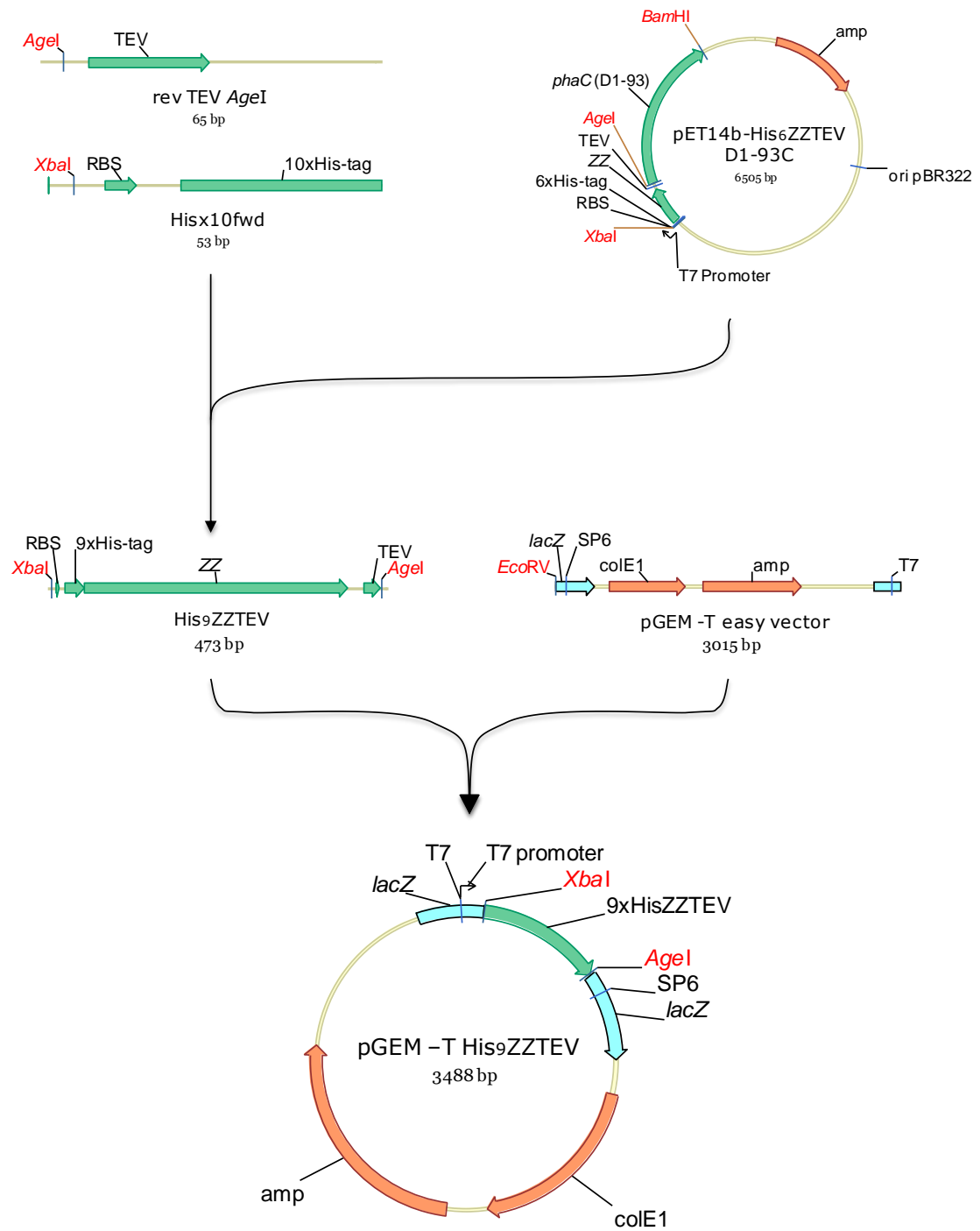
Figure 15. Construction of intermediate cloning plasmid pGEM-T His₉ZZTEV for generation of pET14b-His₉ZZTEVΔ1-93C. The PCR fragment 9xHisZZTEV with flanking *Xba*I and *Age*I restriction sites was generated using primers revTEV_*AgeI* (reverse) and 10xHisxfwd (forward) using plasmid pET14b-His₆TEVΔ1-93C as a template. The resulting 473bp blunt ended PCR product was A-tailed and ligated into intermediate cloning vector pGEM-T easy vector.
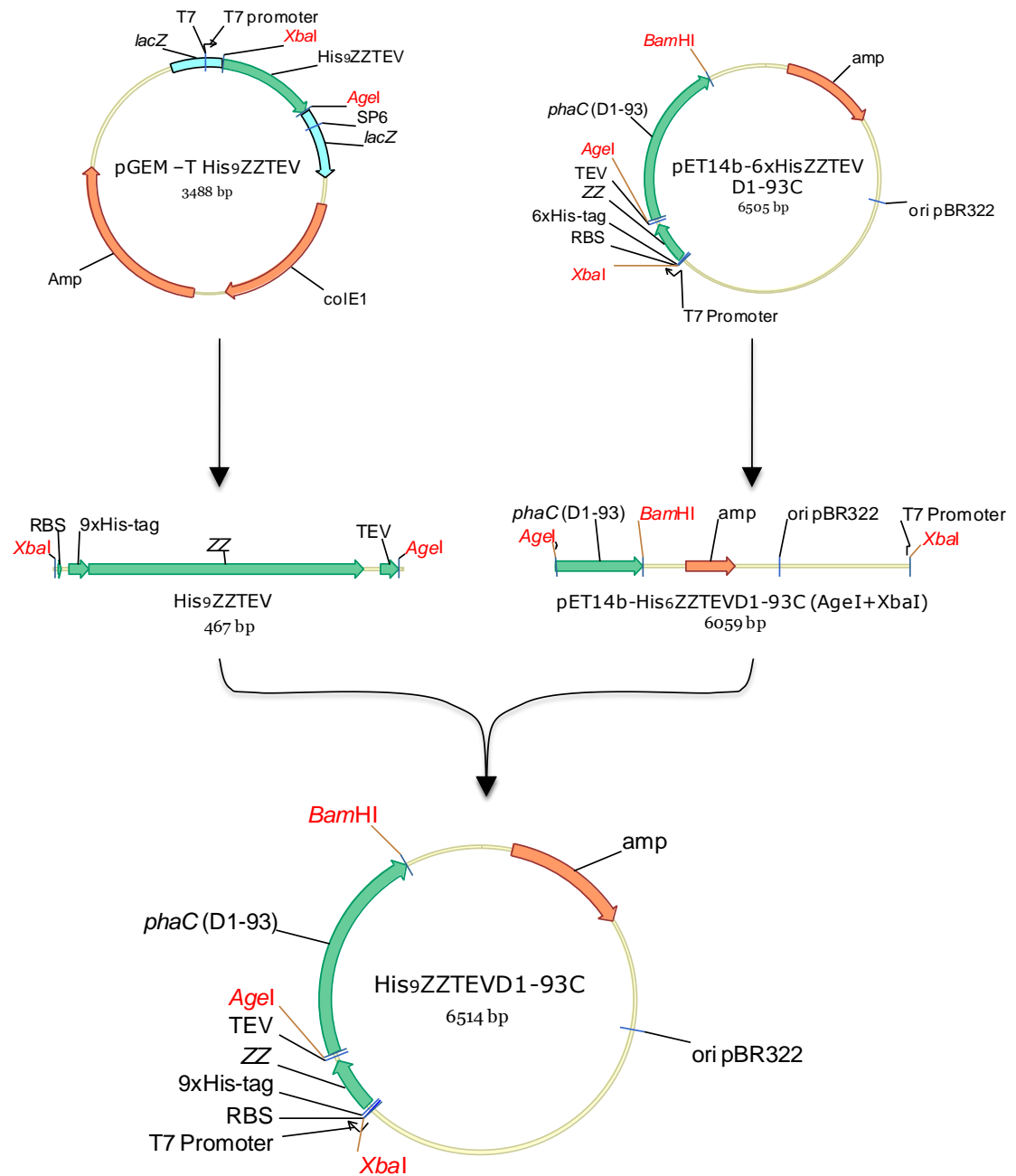
Figure 16. Construction of pET14b-His₉ZZTEVΔ1-93C. Intermediate cloning plasmid pGEM-T His₉ZZTEV was digested with *Xba*I and *Age*I. The resulting 467bp (His₉ZZTEV) fragment was ligated into linearized pET14b-His₆ZZTEVΔ1-93C digested with *Xba*I and *Age*I using T4 DNA ligase.

3.1.4 Plasmid expression and protein production

The overproduction of recombinant protein was achieved using the pET expression system utilising the T7 polymerase for gene expression. Plasmids pET14b-C (WT), pET14b-ZZ(-)C and pET16b-His$_{10}$C were transformed into *E.coli* BL21(DE3) pLysS (2.10.1) to assess whether the ZZ domain or His-tag gave enhanced protein solubility or protein production in comparison to WT (PhaC) (Figure 17). Assessment of the pre and post induction cultures indicates no fusion protein was produced in the absence of an induction factor (final concentration of 1 mM IPTG) in BL21 (DE3) pLysS. Expression of all 3 plasmids resulted in the overproduction of the fusion protein and in comparison to wildtype (PhaC), significantly more protein is produced when plasmids pET14b-ZZ(-)C and pET16b-His$_{10}$C are expressed. Cells were lysed using the French press as described in section (2.12.1.3). The cell lysate was then subjected to low speed centrifugation at 8000 x *g* for 10 mins to remove large insoluble cellular debris and unlysed cells. The resulting insoluble fraction was washed twice with 50 mM potassium phosphate buffer before being assessed by SDS-PAGE (2.13.2). Results indicate there is a correlation between overproduction of the fusion protein and amount of insoluble protein recovered after low speed centrifugation. To access whether the fusion protein was soluble, the crude cell lysate supernatant fraction after low centrifugation was subjected to ultracentrifugation at 100,000 x *g* for 2 hours, the resulting soluble and insoluble fractions were then assessed by SDS-PAGE (2.13.2). Assessment of the protein fractions after ultracentrifugation by SDS-PAGE (Figure 17), indicated fusion protein ZZ-C, containing the IgG binding ZZ domain gave enhanced solubility of the PHA synthase in comparison to the wildtype (phaC) and the His-tagged synthase (His$_{10}$C) (Figure 17 B, lanes 13-15). Expression of plasmid pET16b-His$_{10}$C produced proteins with poor solubility in comparison to wildtype (PhaC) (Figure 17 B, lanes 16-18). Indicating the polyHis-tag may have a negative effect on protein solubility.

Once the solubility was assessed for the affinity tags, plasmids pET14b-His$_9$ZZTEVΔ1-93C and pET16b-His$_{10}$ZZC containing the His-tag and ZZ solubility tag were transformed into both protein production strains *E. coli* strain BL21 (DE3) and *E. coli* strain BL21 (DE3) pLysS (2.10.1) to assess protein production (Figure 18).
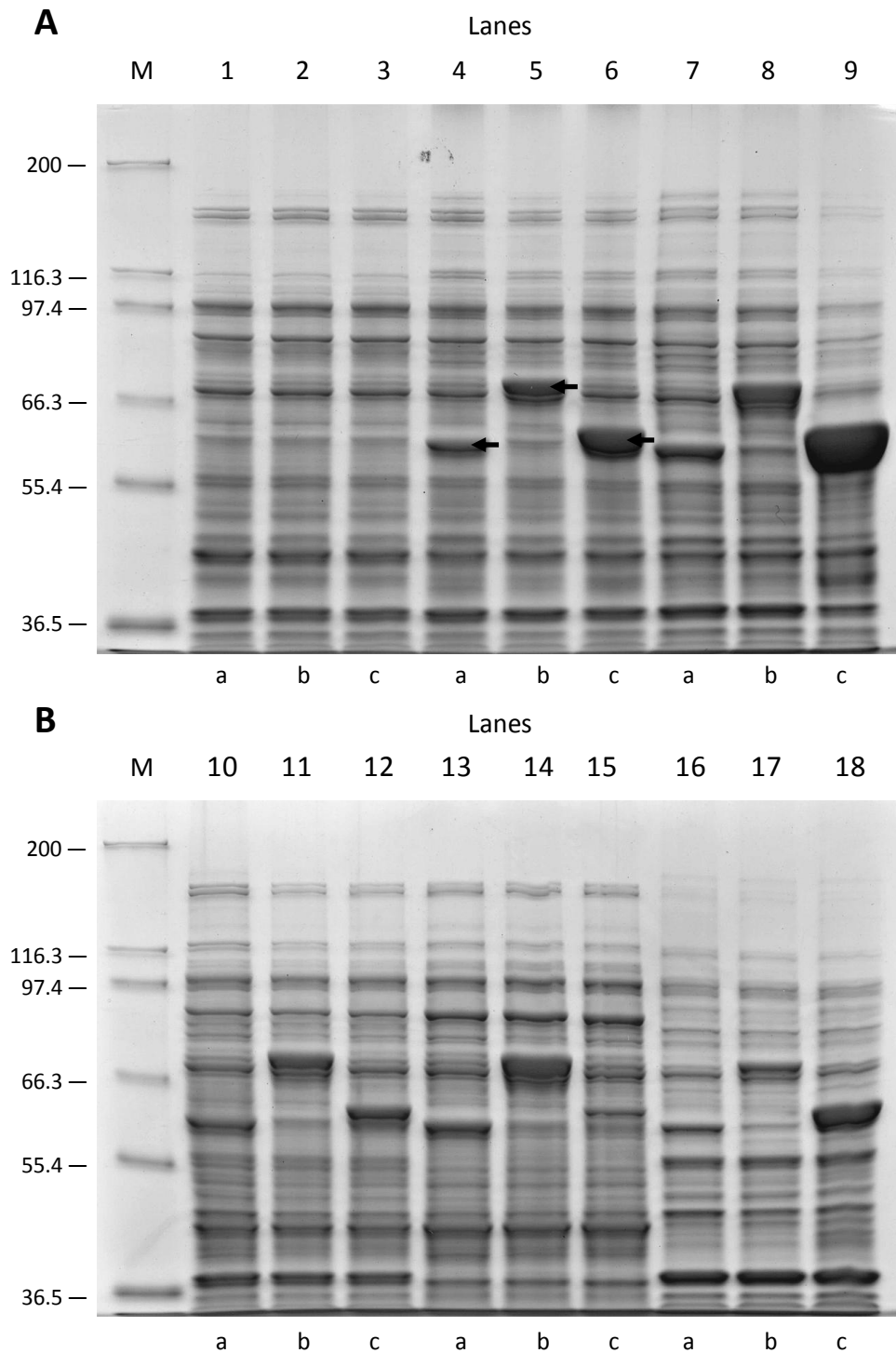
Figure 17. SDS-PAGE gel demonstrating solubility using the ZZ domain of protein A. *E. coli* BL21 (DE3) pLysS strains harbouring plasmid pET-C (WT), pET14b-ZZC and pET16b-His$_{10}$C are arranged in adjacent lanes (labelled a, b and c respectively). **(A)** Lane M; molecular weight standard (Mark 12); Lanes 1-3, pre-cultures post induction; Lanes 4-6, 2 hours post induction with 1 mM IPTG. Cells were lysated using the French press, followed by low centrifugation (Lanes 7-9). The soluble and insoluble fractions of the cell lysate were separated by ultracentrifugation at 100,000 x *g* for 2 hours. **(B)** M; molecular weight standard (Mark 12); Lanes 10-12, cell lysate after low centrifugation spin; Lanes 13-15, cell lysate soluble fraction after ultracentrifugation; and Lanes 16-18, insoluble fraction after ultracentrifugation. Arrows indicate fusion protein.
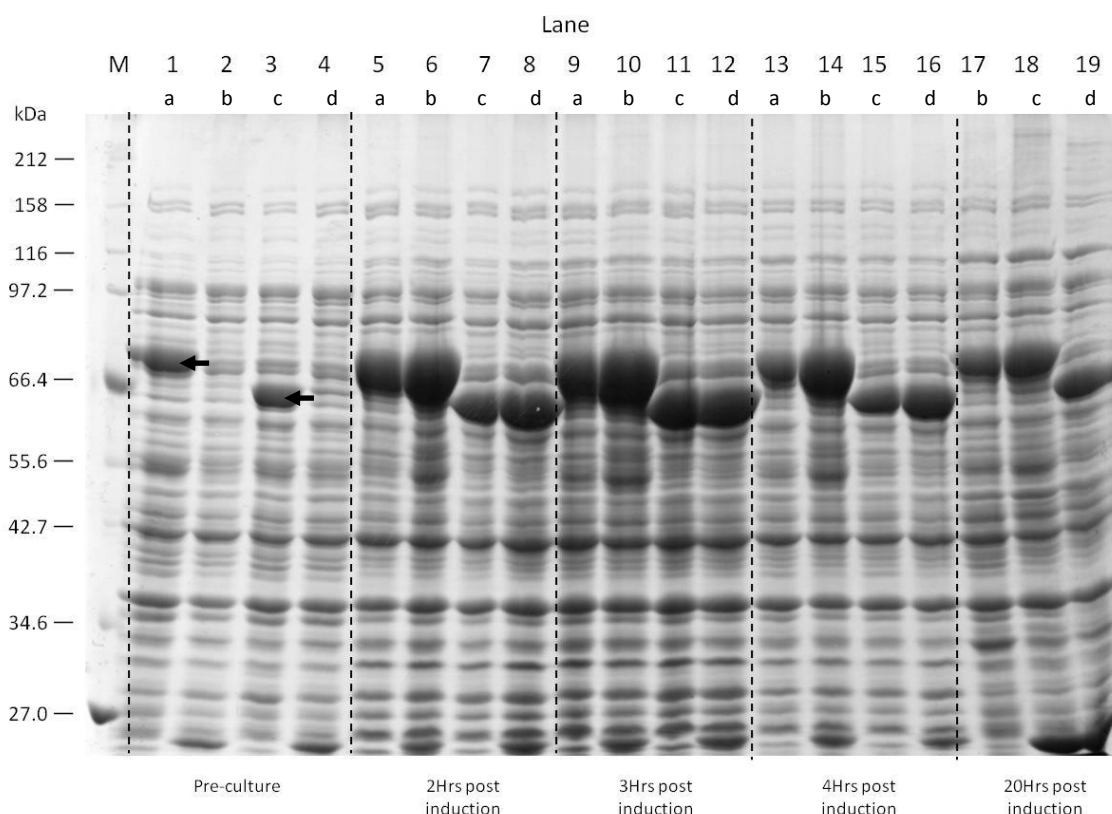
Figure 18. SDS-PAGE gel of recombinant His-tagged PhaC production. *E. coli* BL21 (DE3) strain habouring pET16b-His$_{10}$ZZC and pET14b-His$_9$ZZTEVΔ1-93C represented by a and c respectively. *E. coli* BL21 (DE3) pLysS strain is represented by b and d repectively. Lane 1 Broad Range ladder; lanes 2-5, pre-cultures prior to induction with IPTG; lanes 6-9, 2 hour cultivation post induction with IPTG; lanes 10-13, 3 hour cultivation post induction with IPTG; lanes 14-17, 4 hour cultivation post induction with IPTG; lanes 18-20, 20 hour cultivation post induction with IPTG. All cultivation pre and post induction was done at 37 °C with aeration. Arrows indicate fusion protein.

Figure 18 shows an SDS-PAGE of the whole cell protein prior to lysis. Overproduction of the His-tagged protein was observed for both plasmids when expressed independent of strain upon induction with 1 mM IPTG. In comparison to the non-induced cells (lanes 1-4), the fusion protein was strongly overproduced after induction indicated by the large predominant protein bands at approximately 76 kDa and 66.4 kDa which was relatively consistent with the theoretical molecular weight 81.86 kDa for His$_{10}$ZZC and 71.6 kDa for His$_9$ZZTEVΔ1-93C respectively. This was apparent even only 2 hours after induction (lanes 5-8), with the majority of the protein already being produced. Protein production strain BL21 (DE3) harbouring the pLysS plasmid allowed for tighter regulation of gene expression, thereby, reducing leaky protein production seen in *E. coli* strain BL21 (DE3) pre-cultures in the absence of IPTG (lanes 1 and 3). In addition, BL21 (DE3) pLysS strains independent of plasmid expressed, show greater levels of

protein production in comparison to BL21 (DE3) (b and d) as a result. As incompletely repressed gene expression can impact on recombinant protein production. Similar results were seen for plasmid $His_{10}GB1\Delta1$-93C (Data not shown).

3.1.5 Purification and analysis
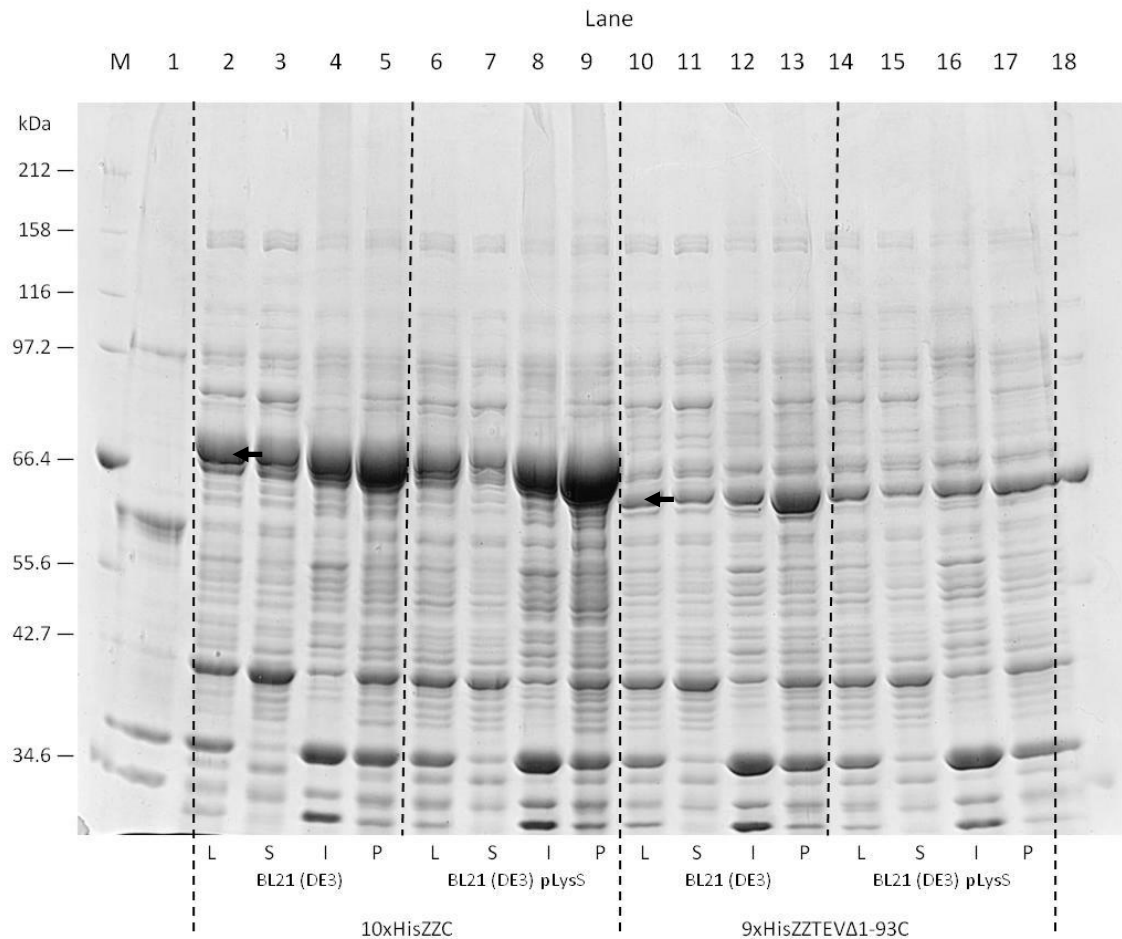
Figure 19. SDS-PAGE gel of recombinant His-tagged PhaC cell lysis. Lane M, Broad Range ladder; Lane 1, *E. coli* BL21 (DE3) with WT PhaC; Lanes 2-5, are the soluble and insoluble fractions from BL21 (DE3) with $His_{10}ZZC$; Lanes 6-9, are the soluble and insoluble fractions from BL21 (DE3) pLysS with $His_{10}ZZC$, Lanes 10-13, are the soluble and insoluble fractions from BL21 (DE3) with $His_{9}ZZTEV\Delta1$-93C, Lanes 14-17, are the soluble and insoluble fractions from BL21 (DE3) pLysS with $His_{9}ZZTEV\Delta1$-93C. All fractions are arranged in order of (L) crude cell lysate, (S) soluble fraction after ultracentrifugation, (I) insoluble sediment from ultracentrifugation, and (P) insoluble sediment from low centrifuge spin. Arrow indicates fusion protein.

For the purification and analysis of recombinant proteins produced in *E. coli* BL21 strains. Strains harbouring their respective plasmids were cultivated for 2 hours post

induction and lysed in 50 mM KPO_4 buffer containing 50 mM KCl and protease inhibitor using the cell disruptor method for the isolation of protein (2.12.1.2). To separate the soluble fraction from the insoluble fraction, crude cell lysate was subjected to ultracentrifugation at 100, 000 x g for 2 hour after the first low speed centrifugation spin. All protein fractions were analysed using SDS-PAGE (2.13.2). SDS-PAGE results indicated high overproduction of our fusion protein as mentioned above (Figure 19). Expression of Plasmid pET16b-His$_{10}$ZZC showed greater production of its fusion protein in comparison to the expression of plasmid pET14b-His$_9$ZZTEVΔ1-93C. A large proportion of the overproduced protein was seen to be insoluble, as indicated by the large predominant protein bands in the low speed centrifugation sediment fractions (lanes 5, 9, 13, and 17) and more importantly the insoluble fractions after ultracentrifugation (lanes 4, 8, 12, and 16). Cultures which were cultivated for > 2 hours post induction showed increasing levels of insolubility of the fusion protein, with little to no soluble fusion protein seen in the soluble fraction after 4 hours post induction cultivation (data not shown). However, a small fraction of the overproduced protein in the 2 hour post induction cultivation remains soluble for both plasmids (lanes 3, 7, 11, and 15). The soluble fractions also show contamination with insoluble proteins of approx 27 kDa; this has previously been identified as an outer membrane protein.

The N-terminally His-tagged proteins were firstly purified on a small scale using Ni^{2+} - NTA based His-affinity purification (2.13.6.1) and its purity assessed by SDS-PAGE analysis (Figure 20). The washing steps successfully separated most of the contaminating protein from the fusion protein (Figure 20, lane 8). The purified His-tagged fusion proteins His$_{10}$ZZC, His$_9$ZZTEVΔ1-93C, and His$_{10}$GB1TEVΔ1-93C was highly purified (to >90 %) with little contaminating host proteins remaining in the his-elution fractions (Figure 20, lane 6). The protein band for His$_{10}$GB1Δ1-93C was still present in the His-spin flow fraction when incubated with the affinity resin (Figure 20, lane7), this suggests the resin had been overloaded. Purified protein from Ni^{2+} NTA column was observed to remain soluble at a concentration of ~6 mg/ml for greater than 2 weeks at 4°C independent of fusion protein and buffer used, indicating protein is reasonably stable (Data not shown).

In addition, various buffer conditions were tested with and without salts (ranging from 5 mM to 200 mM) to optimise solubility and decrease nonspecific binding of contaminating proteins.
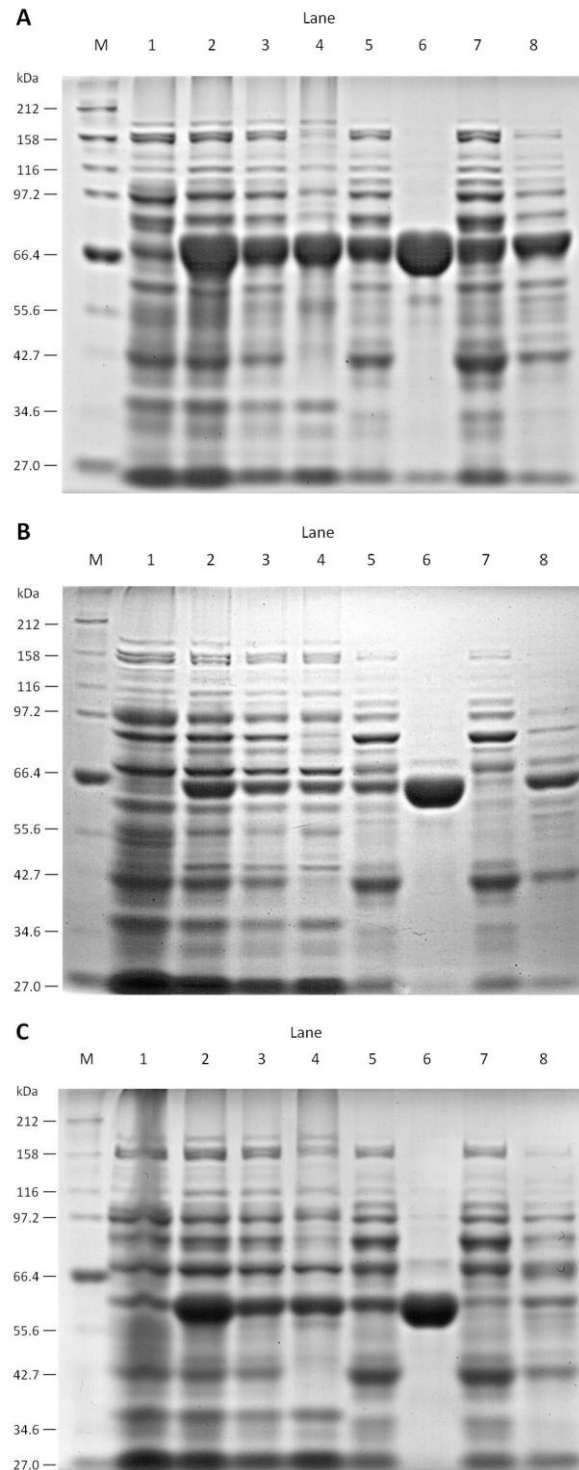
Figure 20. SDS-PAGE gel of affinity purification fractions for His-tagged PhaC proteins. Affinity purification fractions from various expressed plasmids in strain *E. coli* BL21 (DE3) pLysS and purified using Zymo His-spin columns (Ni^{2+} -NTA). Protein **(A)** His$_{10}$ZZC, **(B)** His$_9$ZZTEVΔ1-93C, and **(C)** His$_{10}$GB1TEVΔ1-93C. M, molecular weight standard (Broad Range); lane 1, pre-culture prior to induction with IPTG; Lane 2, 2 hours cultivation post induction with IPTG; Lane 3, crude cell lysate after cell disruption and low centrifugation at 4000 x *g* for 10 mins; Lane 4, insoluble fraction from crude cell lysate after ultracentrifuation at 100,000 x *g* for 2 hours; Lane 5 soluble fraction from crude cell lysate after ultracentrifuation at 100,000 x *g* for 2 hours; Lane 6, His-spin (Ni^{2+} -NTA) elution fraction; Lane 7, His-spin sample flow through fraction; and Lane 8, His-spin wash flow though fraction.

The buffers which were tested were 50 mM potassium phosphate buffer, 1x PBS buffer and 50 mM HEPES buffer at pH 7.5. The fusion protein independent of plasmid expressed remained soluble in all buffers tested. No significant difference can be seen between the different buffers used during cell lysis (2.12.1) and purification, indicating stability of the purified protein (2.13.6) (Data not shown).

3.1.6 Proteolytic digest

To assess whether the fusion partner could be successfully cleaved from the PHA synthase, fusion proteins $His_9ZZTEV\Delta1$-93C and $His_{10}GB1TEV\Delta1$-93C were treated using ProTEV protease (2.13.5), removing the N-terminal His-tag IgG binding domain fusion from the PHA synthase. Figure 21 illustrates the cleavage of both His-tagged fusion proteins. The resulting fractions were analysed by SDS-PAGE (2.13.2). Results for $His_9ZZTEV\Delta1$-93C are illustrated in Figure 21 (A). The absence of $His_9ZZTEV\Delta1$-93C fusion protein in the column flow through from protein being produced either in *E. coli* strain BL21 (DE3) or BL21 (DE3) pLysS after incubation with affinity resin, suggests all His-tagged fusion proteins have successfully bound (lanes 1-2). Lanes 3-8 represents the wash fractions (I, II and III), and results suggests most of the contaminating protein can be removed after 2 washes. Only one predominant band is seen at ~55.6 kDa in the elution fractions (lanes 9-10), which is consistent with the theoretical molecular weight of 54.7 kDa for the resulting cleaved ($\Delta1$-93C) product, indicating successful cleavage. However, lanes 11-12 indicate that a significant amount of fusion protein still remained in the resin after centrifugation suggesting not all the cleaved fusion protein had been removed. A faint band corresponding to $His_9ZZTEV\Delta1$-93C around 71 kDa in lane 12 indicates not all the fusion protein was successfully digest during the overnight protease treatment in the BL21 (DE3) pLysS sample.

ProTEV digestion of protein $His_{10}GB1TEV\Delta1$-93C resulted in successful cleavage of the fusion protein indicated by a band at 55.6 kDa correlating to $\Delta1$-93C (54.7 kDa). However, two extra lower molecular weight protein bands are seen after protease treatment with molecular weight of 50 kDa and 47 kDa. The 50 kDa band is consistent with the molecular weight of ProTEV protease (50 kDa), while the 47 kDa band has not yet been identified.
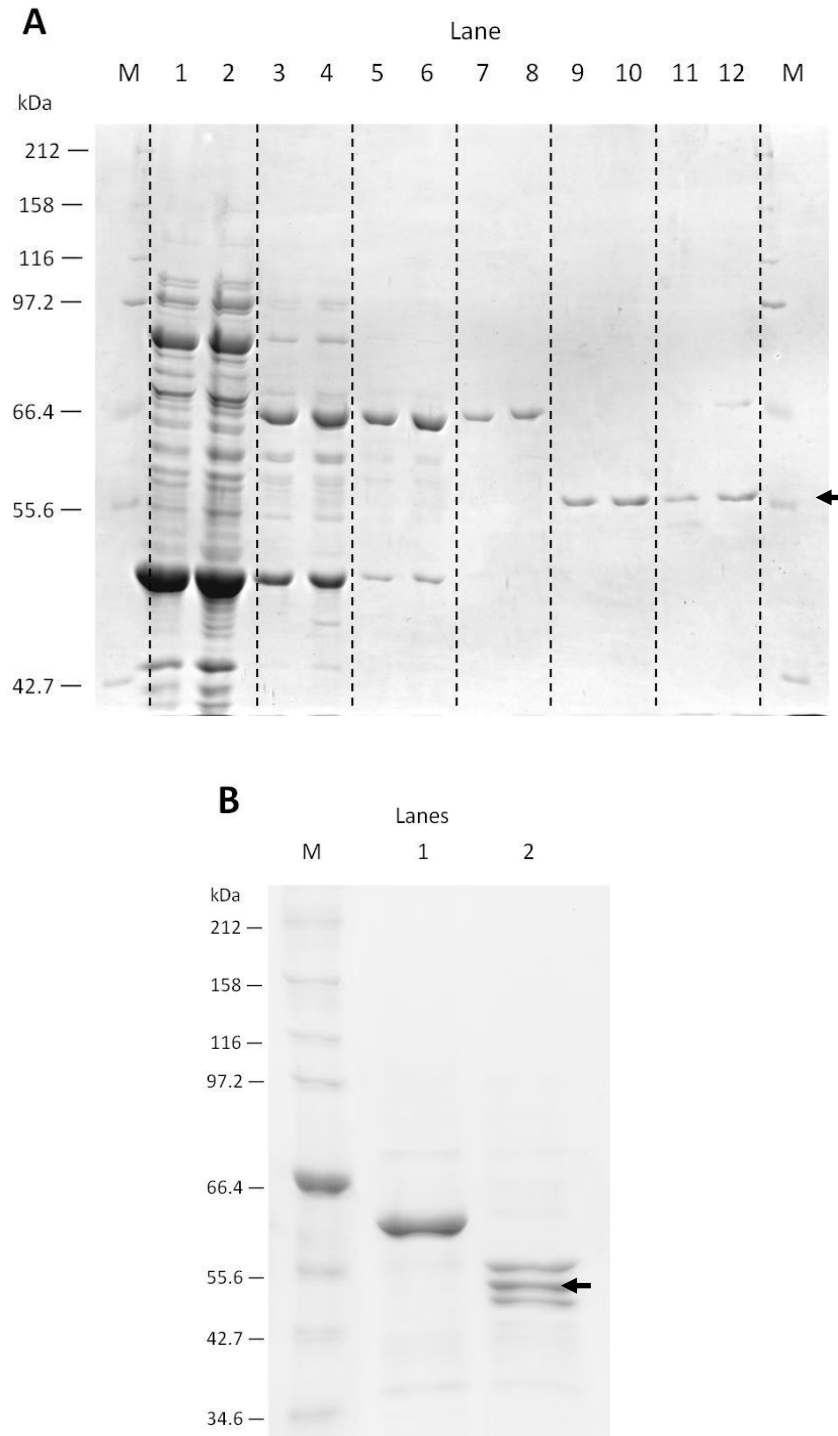
Figure 21. SDS-PAGE gel of TEV protease digestion of purified His9ZZTEVΔ1-93C, and His10GB1TEVΔ1-93C. (A) Protein His9ZZTEVΔ1-93C, M, molecular weight standard; Lanes 1, 3, 5, 7, 9, and 11 represents protein produced in BL21 (DE3) and Lanes 2, 4, 6, 8, and 10 represent protein produced in BL21 (DE3) pLysS. Lanes 1-2, His-spin sample flow though; Lanes 3-4, wash fraction I; Lanes 5-6, wash fraction II; Lanes 7-8, wash fraction III; Lanes 9-10, TEV digested elution fraction; and Lanes 11-12, elution fraction using imidazole. **(B)** Protein His10GB1TEVΔ1-93C, M, molecular weight ladder; Lane 1, purified protein; and Lane 2, TEV digested fraction. Arrows indicate cleaved fusion protein.

3.1.7 Up scaling purification

The His-Trap HP 5ml was used in conjunction with cell lysis using French press method (2.12.1.3) for up scaling purification of fusion protein. Figure 22 (A) illustrates the results for affinity purification using His-Trap HP as described in section (2.13.6.2) for the fusion protein $His_{10}ZZC$ and Figure 22 (B) for the fusion protein $His_{10}GB1TEV\Delta1$-93C. Each figure (A and B) shows a UV 280 nm trace and its corresponding SDS-PAGE. For $His_{10}ZZC$, 3 large peaks can be seen in Figure 22 (A). From left to right, the first large peak contains mostly *E. coli* host cell proteins, the second peak correlates to the elution of nonspecifically bound contaminating proteins at around 75 mM imidazole concentration and the last peak correlating to the point where the most fusion protein is eluted at ~375 mM imidazole concentration. The first two peaks of $His_{10}GB1TEV\Delta1$-93C are similar to that of $His_{10}ZZC$, however, the former and latter fusion protein comes off the colum over a range from 200 mM imidazole to ~450 mM imidazole as indicated by SDS-PAGE (Figure 22 A and B). In addition, the fusion proteins independent of plasmid being expressed shows a broad peak and may indicate overloading of the column (Figure 22 A and B). The eluted fusion proteins show > 90% purity (Figure 23 A, lanes g-r and B, lanes j-p). Various buffers at (50 mM) and salts at different concentrations (5-200 mM) were used in conjunction with different imidazole concentrations in the binding (5-10 mM), washing (30-150 mM) and eluting (200-500 mM) buffers to minimise contaminates in the elution fraction.
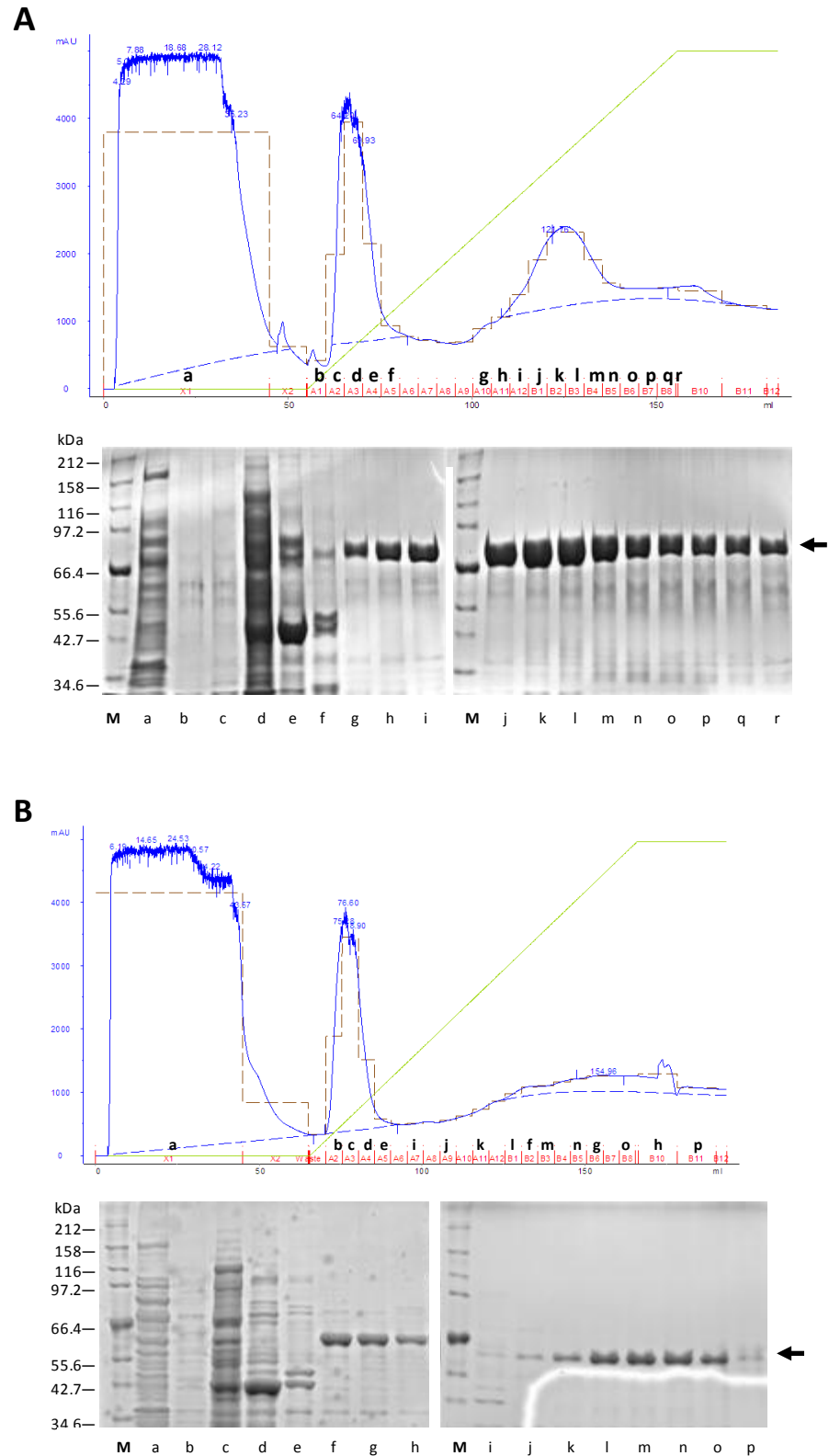
Figure 22. Affinity purification of proteins His$_{10}$ZZC and His$_{10}$GB1TEVΔ1-93C using His-Trap HP on an AKTA explorer 100. **(A)** UV 280 trace of protein His$_{10}$ZZC and its corresponding SDS-PAGE, and **(B)** UV280 trace of protein His$_{10}$GB1Δ1-93C and its corresponding SDS-PAGE. M, molecular weight standard; a-r, represent fractions; UV 280 trace (blue); Imidazole concentration from 0 to 500 mM (green); and collection fractions (brown/red). Fusion protein is indicated by the arrow.

3.1.8 Gel filtration chromatography

In order to analyse and further purify the respective His-tagged fusion proteins, gel filtration chromatography was employed. For analytical gel filtration approximately 200 μl of His-tagged fusion protein at a concentration of 1 mg/ml was subjected to gel filtration chromatography on a Superdex 200 10/300 as described in section (2.13.7). For the fusion protein $His_{10}ZZC$, several peaks were obtained at 8.24 ml, 12.81 ml, 14.22 ml, 16.27 ml, 20.29 ml, 25.95 ml, and 27.04 ml (Figure 23). Only the peaks at 12.81 ml, 14.22 ml, 16.27 ml, and 20.29 ml were within the resolving range of the column used and indicated an apparent molecular weight of 200 kDa, 60k kDa, 20 kDa, and 6 kDa respectively. The 8.24 ml peak was within the void volume, suggesting that its apparent molecular weight was > 699 kDa and most likely to correspond to protein aggregates, while the smallest peaks at 25.95 ml and 27.04 ml were most likely to correspond to imidazole or other small contaminating molecules. SDS-PAGE analysis indicated peaks 12.81 ml (~200 kDa) and 14.22 ml (~60 kDa) contained our fusion protein of interest and the smaller peaks below 20 mAU were too dilute to be detected using SDS-PAGE with coomassie blue staining. The theoretical molecular weight of $His_{10}ZZC$ is 81.86 kDa (Table 10), which doesn't correspond well with the results indicated by gel filtration. However, the results from gel filtration are only an approximation, variations between runs with the same fusion protein were observed (data not shown). Therefore, the peak at 14.22 ml (~60 kDa) was most likely to correspond to the monomer and the larger peak at 12.81 ml (~200 kDa) corresponding to a larger complex such as a dimer or trimer. It is important to note the ratio between the two peaks, with the putative monomer being approximately 2x greater in absorbance than the putative dimer/trimer.
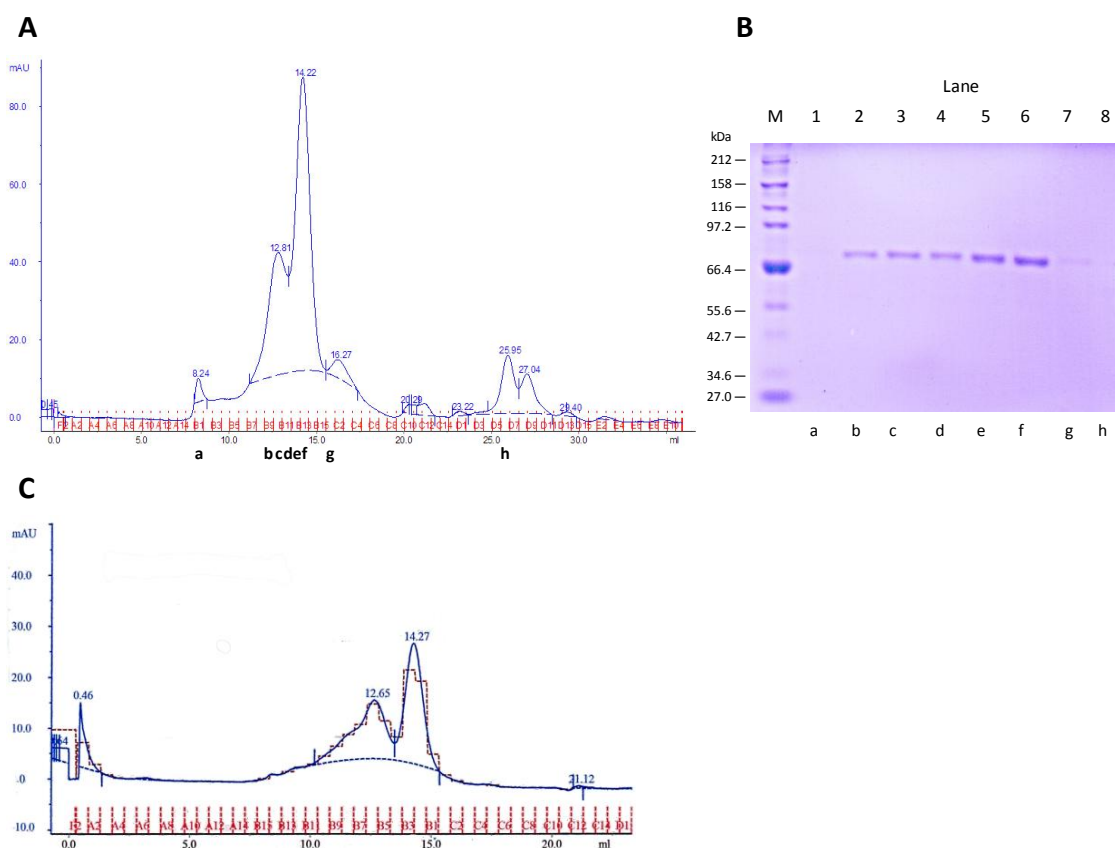
Figure 23. Analytical gel filtration chromatography on an AKTA explorer 100 for protein His₁₀ZZC. (A) UV 280 trace of protein His$_{10}$ZZC and **(B)** its corresponding SDS-PAGE. Lanes 2 to 7 correspond to consecutive fraction b-f representing peaks at 12.81 ml. 14.22 ml, and 16.27 ml with a molecular weight consistent with His$_{10}$ZZC. Peak fraction at 12.81 ml was concentrated and re-analysed using gel filtration chromatography with using the same running parameters as previous run. **(C)** UV 280 trace for the re-analysis fraction. M, molecular weight standard; and a-h, represent consecutive elution fractions.

To assess whether this ratio between monomer and dimer/trimer is dynamic, the larger 12.81 ml (~200 kDa) peak fraction (2.13.7) was concentrated and re-analysed using gel filtration. Results suggest that the PHA synthase is dynamic and maintains a ratio of monomer to dimer/trimer of approximately 2:1 (Figure 23 C).

For the fusion protein His$_{10}$GB1TEVΔ1-93C, several peaks were obtained (Figure 24), with peak 8.40 ml in the void volume, peaks 11.77 ml, 14.49 ml, 18.59 ml within the resolving range of the column and peaks 25.73 ml and 26.74 ml being too small to be resolved by column. SDS-PAGE analysis of the peak fractions indicated peaks at 8.40 ml, 11.77 ml and 14.49 ml contained our fusion protein of interest with a theoretical molecular weight of 63 kDa (Table 10). As previously mentioned the smaller peaks, greater than 25 ml, most likely corresponds to imidazole or other small molecules. The

smaller 11.77 ml peak had an approximate molecular weight of 350 kDa, while the larger 14.49 ml peak had an approximate molecular weight of 50 kDa. These values roughly correspond to the monomer and a larger complex, possible a tetramer or bigger. The ratio between the larger product and smaller product should be noted.
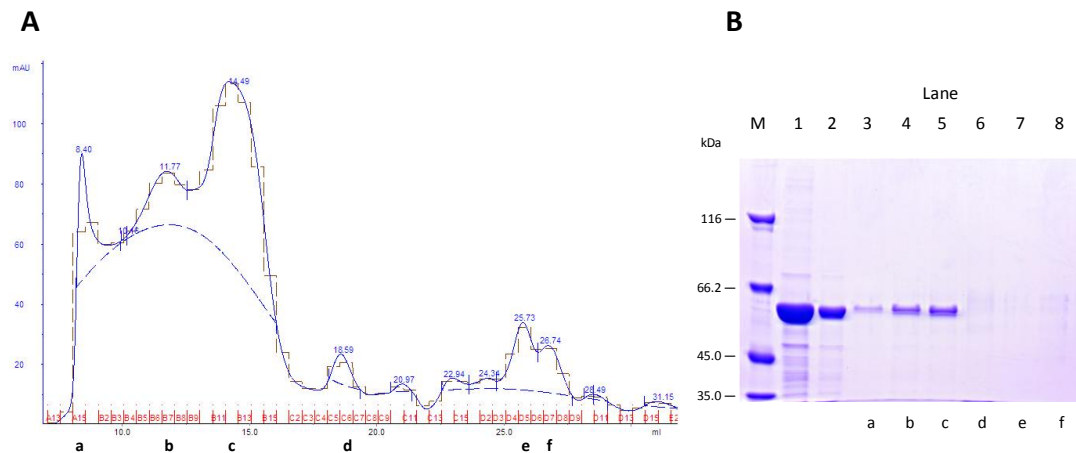
Figure 24. Gel filtration chromatography on an AKTA explorer 100 for protein His$_{10}$GB1TEVΔ1-93C. **(A)** UV 280 trace of protein 10xHisGB1TEVΔ1-93C and **(B)** its corresponding SDS-PAGE. Lane M, molecular weight standard (unstained marker); Lane 1-2, purified 10xHisGB1Δ1-93C PHA synthase; Lanes 3 to 5 correspond to the first 3 peaks on the left at 8.40 ml, 11.77 ml, and 14.49 ml, with a molecular weight consistent with 10xHisGB1TEVΔ1-93C; and a-f, represent consecutive elution fractions.

For fusion protein His$_9$ZZTEVΔ1-93C, several significant peaks were seen at 8.50 ml, 14.60 ml, 16.80 ml, 25.8 ml and 27.0 ml (Figure 25). SDS-PAGE analysis of all the peak fractions indicated our fusion protein was in the 8.50 ml peak, which was in the void volume and out of the resolving range of the column, indicating the weight was >699 kDa. This large complex is most likely due to aggregation of the fusion protein. However, the smaller peak fractions at 14.60 ml, 16.80 were too dilute to be detected by SDS-PAGE staining with coomassie blue and peaks greater then 25 ml most likely corresponded to imidazole or small contaminating molecules.
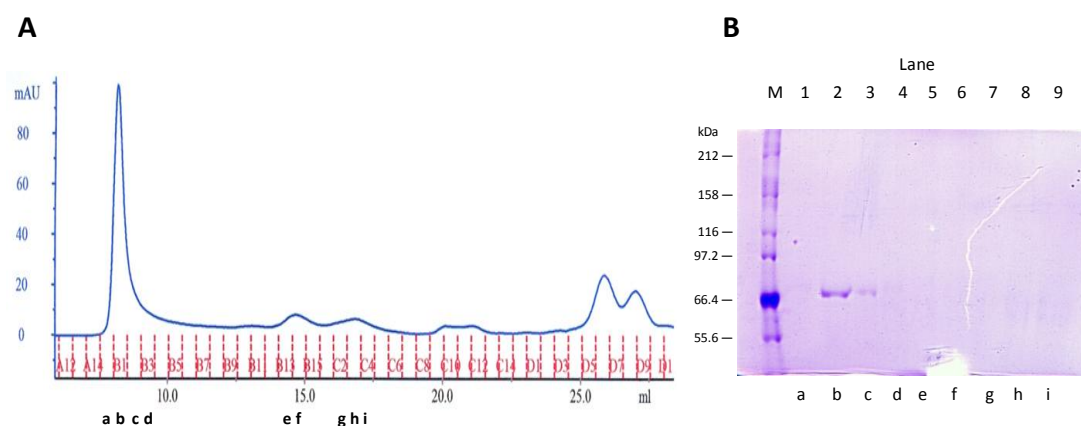
Figure 25. Gel filtration chromatography on an AKTA explorer 100 for protein His$_9$ZZTEVΔ1-93C. (A) UV 280 trace of protein His$_{10}$ZZTEVΔ1-93C and **(B)** its corresponding SDS-PAGE. Lane M, molecular weight standard (BroadRange); Lanes 1-9 elution fractions ; Lanes 2-3 correspond to the single large peak, with a molecular weight consistent to His$_9$ZZTEVΔ1-93C. Lanes a-i, represent consecutive elution fractions.

3.1.9 Crystal screening trials

Based on the gel filtration results and SDS-PAGE, only uncleaved purified fusion protein His$_{10}$ZZC and His$_{10}$GB1TEVΔ1-93C was used initially as a first attempt for crystal screening as described in section 2.13.8, using the HAMPTON crystal screen I and II and/or Molecular Dimensions PACT premier. The hanging drop method by vapour diffusion was used for the purified fusion protein His$_{10}$ZZC in KPO$_4$ buffer. Purified fusion protein His$_{10}$ZZC was used at a concentration of approximately 5 mg/ml using both crystal screen (HAMPTON and Molecular Dimensions), plates were incubated at 21 °C. Initial results showed precipitation of the protein in most wells and the formation of salt crystals. However, this was most likely due to the presence of phosphate in the buffer and no protein crystals were visable after 6 months incubation.

Purified fusion protein His$_{10}$GB1TEVΔ1-93C in 50 mM HEPES buffer containing 50 mM NaCl was used with the sitting drop method and HAMPTON crystal screen I and II. Two crystal screens were setup with 2 sitting drop reactions per reaction condition containing approximately 5 mg/ml and 10 mg/ml protein. Plates were incubated at 4 °C and 21 °C. No protein crystals were visible in either incubation condition after 5 months.

3.2 *In vivo* polyhydroxyalkanoate inclusions

In order to assess the functionalised PHB beads produced *in vivo*, the following plasmids were used: pET14b-His$_9$ZZTEVΔ1-93C, pET16b-His$_{10}$ZZC, and pET14b-His$_{10}$GB1TEVΔ1-93C. The controls were plasmid pET16b-His$_{10}$C and pET14b-ZZΔ1-93C. Please refer to section 3.1.1 for the cloning of plasmids pET14b-His$_9$ZZTEVΔ1-93C, pET16b-His$_{10}$ZZC, pET16b-His$_{10}$C and pET14b-His$_{10}$GB1ETVΔ1-93C. Cloning of plasmid pET14b- ZZΔ1-93C is described below (3.2.1). To demonstrate functionality, each plasmid was designed to encode an IgG binding domain (either a GB1 domain of protein G or ZZ domain of protein A) fused to the end of the gene representing the N-terminus of the PHA synthase, as described below (3.2.1). Both the full length and truncated forms of the codon optimised PHA synthase gene from *C. necator* (for expression in *E. coli*) were used to make plasmids.

3.2.1 Construction of pET14b-ZZTEVΔ1-93C

Plasmid pET14b-ZZTEVΔ1-93C is a non-affinity tagged control for plasmid pET14b-His$_{10}$ZZTEVΔ1-93C. This plasmid is used to assess the effects of the polyHis-tag on PHA granule formation under PHA accumulating conditions *in vivo* and *in vitro*. The DNA region encoding the ZZ domain of protein A and TEV site was amplified using PCR (2.11.2) and pET14b-His$_9$ZZTEVΔ1-93C was used as a template (Figure 26). Primers were designed to clone the ZZ domain and TEV site while excluding the 10xHis-affinity tag and introducing the appropriate restriction sites (*Xba*I and *Age*I) for subcloning. The fragment was amplified using *Pfx* polymerase due to its high fidelity. The PCR product (473bp) was verified by running a small aliquot on AGE (2.11.5). The remaining PCR product was isolated and purified using AGE with SYBR safe DNA gel stain (2.11.5) and gel purification kit (2.11.6) respectively. The purified blunt end PCR product was "A-tailed" (2.11.8) to allow cloning into pGEM –T Easy vector. The resulting A-tailed PCR product was then ligated into the pGEM –T Easy vector (2.11.8). After ligation, the product was transformed into XL1-blue (2.10.1) and plated onto X-Gal medium agar (2.4.1) containing 75 µg/ml ampicillin. Single white colonies were selected for subsequent plasmid isolation (2.11.1) and RE analysis (2.11.4). DNA sequencing (2.11.10) was performed on plasmids which showed the correct restriction patterns with RE analysis (2.11.4) to determine if any sequencing errors were present.

After confirmation by DNA sequencing, plasmids were subjected to RE analysis (2.11.4) using restriction enzymes *Xba*I and *Age*I, excising the ZZTEV (440 bp) fragment which was separated from other fragments using AGE (2.11.5), followed by isolation and purification (2.11.6) (Figure 27). The purified ZZTEV fragment was then cloned into vector pET14b-His$_{10}$ZZTEVΔ1-93C using T4 DNA ligase (2.11.9). Vector pET14b-His$_{10}$ZZTEVΔ1-93C was prepared by RE analysis (2.11.4) using *Xba*I and *Age*I, followed by AGE (2.11.5) and gel purification (2.11.6). After ligation (2.11.9), the product was transformed into *E. coli* XL1-blue (2.10.1) and plated on LB medium containing 75 µg/ml ampicillin. Single white colonies were selected for plasmid isolation and RE analysis to confirm successful ligation and transformation of the plasmid. -80 °C freezer stocks of confirmed transformations were made (2.8).
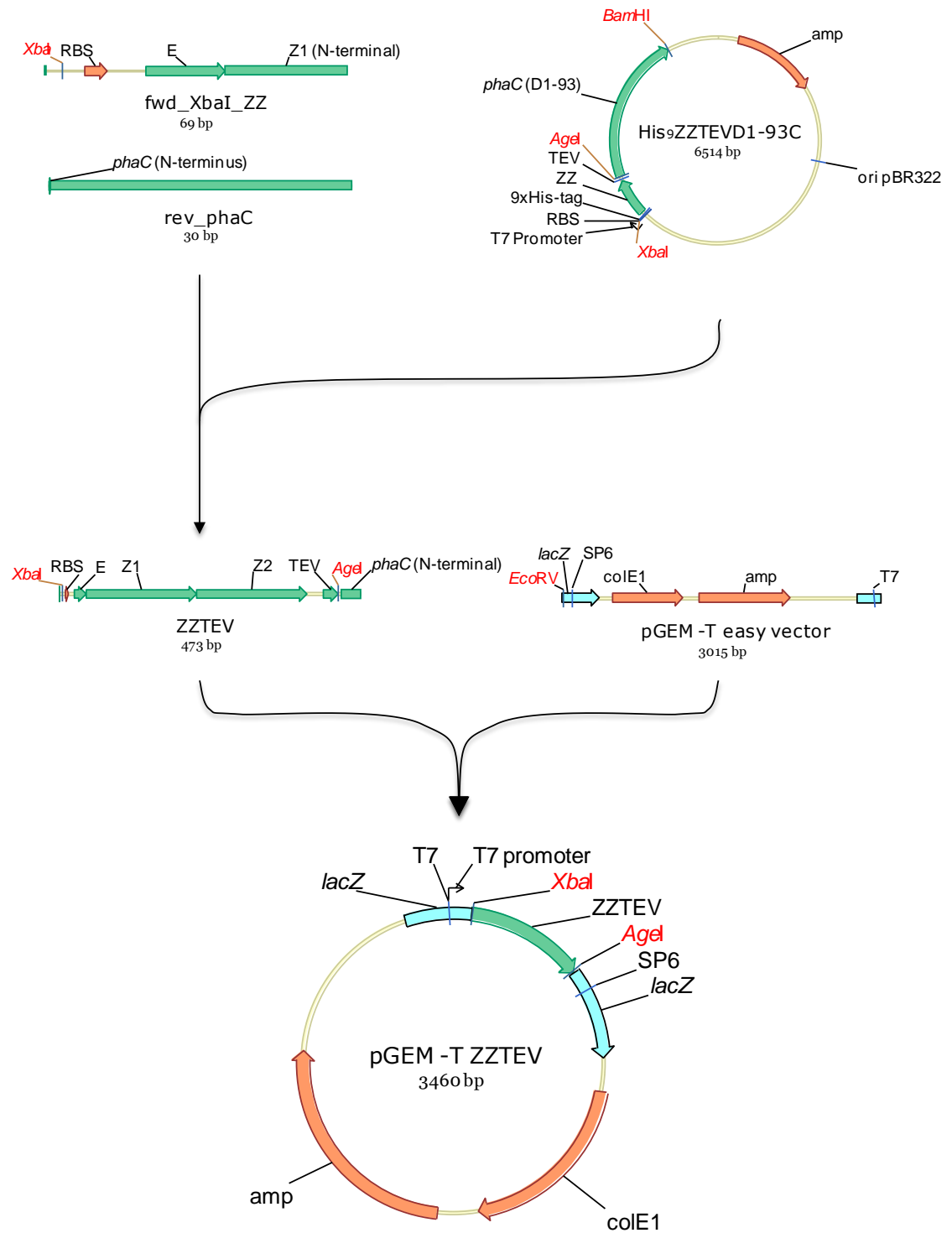
Figure 26. Construction of intermediate cloning plasmid pGEM-T ZZTEV for the generation of pET14b-ZZTEVΔ1-93C. The PCR fragment ZZTEV with flanking *Xba*I and *Age*I restriction sites was generated using primers rev_*phaC* (reverse) and fwd_*Xba*I_ZZ (forward) using plasmid pET14b-His₉TEVΔ1-93C as a template. The resulting 473bp blunt ended PCR product was A-tailed and ligated into intermediate cloning vector pGEM-T easy vector.
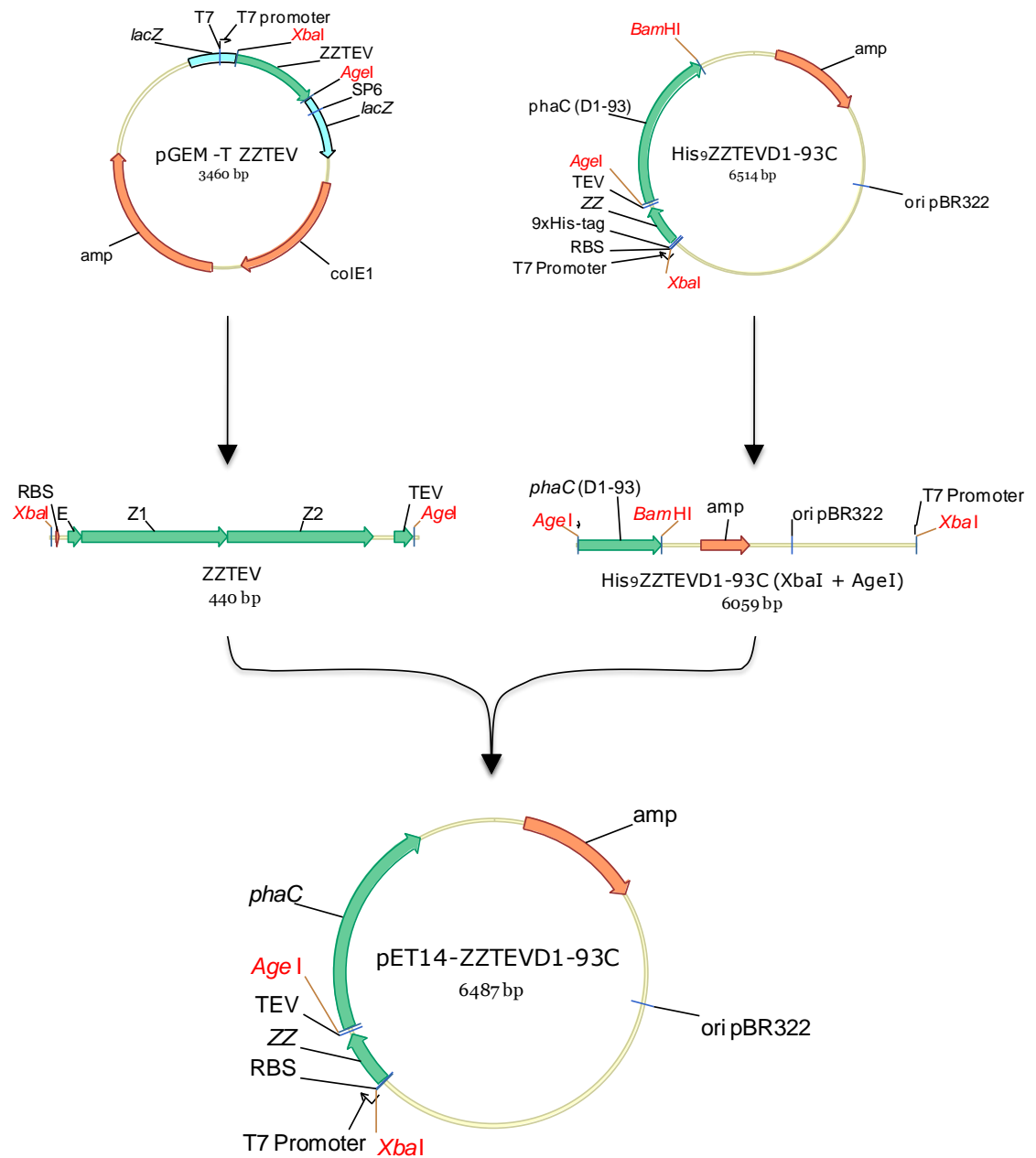
Figure 27. Construction of pET14b-ZZTEVΔ1-93C. Intermediate plasmid pEM-T ZZTEV was digested with *Xba*I and *Age*I. The resulting 440bp (His₉ZZTEV) fragment was ligated into linearized pET14b-His₉ZZTEVΔ1-93C digested with *Xba*I and *Age*I using T4 DNA ligase.

3.2.2 Plasmid expression and PHA bead biogenesis

All plasmids used for *in vivo* PHA bead biogenesis were designed using the pET vector. The pET vector contains a *lacI* gene (*lac* repressor), a T7 promoter, a *lac* operator (*lacO*), an amp resistance gene, and a ColE1 origin of replication. The pET vector is part of the pET expression system and expression of the pET vector requires a host which has been genetically engineered to contain genes for the T7 RNA polymerase, and *lac* promoter in its genome, in this study commercial *E. coli* strain BL21(DE3) (Stratagene) was used for the production of PHB beads *in vivo*.

All plasmids for *in vivo* production of PHB beads were transformed (2.10.1) into *E. coli* strain BL21(DE3) harbouring plasmid pMCS69. Plasmid pMCS69 encodes for genes *phaA* and *phaB*, required for substrate synthesis (Table 3). The recombinant strains were cultivated under PHB accumulating conditions (2.6.1) and beads were isolated (2.12.2). Theoretical molecular weight of the fusion proteins were calculated using the ProtParam tool from the ExPASy Proteomics Server (http://www.expasy.org/). The theoretical molecular weight of each of the expected fusion proteins is listed in the table below:

Table 10. Theoretical molecular weight of the PHA synthase fusion proteins as predicted by ProtParam

Fusion protein	Molecular weight (kDa)
PhaC (WT)	64.3
His$_9$ZZTEVΔ1-93C	71.6
ZZTEVΔ1-93C	70.36
His$_{10}$C	66.83
His$_{10}$ZZC	81.86
His$_{10}$GB1TEVΔ1-93C	63.0

Bands of the approximate expected weight for each fusion protein were detected and shown to be strongly overproducedon the beads surface, as indicated by relative

intensity in comparison to other proteins on SDS-PAGE (Figure 28). Other dominant protein bands were present at approximately 97.0 kDa, 42 kDa, 37.5 kDa, and 34.5 kDa and these have been previously identified as ATPase, Elongation factor-Tu and outer-membrane proteins OM-F and OM-A respectively.
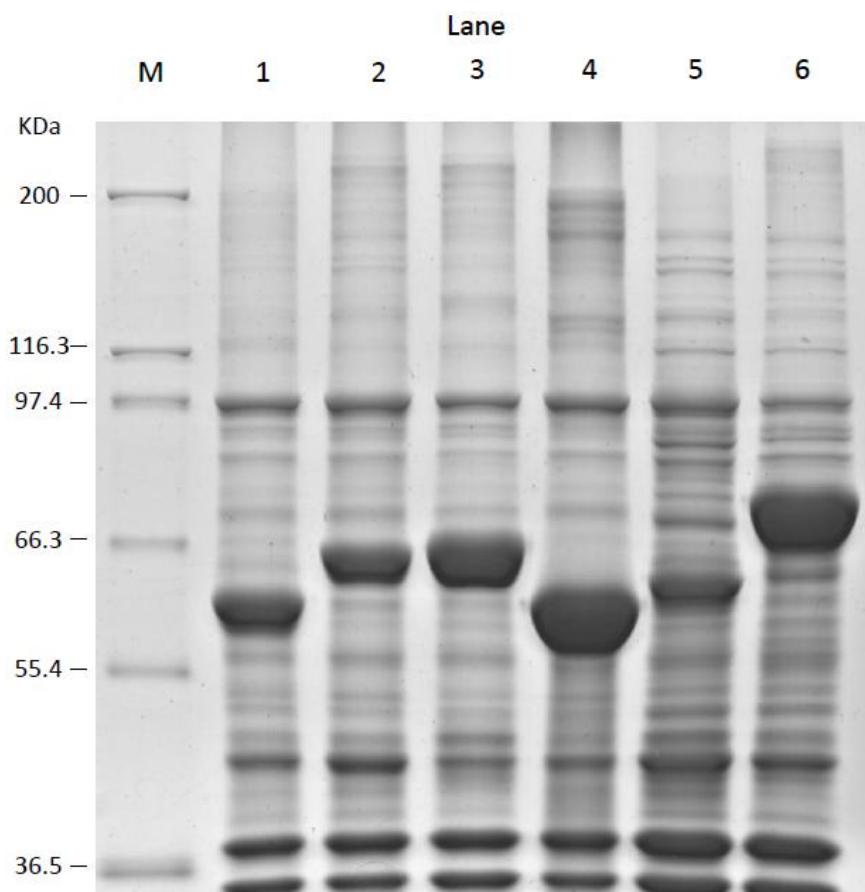
Figure 28. SDS-PAGE gel of isolated PHA beads produced *in vivo* from *E. coli*. Lane M, molecular weight standard (Mark 12); Lane 1, PhaC (WT); Lane 2, ZZTEVΔ1-93C; Lane 3, His$_9$ZZTEVΔ1-93C; Lane 4, His$_{10}$GB1TEVΔ1-93C; Lane 5, His$_{10}$C; and Lane 6, His$_{10}$ZZC.

3.2.3 Microscopy (FM and TEM) and GC/MS analysis

PHB accumulating *E. coli* cells were routinely stained with Nile-red and visualised using fluorescence microscopy (2.12.3). The positive florescence seen with *E. coli* samples under PHB accumulating conditions (Figure 29) suggested intracellular PHB accumulation and hence PHA synthase activity. Strains which were expressing plasmids

encoding fusion proteins with a polyHis-tag were observed to form extremely small PHB beads in comparison to wildtype or nonpolyHis-tagged fusion proteins, suggesting that the polyHis-tag effects bead size *in vivo*. Accumulation of intracellular PHB was further confirmed and quantified by GC/MS analysis (Table 11). GC/MS analysis confirmed the presence of PHB accumulation in all *in vivo* samples, indicating activity of the PHA synthase for all plasmids.

Table 11. GC/MS results for PHB accumulation *in vivo* synthesised beads

Plasmid construct	Dry weight of sample (mg)	PHB per sample (mg)	PHB per mg dry weight	% PHB per mg dry weight
WTphaC	15	8.65	0.58	57.63
His$_{10}$ZZC	15.7	6.01	0.38	38.27
His$_9$ZZTEVΔ1-93C	15.7	6.97	0.44	44.42
His$_{10}$GB1TEVΔ1-93C	15	6.10	0.41	40.68
ZZTEVΔ1-93C	15	3.57	0.24	23.82

To confirm the observation made earlier with florescence microscopy (FM), TEM analysis was done on PHB accumulating *E. coli* cells harbouring plasmids pET14b-C (WT), pET16b-His$_{10}$C, pET14b-His$_{10}$ZZTEVΔ1-93C and pET14b-ZZTEVΔ1-93. The results are shown in Figure 30. TEM results of PHB accumulating *E.coli* harbouring His$_{10}$ZZC and His$_{10}$ZZTEVΔ1-93C confirmed the FM observations. Bead diameter was measured using iTEM software imaging (Olympus soft imaging solutions GmbH) from 10 -30 cells giving between $200 - 600$ data points. PHB beads from His$_{10}$C had a bead diameter ranging from 31 nm to 249 nm with an average diameter of 97 nm (Figure 31). In comparison to nonHis-tagged phaC beads which were from 62 nm to 424 nm with an average of 174 nm, the His$_{10}$C beads were are 53 % smaller. Similarly, PHB beads isolated from His$_9$ZZTEVΔ1-93C showed beads from 54 nm to 410 nm with an average diameter of 175 nm, while nonHis-tagged ZZTEVΔ1-93C were 61% smaller (51-933 nm with an average of 295 nm). It is interesting to note that PHA beads from ZZTEVΔ1-93C were considerably larger on average than that of the WT (PhaC). This suggests either the 93 amino acid truncation or the IgG binding domain, or a combination of both, may be affecting bead size.
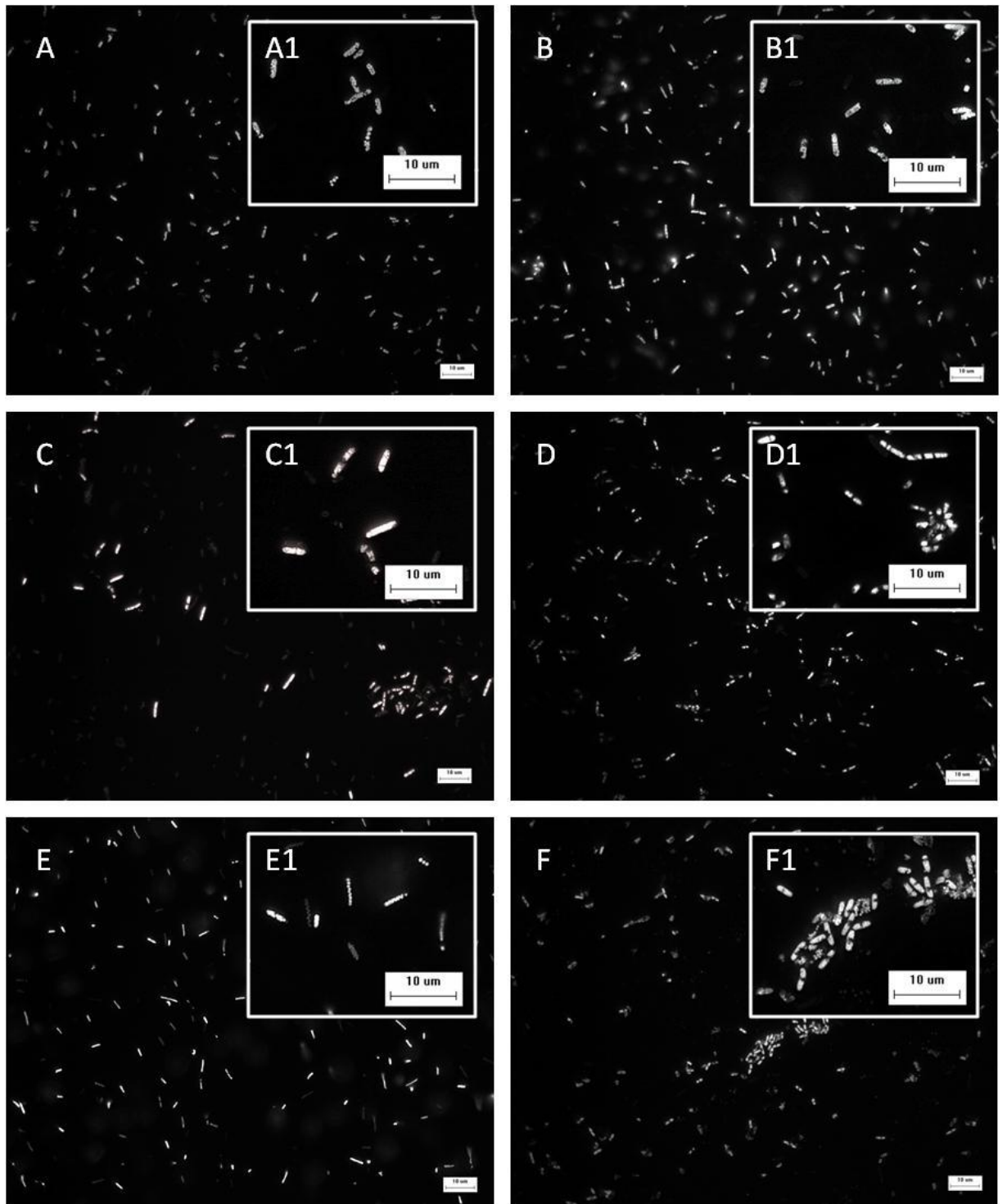
Figure 29. Fluorescence microscopy images of PHA beads produced in *E. coli*. *E. coli* BL21 (DE3) harbouring the relevant plasmid was expressed under PHB accumulating conditions. (A) PhaC (WT); (B) $His_{10}GB1TEV\Delta1-93C$; (C) $His_{10}C$; (D) $His_{10}ZZC$; (E) $ZZ\Delta1-93C$; (F) $His_9ZZTEV\Delta1-93C$. (A1) to (F1) represents a magnified section of the respective FM image.
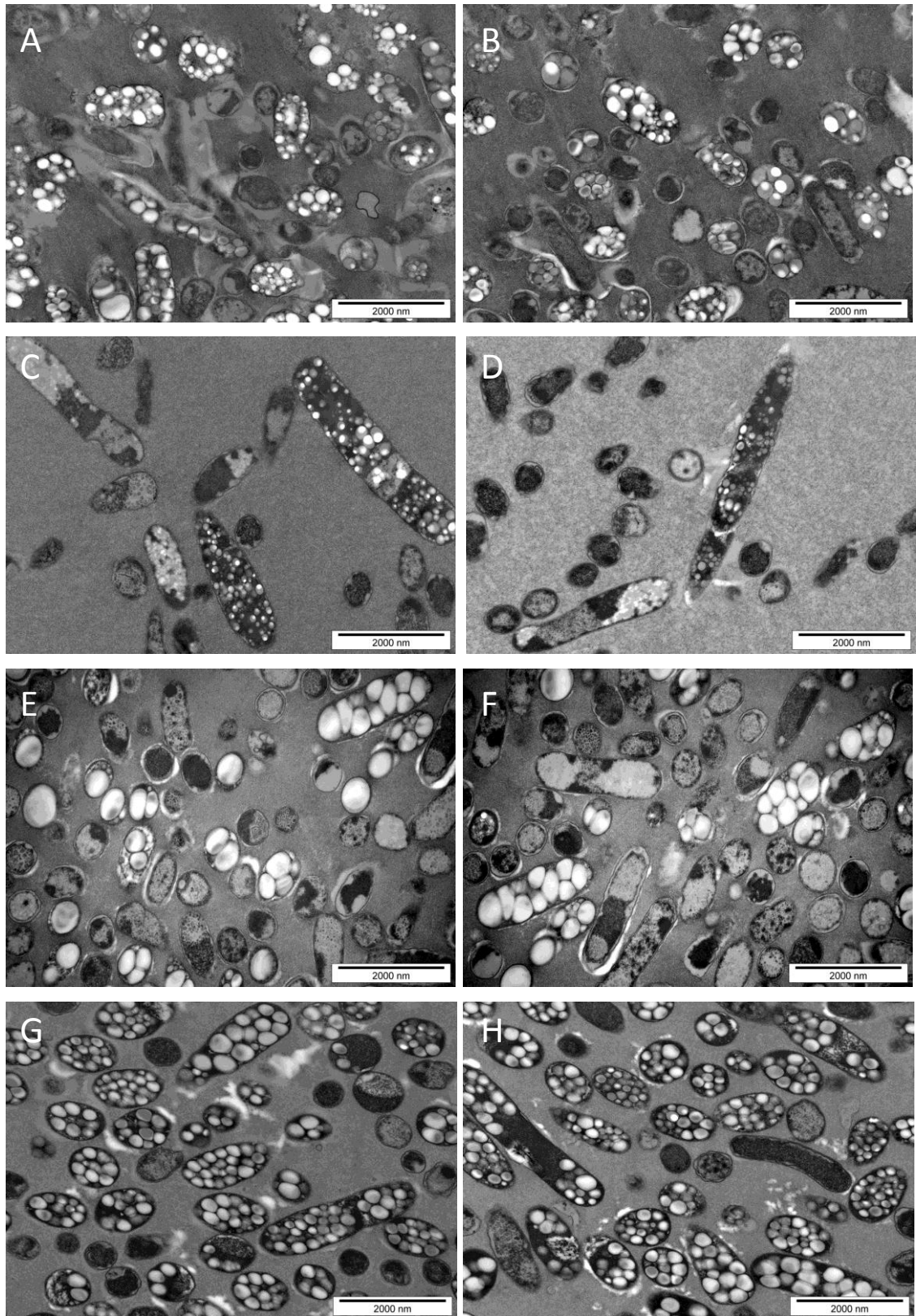
Figure 30. TEM analysis of His-tag fusion on PHA beads formed *in vivo*. *E. coli* BL21 (DE3) harbouring the relevant plasmid was expressed under PHB accumulating conditions. (A-B) PhaC (WT); (C-D) His$_{10}$C; (E-F) ZZΔ1-93C; (G-H) His$_9$ZZTEVΔ1-93C.
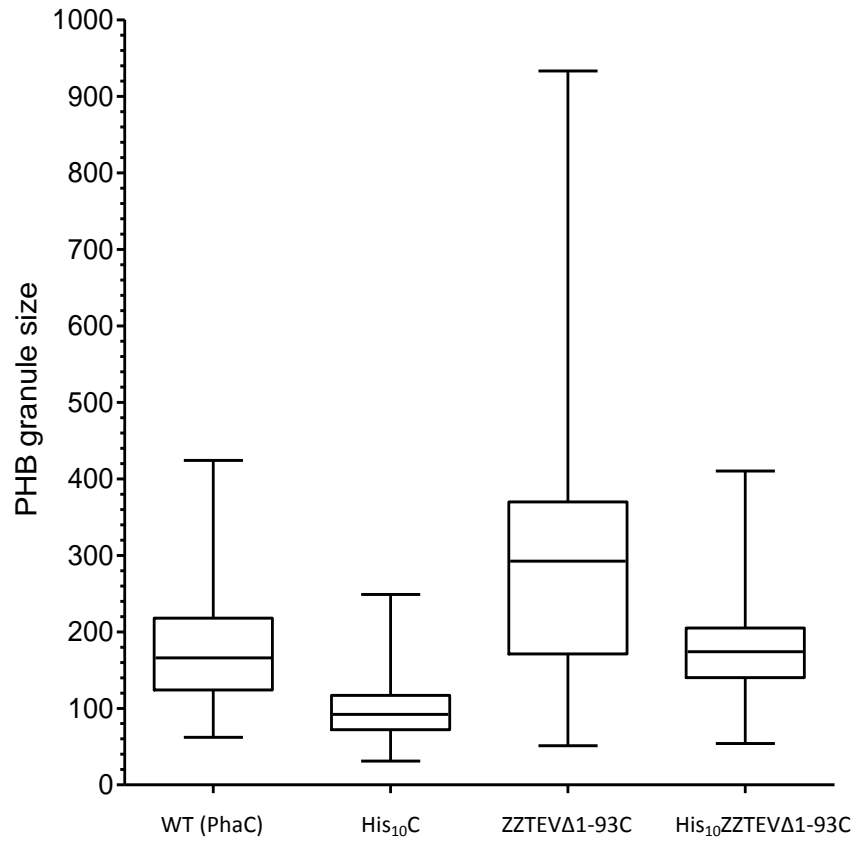
Figure 31. His-tag effect on bead size distribution. *E. coli* BL21 (DE3) expressing His-tagged plasmids $His_{10}C$ and $His_9ZZTEV\Delta1-93C$ and their nonHis-tagged controls WT (PhaC) and $ZZTEV\Delta1-93C$ repectively under PHB accumulating conditions for 48 hours. Cultures where subsequently analysed using TEM and bead diameters quantified using iTEM imaging software (Olympus soft imaging solutions GmbH) from 10 to 30 cells giving between 200 to 600 data points. Analysis was done using GraphPad Prism 5 (GraphPad software inc.).

3.2.4 Functional assessment of IgG binding domain

The functional activity of the IgG binding domain expressed on the surface of the PHB beads was confirmed by ELISA (2.13.4.1). A positive result was indicated by increased absorbance at 490 nm. *In vivo* produced PHA beads in *E. coli* displaying fusion ZZ binding domain (see section 3.2) demonstrated that IgG from human serum bound specifically to these domains, indicated by the positive fluorescence (Figure 32). Both His-tagged plasmids (His$_{10}$ZZC and His$_9$ZZTEVΔ1-93C) showed significant levels of bound IgG in comparison to negative control (PhaC) (Figure 32).
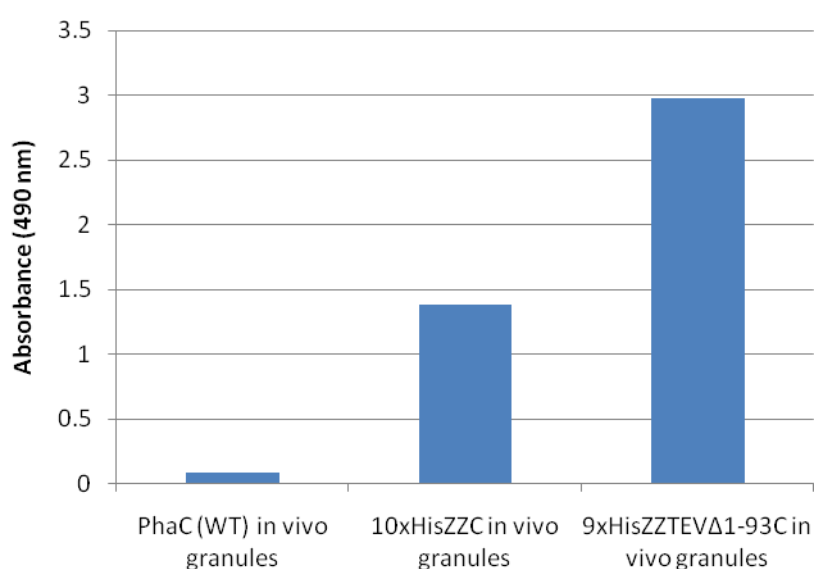
Figure 32. Functional assessment of the ZZ domain on PHB beads produced *in vivo* from *E. coli* by ELISA.

In vivo produced PHB beads using plasmid His$_{10}$GB1TEVΔ1-93C, demonstrated that IgG also bound specifically to the GB1 domain of protein G (Figure 33). Negative controls showed insignificant levels of bound IgG.
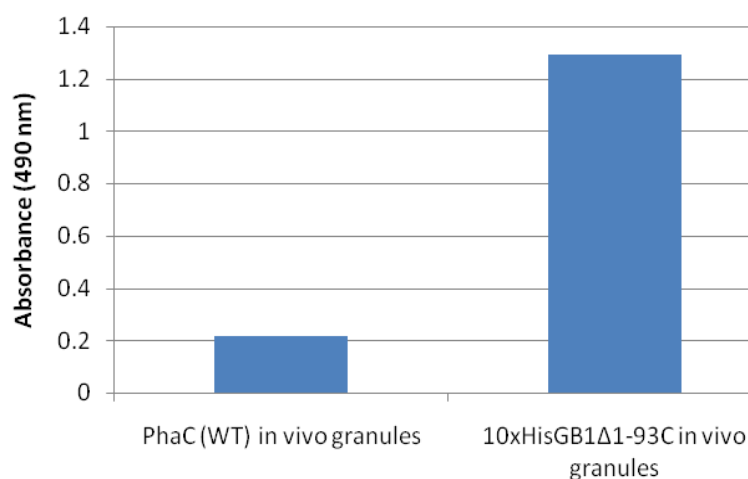
Figure 33. Functional assessment of the GB1 domain on PHB beads produced *in vivo* from *E. coli* by ELISA.

In vivo produced PHA beads displaying the IgG binding (ZZ or GB1) domain were further assessed for their ability to bind and purify IgG from human serum (2.13.4.2). IgG elution fractions were quantified by Bradford assay (2.13.1.1) and results are displayed in Figure 34. Commercially available protein A-sepharose beads with immobilised protein A from GE were used in parallel with PHA beads for comparative analysis. IgG purification was conducted as described in the material and methods section (2.13.4.2). Bradford analysis (2.13.1.1) on the IgG elution fractions showed that significant IgG is eluted from the PHA beads displaying the His-tagged IgG binding domain (ZZ or GB1) and this is comparable to, although slightly less than the commercial protein A beads (Figure 34).

SDS-PAGE was used to check the purity of the eluted IgG fractions (Figure 35). Two protein bands can be seen for IgG, with the ~50 kDa and ~25 kDa bands corresponding to the heavy and light chain. In comparison to commercially available protein A beads, ZZ or GB1 surface displaying PHA beads show eluted IgG with similar purity. No protein bands were seen in the IgG elution using the negative control WT PhaC or $His_{10}C$ on SDS-PAGE, indicating that no non-specific IgG bound to beads, confirming the results from the Bradford assay.
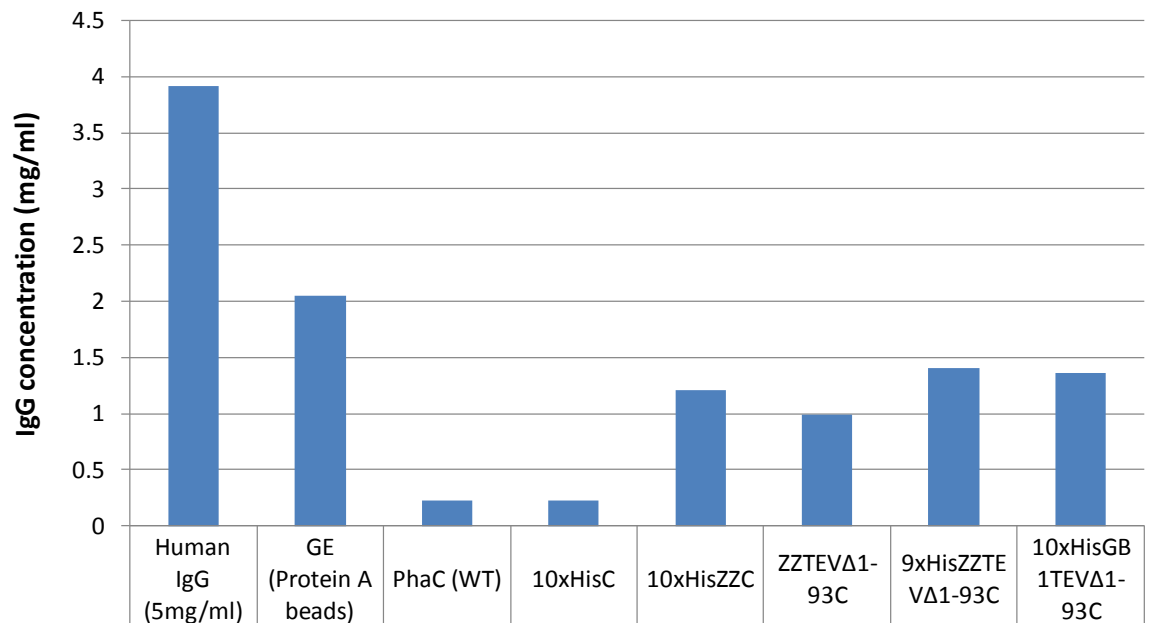
Figure 34. IgG binding assay for *in vivo* PHA beads from *E. coli*.
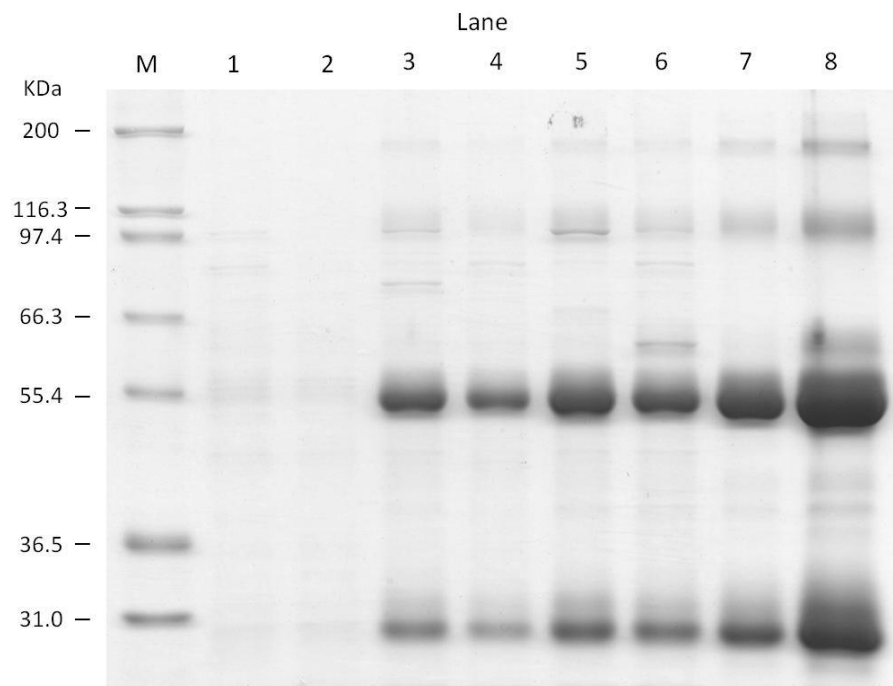
Figure 35. SDS-PAGE gel of the IgG binding assay elution fraction from PHA beads produced *in vivo* by recombinant *E. coli*. M, molecular weight standard (Mark 12); Lane 1, PhaC (WT); Lane 2, $His_{10}C$; Lane 3, $His_{10}ZZC$; Lane 4, ZZTEVΔ1-93C; Lane 5, $His_9ZZTEV\Delta$1-93C; Lane 6, $His_{10}GB1TEV\Delta$1-93C; Lane 7, GE (Sephorose protein A beads); and Lane 8, pure human IgG (5 mg/ml).

3.3 *In vivo* production of PHA in *L. lactis*

The design of the cloning strategy involving the immobilisation of influenza A virus (H2N2) Hemagglutinin (HA) antigen and Hepatitis C virus core antigen (HepC) on the beads surface in *L. lactis* was done by Katrin Grage (IMBS, Massey University). All subsequent work involving cloning, expression, biogenesis and isolation of PHA beads was done by the author. Functional analysis of the purified antigen displaying beads was done in collaboration with Natalie Parlane (Hopkirk Research Institute, AgResearch). In order to display the influenza A virus (H3N1) Hemagglutinin antigen (GI: 158188134) and Hepatitis C virus subtype 1b core antigen (amino acids 1-191) on the surface of PHA beads in *L. lactis*, two plasmids were made by cloning (1) the genes required for the production of the respective antigens and (2) genes required for PHA biogenesis (*pha*C, *pha*A and *pha*B) into a *L. lactis* expression vector (pNZ), which were subsequently electroporated into *L. lactis*.

In order to highly overproduce functional recombinant proteins from another organism in *L. lactis* NZ9000, both the HA and HepC core antigens genes were synthesised and optimised for codon usage to *L. lactis* by Genescript corporation (USA). Both the HA and HepC genes were designed with a small proportion of the DNA encoding the N-terminus of PhaC linked to the DNA corresponding to the antigens C-terminus, with flanking restriction sites (*Nco*I and *Nhe*I), in order to easily subclone into a pre-existing vector (pNZ-CAB) designed by Mifune *et al* (2009). Plasmid pNZ-CAB harbours the codon-optimised PHB biosynthesis operon form *C. necator* under P_{nisA} control.

3.1.1 Construction of pNZ-HA*CAB* and pNZ-HepC*CAB*

Firstly, the codon optimised HA and HepC genes encoding the relevant antigens were excised from the pUC57 vector obtained from Genescript corporation (USA) by restriction analysis (2.11.4) using *Nco*I and *Nhe*I, resulting in 1871 bp and 746 bp fragments respectively. In parallel, purified plasmid pNZ-CAB was also linearised with the same restriction enzymes. Each restriction enzyme reaction mixture was then analysed by AGE (2.11.5) containing SYBR safe DNA gel stain. Bands identified as

being of the correct size were then isolated and purified from the gel using a gel purification kit (2.11.6) for subsequent cloning steps.

The construction of pNZ-HA*CAB* and pNZ-HepC*CAB* was conducted as a single step ligation as described below. A schematic outline of the cloning strategy is illustrated in Figure 37 for pNZ-HA*CAB* and Figure 38 for pNZ-HepC*CAB*. The resulting purified DNA fragments were subsequently ligated into the linearised vector pNZ-*CAB* (6739 bp) down stream of the Nis$_A$ promoter using T4 DNA ligase (2.11.9). The ligation mixture was transformed directly into *L. lactis* NZ9000 by electroporation (2.10.2). Plasmid was isolated from single colony transformants (2.11.1.3) grown on M17 media (2.3.2) containing 30 µg/ml chloramphenicol after 48 hours incubation at 30 °C, followed by confirmation with restriction analysis (2.11.4) using restriction enzymes *Xba*I and *Spe*I (Figure 36). Plasmids which gave the correct restriction patterns were subsequently confirmed by DNA sequencing (2.11.10) using primer Pnis1 directed to the nisin promoter.
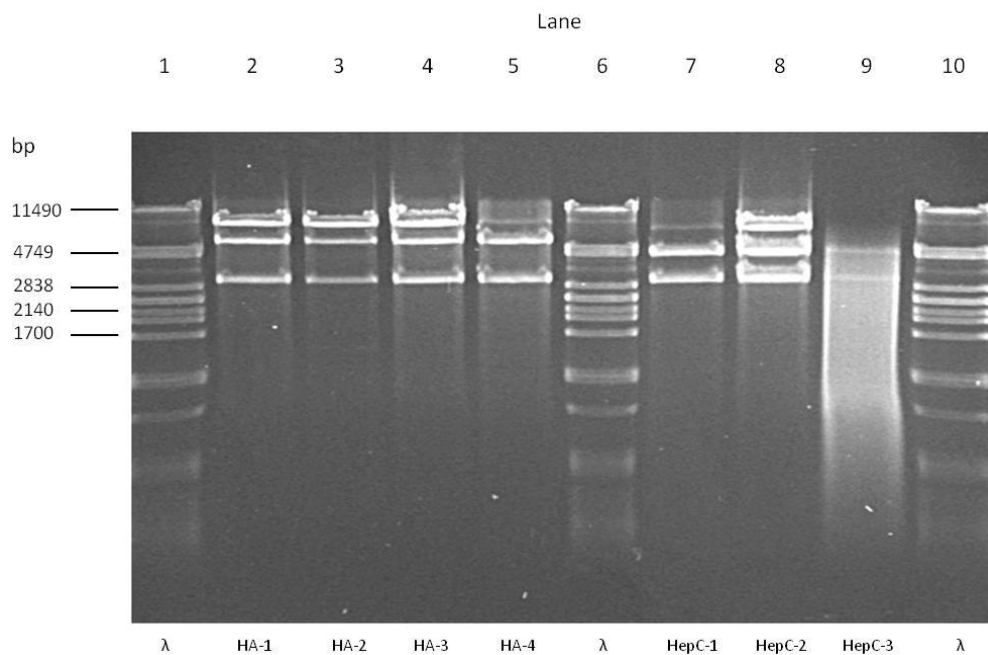
Figure 36. *Xba*I + *Spe*I double digest of pNZ-HA*CAB* and pNZ-HepC*CAB*. Lanes 1, 6, & 10, DNA ladder standard (λ-*Pst*I); Lanes 2-5, digest of pNZ-HACAB with expected fragments of 5580bp and 3018bp for a complete digest and 8598bp for partial digest. Lanes 7-9, digest of pNZ-HepCCAB with expected fragments sizes of 4455bp and 3018bp for a complete digest and an expected fragment size of 7473bp for partial digest.
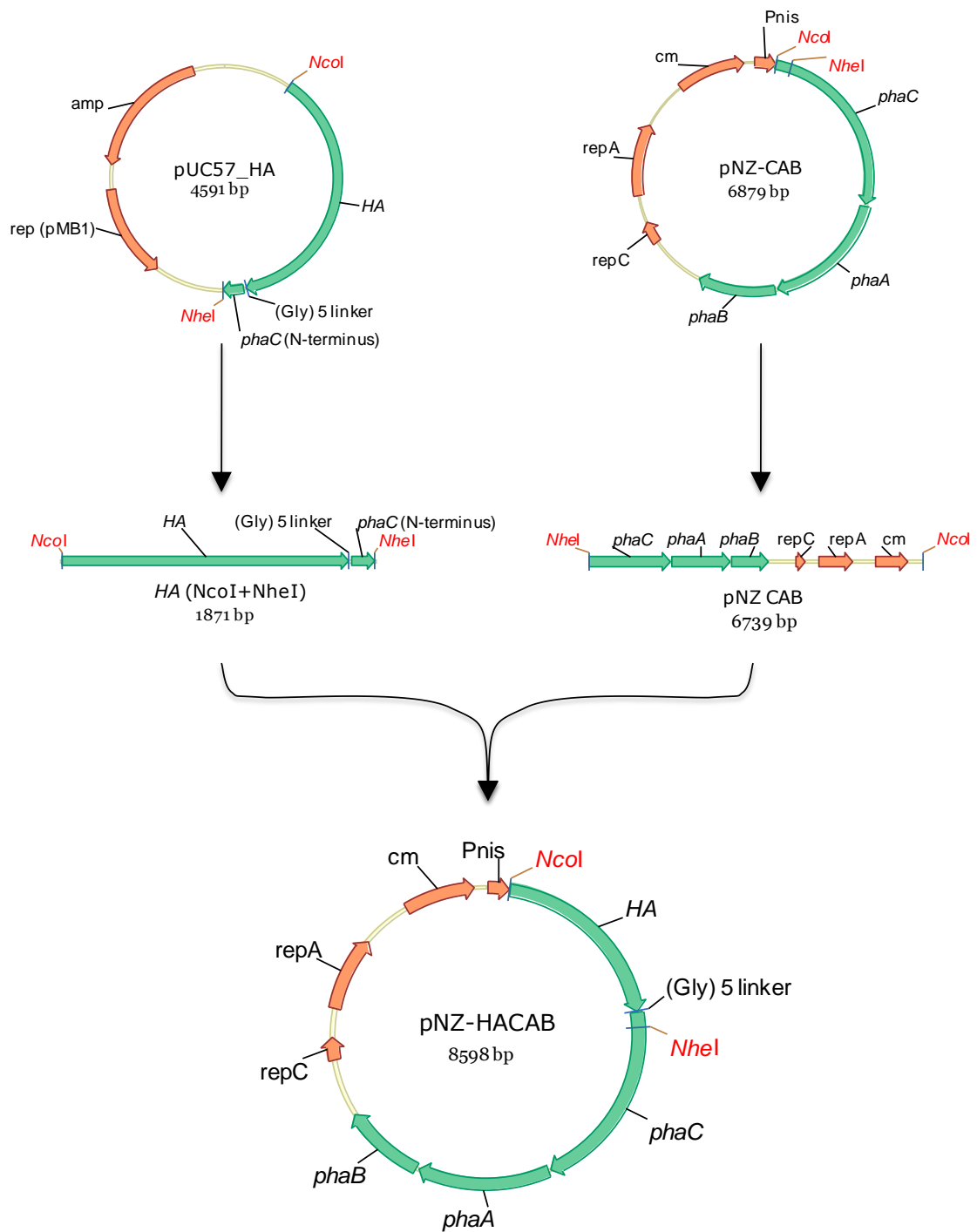
Figure 37. Construction of plasmid pNZ-HA*CAB*. Codon optimised HA was isolated from pUC57_HA by restriction digest with *Nco*I and *Nhe*I (1871bp), followed by separation of DNA fragments by agarose gel electrophoresis and gel extraction. The HA gene was ligated into linearized pNZ-CAB digested with *Nco*I and *Nhe*I downstream of the Nis$_A$ promoter using T4 DNA ligase.
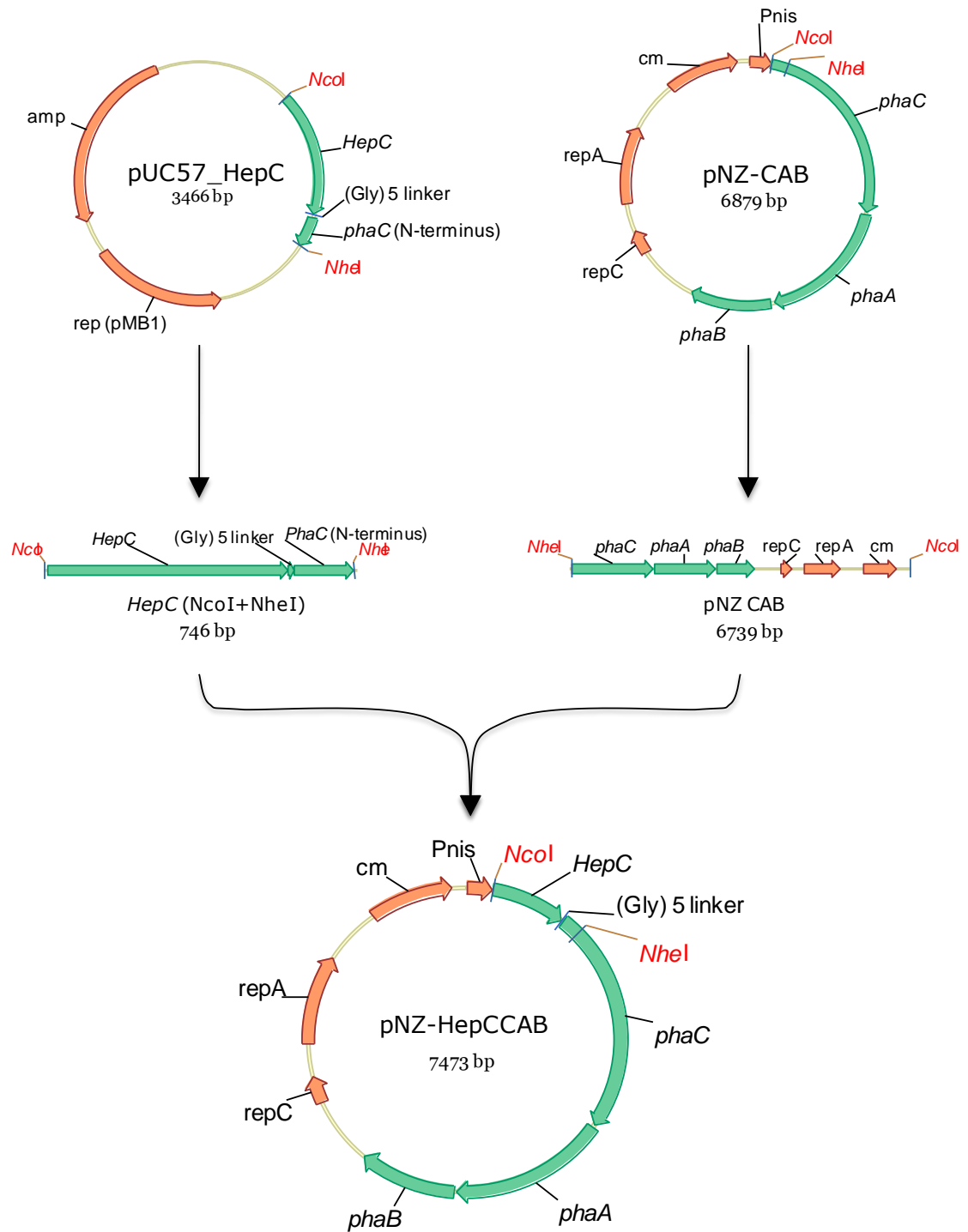
Figure 38. Construction of plasmid pNZ-HepC*CAB*. Codon optimised HepC was isolated from pUC57_HepC by restriction digest with *Nco*I and *Nhe*I (746bp), followed by separation of DNA fragments by agarose gel electrophoresis and gel extraction. The HA gene was ligated into linearized pNZ-CAB digested with *Nco*I and *Nhe*I downstream of the Nis_A promoter using T4 DNA ligase.

3.3.2 Plasmid expression and PHA bead biogenesis

PHA beads were produced in *L. lactis* NZ9000 with surface displayed antigens by expressing plasmids pNZ-HA*CAB* and pNZ-HepC*CAB* under PHA accumulating cultivation conditions in *L. lactis* as described in (2.6.1). PHA beads were isolated (2.12.1 and 2.12.2) and the protein profiles of isolated PHA beads were visualised by SDS-PAGE (2.13.2) and are shown in Figure 39. Theoretical molecular weight of the fusion proteins were calculated using the ProtParam tool from the ExPASy Proteomics Server (http://www.expasy.org/). Protein was quantified by Bradford assay (2.13.1.1) before being loaded on to SDS-PAGE (2.13.2).

A theoretical molecular weight of 128.3 kDa was expected for the HA-PhaC fusion protein. No dominant protein bands were apparent in lane 1 of Figure 39 corresponding to expression of plasmid pNZ-HA*CAB*, suggesting little to no fusion protein was produced. The theoretical molecular weight for HepC-PhaC was 85.4 kDa. A single predominant band at approximately 85.4 kDa representing HepC-PhaC fusion was apparent. The protein band intensity relative to other proteins in lane 2 indicates high overproduction of the fusion protein on the surface of the PHA beads. The identity of the HepC-PhaC fusion protein was further confirmed by Maldi-TOF/MS analysis (2.13.3) with a sequence coverage of 50 % with an average ion score > 100 (data not shown).
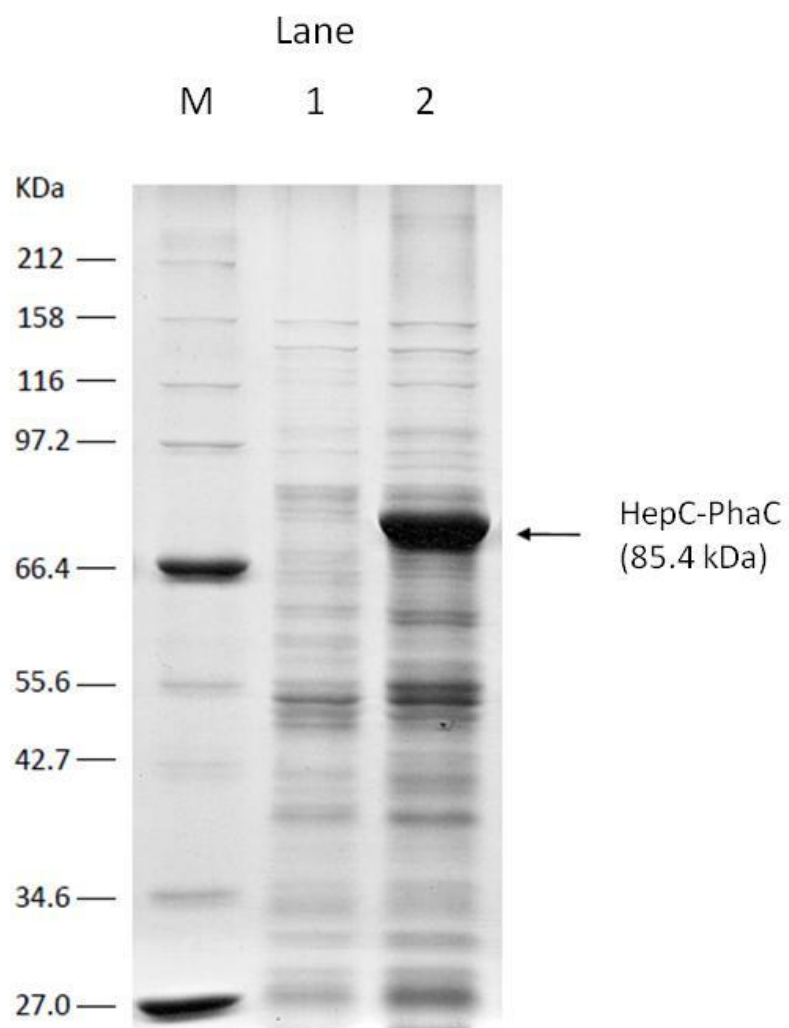
Figure 39. SDS-Page gel of *L. lactis* isolated beads harbouring pNZ plasmids. Lane M, molecular weight standard (BroadRange) ; Lane 1, protein profile for HA-PhaC beads, with an expected theroretical molecular weight of 128.3 kDa; Lane 2, protein profile for HepC-PhaC beads, with an expected theroretical molecular weight of 85.4 kDa.

3.3.3 FM and TEM analysis of PHB bead formation in *L. lactis* NZ9000

L. lactis strains harbouring plasmid pNZ-HepC*CAB* expressed under PHA accumulating conditions were stained with Nile-red and visualized using fluorescence microscopy (2.12.3). The positive fluorescence seen with *in vivo* samples in Figure 40 was indicative of intracellular PHA accumulation and indicated PHA synthase activity. However, it is important to note that the cell poles typically stain with Nile-red.

Based on FM and SDS-PAGE analysis results, only recombinant *L. lactis* harbouring plasmid pNZ-HepC*CAB* under PHA accumulating conditions was subjected to TEM analysis (2.12.5) to assess PHA bead formation, in particular shape and size. TEM results for *L. lactis* N9000 harbouring pNZ-HepC*CAB* (Figure 41) showed the formation spherical intracellular inclusion bodies of regular size distribution of 80-180 nm, with an average diameter of 140 nm.

3.3.4 Functional assessment of Hepatitis C beads in a mouse model

All subsequent work done assessing the functionality of the isolated surface displaying HepC antigen beads was done in collaboration with Natalie Parlane (Hopkirk Research Institute, AgResearch). The immunogenicity of the HepC PHA beads produced in *L. lactis* host was compared to HepC PHA beads produced in *E. coli* host using a mouse model. Results from the immunisation of mice with HepC microbeads produced in *L. lactis* stimulated the generation of a significant antigen-specific cellular immune response (346 pg/ml) by measuring cytokine IFN-γ *in vitro,* which is comparable with HepC microbeads produced in *E.coli* (557 pg/ml) and recombinant HepC (455 pg/ml). All negative controls showed insignificant levels of IFN-γ (< 70 pg/ml).
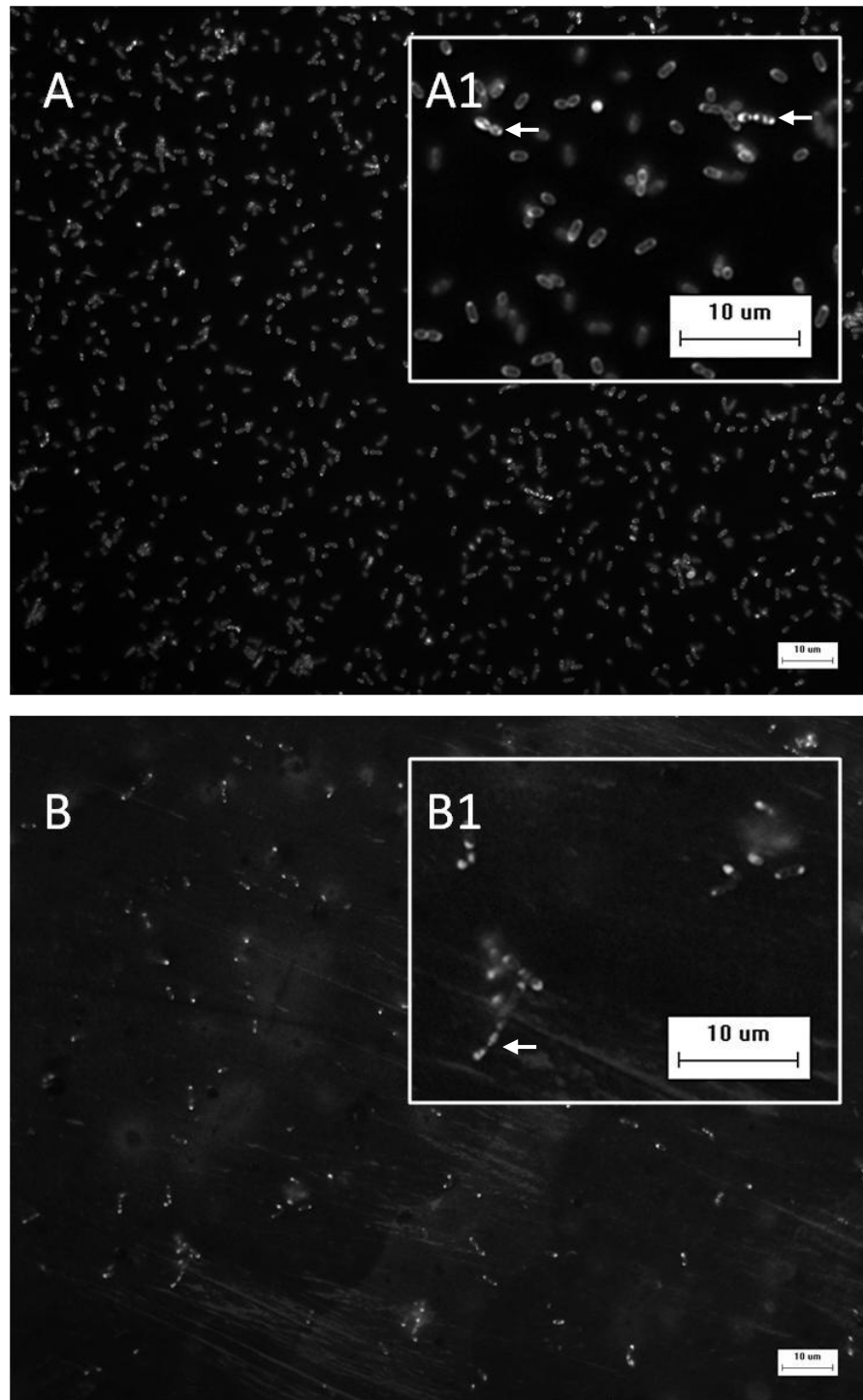
Figure 40. Fluorescence microscopy images of *L. lactis* harbouring pNZ-HA*CAB* and pNZ-HepC*CAB* expressed under PHB accumulating conditions. *L. lactis* strains were grown for 24 hours under PHB accumulating conditions harbouring either (A) pNZ-HA*CAB* or (B) pNZ-HepC*CAB*. Cells were stained with Nile-red and viewed florescence
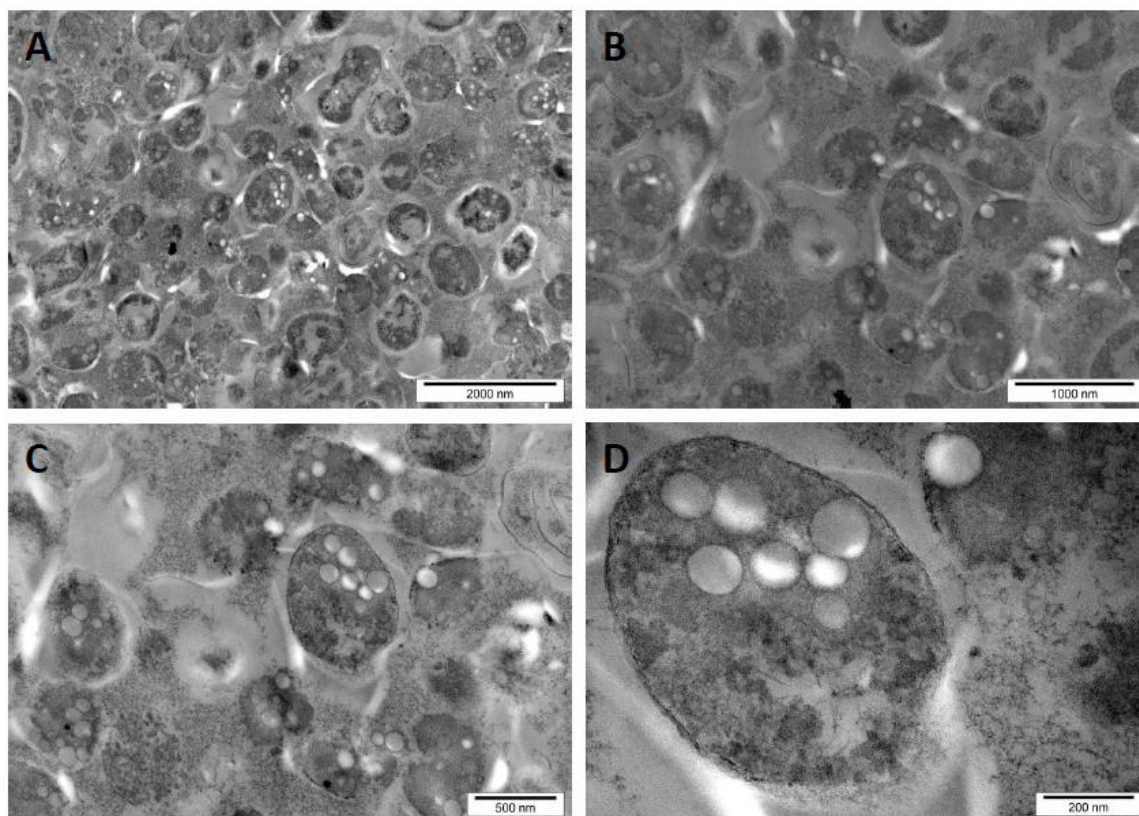
Figure 41. TEM analysis of *L. lactis* NZ9000 expressing plasmid pNZ-HepC*CAB*. (A) to (D) *L. lactis* NZ9000 cells expressing plasmid pNZ-HepC*CAB* under PHA accumulating conditions resulted in the formation of small spherical regular sized PHB inclusion bodies.

3.4 Phenotypic characterisation of NZ mutants

L. lactis is known to produce large amounts of lactate under conditions of homolactic fermentation. In a recent study by Mifune *et al.* (2009), it was suggested that PHB yield could be improved by using lactate dehydrogenase (LDH) mutant strains to help redistribute the pyruvate pool/flux towards PHB biogenesis indirectly by increases in acetyl-CoA (Figure 5). To characterise the effects of knocking out the lactate dehydrogenase pathway on PHB yield, two LDH knockout strains (NZ9010 and NZ9020) and NZ9000 (positive control) were transformed with plasmids pNZ-*CAB* (Mifune *et al*, 2009) harbouring the codon optimised PHA operon from *C. necator* and empty vector pNZ-8148 was used as the negative control. Plasmid was isolated from single colony transformants (2.11.1.3) grown on M17 media (2.3.2) containing 30 µg/ml chloramphenicol (2.5) after 48 hours incubation at 30 °C, followed by confirmation with restriction analysis (2.11.4) using restriction enzymes *Bgl*II or *Nhe*I and *Bam*HI (Figure 42). Bands of expected sizes of 4029bp and 2850bp were obtained for complete digestion and confirming successful transformation.
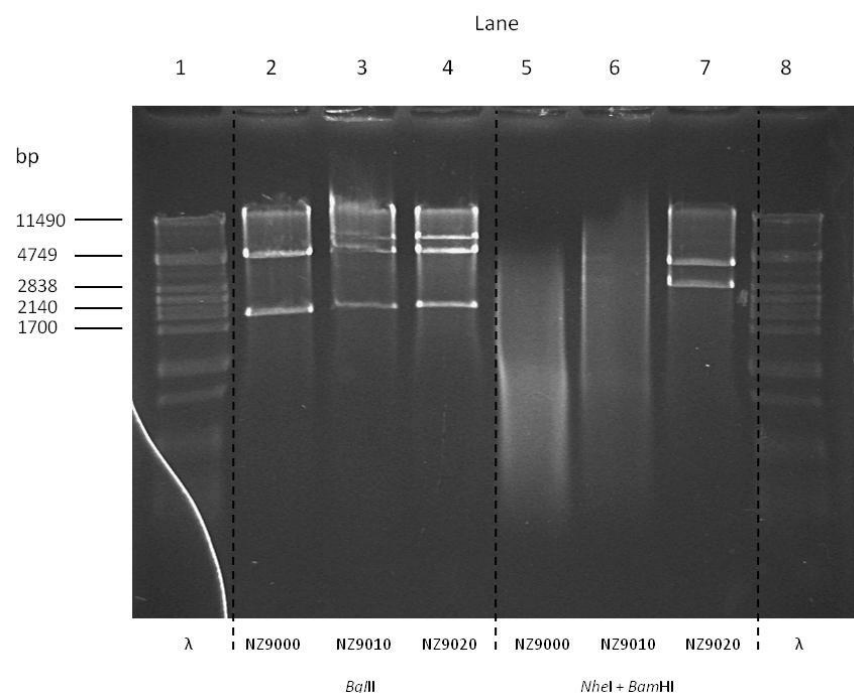
Figure 42. Restriction analysis of pNZ-CAB from NZ9000, NZ9010, and NZ9020 transformants. Lanes 1 & 8, DNA ladder standard (λ-*Pst*I); Lanes 2-4, pNZ-CAB isolated from NZ9000, NZ9010, and NZ9020 digested with *Bgl*II respectively with expected sizes of 4906bp and 1973bp (complete digestion); Lanes 5-7, pNZ-CAB isolated from NZ9000, NZ9010, and NZ9020 digested with *Nhe*I and *Bam*HI respectively with expected band sizes of 4029bp and 2850bp. The undigested DNA fragment runs at the expected size >11,000bp and partially digested DNA fragment runs at the expected size of 6879bp.

3.4.1 Growth and pH analysis of recombinant *L. lactis*

L. lactis NZ strains harbouring plasmid pNZ-*CAB* or pNZ-8148 were grown under PHB accumulating conditions (2.6.1) in the presence of 10 µg/ml chloramphenicol for NZ9000 strain, 10 µg/ml erythromycin and 10 µg/ml chloramphenicol for NZ9010 and NZ9020 strains. Experiments were conducted in triplicate.

There were no significant differences seen in the growth characteristics or media pH when *L. lactis* NZ strains (NZ9010, and NZ9020) were grown in GM17 media harbouring plasmid pNZ-*CAB* or pNZ-8148 (Figure 43) under PHA accumulating conditions, over the 24 hour period. Both LDH mutant strains NZ9010 and NZ9020 were seen to reach higher cell densities in comparison to the control strain (NZ9000) independent of plasmid. NZ9010 and NZ9020 reached maximum optical cell density (OD_{600}) of approximately 6.7 and 5.9 respectively, while NZ9000 only reached maximum optical cell density (OD_{600}) of approximately 4. The initial growth rate (first 9 hours) of NZ9010 was comparable to NZ9000. However, NZ9020 in comparison to NZ9000 or NZ9010 had a much longer lag phase approximately 6 hours compared to 4 hours seen in the other strains. As expected, there was no significant drop in the pH of the culture medium for LDH mutants harbouring plasmid pNZ-*CAB* and control vector (pNZ-8148), indicating the production of a small amount of lactic acid in comparison to NZ9000 which had a significant drop in pH, from pH 8.0 to pH 5.0.
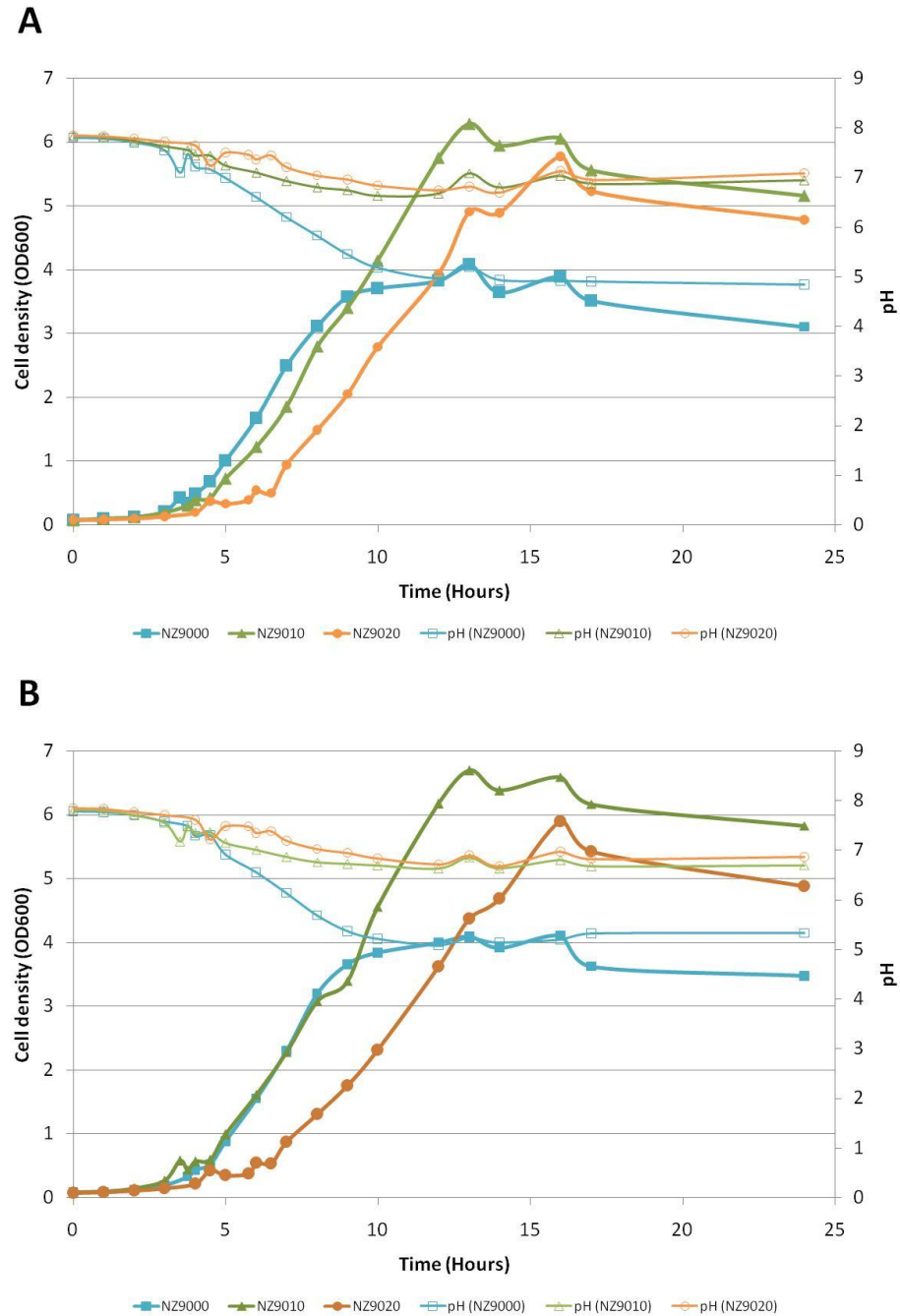
Figure 43. Growth curves of *L. lactis* NZ9000, NZ9010, & NZ9020 habouring plasmids pNZ-*CAB* & pNZ-8148. *L. lactis* strains were either transformed with (**A**) pNZ-8148 (vector control) or (**B**) pNZ-*CAB* (PHA operon) and expressed under PHB accumulating conditions for 24 hours. The optical density of the cells (measured at 600 nm) and pH was acquired at various time points. No significant difference can be seen between strains harbouring plasmid pNZ-8148 or pNZ-*CAB*. Both LDH deficient strains (NZ9010 and NZ9020) reached higher cell densities and showed minor decrease in pH in comparison to stain NZ9000. Experiments conducted in triplicate, and the mean values are shown.

3.4.2 Lactate and Acetate formation by recombinant *L. lactis*

The formation of lactate and acetate by recombinant *L. lactis* mutants was investigated to confirm LDH knockout phenotype and redistribution of carbon flux towards the acetate pathway. The culture supernatant of *L. lactis* LDH deficient mutant strains (NZ9010 and NZ9020) and wildtype control (NZ9000) harbouring both pNZ-*CAB* and pNZ-8148 (negative control) under PHB accumulating conditions were obtained at various time points during the 24 hour cultivation. The concentrations of lactate and acetate in the culture supernatant were determined as described in materials and methods (2.12.6).
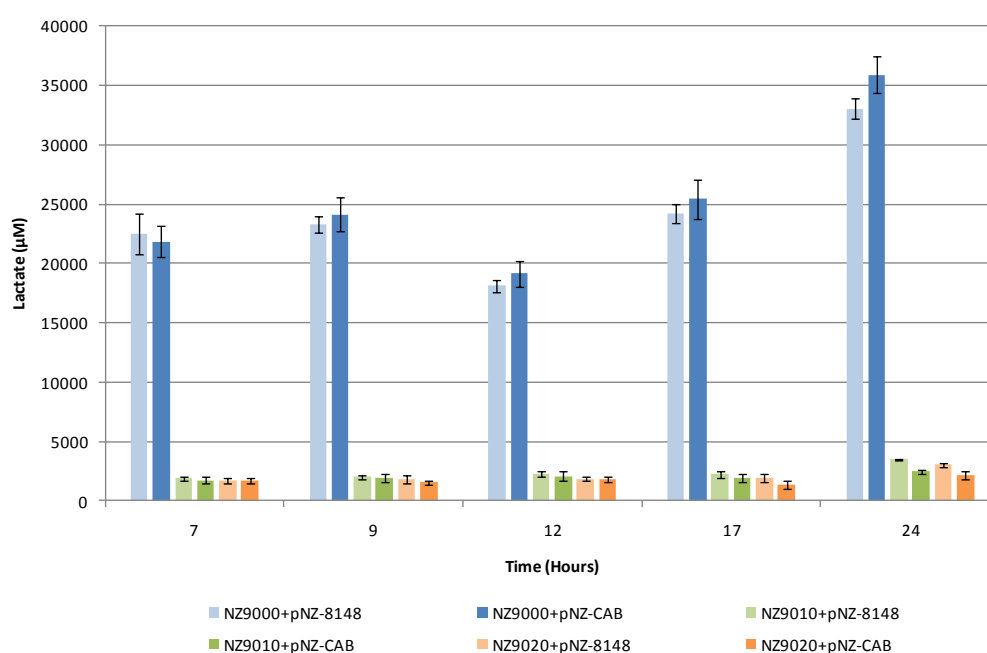
Figure 44. Lactate production by recombinant *L. lactis* NZ9000, NZ9010 and NZ9020 under PHB accumulating conditions. *L. lactis* strains NZ9000 (control strain), NZ9010, and NZ9020 were transformed with pNZ-8148 (vector control) or pNZ-*CAB* (PHA operon) and expressed under PHB accumulating conditions for 24 hours. Cell culture samples were taken at various time intervals throughout the cultivation period and processed by centrifugation to remove cells and supernatant analysed using a lactate assay kit (2.12.6). Experiments conducted in triplicate, and the mean values are shown.

By knocking out the LDH gene in *L. lactis* NZ9000, strains NZ9010 and NZ9020 were expected to produce little to no lactate during cultivation. Independent of the plasmid expressed, the LDH defective strains NZ9010 and NZ9020 did not show significant levels of lactate production (below 5 mM) over the 24 hour cultivation period in comparison to wildtype strain NZ9000 (Figure 44). No significant difference in the

level of lactate was seen between plasmids pNZ-*CAB* and pNZ-8148 in all strain, suggesting PHB production does not significantly affect lactate production.
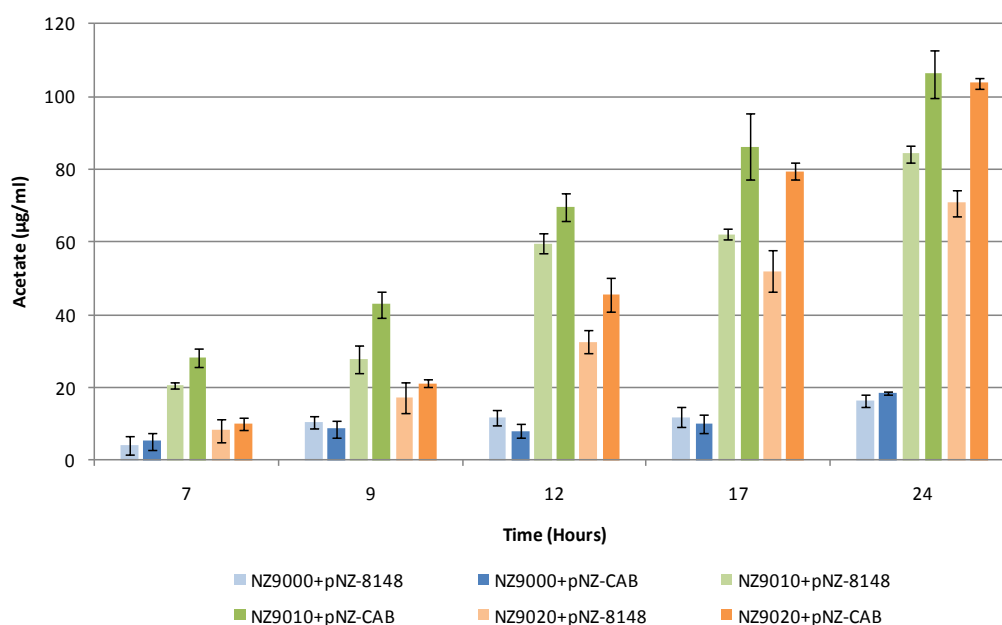
Figure 45. Acetate production by recombinant *L. lactis* NZ9000, NZ9010, and NZ9020 under PHB accumulating conditions. *L. lactis* strains NZ9000 (control strain), NZ9010, and NZ9020 were transformed with pNZ-8148 (vector control) or pNZ-*CAB* (PHA operon) and expressed under PHB accumulating conditions for 24 hours. Cell culture samples were taken at various time intervals throughout the cultivation period and processed by centrifugation to remove cells and supernatant analysed using an acetate assay kit (2.12.6). Experiments conducted in triplicate, and the mean values are shown.

After confirming the *L. lactis* LDH knockout phenotype in NZ9010 and NZ9020, a redistribution of carbon from pyruvate flux/pool through the acetate pathway and therefore, increased levels of acetyl-CoA was expected. Acetate analysis indicated both *L. lactis* LDH deficient mutant strains had significant levels of acetate production in comparison to wildtype (Figure 45). Over the 24 hour cultivation period, the level of acetate increased significantly in LDH deficient strains in comparison to the wildtype (NZ9000), which showed only a minor increase. The acetate levels in LDH deficient mutants correlate with cell density for example, NZ9010 reaches log phase sooner than NZ9020 and produces higher levels of acetate sooner, but differences between acetate concentrations become less marked towards the later phases of growth. This confirms that knocking out LDH activity leads to increased distribution of carbon through the acetate pathway.

3.4.3 Quantification of PHB in NZ strains under PHA accumulating conditions

GC/MS (2.12.4) was used to confirm the presence of PHB accumulation in *L. lactis* strains grown under PHB accumulating conditions (2.6.1) aerobically and anaerobically and results are shown as a % PHB per mg dry weight (Table 12). Results indicated that when grown under PHB accumulating conditions aerobically, there was little to no PHB present in the LDH deficient mutants NZ9010 and NZ9020. All negative controls were negative and positive control (NZ9000) harbouring pNZ-*CAB* showed an average yield of 3.57 % PHB per mg/dry weight.

Under PHB accumulating conditions anaerobically, GC/MS showed that both LDH deficient mutant strains NZ9010 and NZ9020 showed similar PHB accumulation to the positive control (NZ9000) harbouring pNZ-*CAB* (Table 12) although this produced considerably less than when grown aerobically. These results may suggest that LDH knockout mutants have a negative impact on PHB biosynthesis especially in the presence of oxygen.

Table 12. Effects of aerobic and anaerobic cultivation conditions on PHB accumulation in *L. lactis* NZ9000, NZ9010 & NZ9020

Strain	Plasmid	% PHB per mg dry weight	
		Aerobic cultivation[a]	Anaerobic cultivation[b]
NZ9000	pNZ-8148	0	0
	pNZ-CAB	3.57	1.14
NZ9010	pNZ-8148	0	0
	pNZ-CAB	0	0.71
NZ9020	pNZ-8148	0	0
	pNZ-CAB	0.04	1.93

[a] Experiments were conducted in triplicate and the mean values are shown.
[b] Experiment has not been repeated and only strains with plasmid pNZ-CAB was used

Chapter 4: Discussion

4.1 Molecular characterisation of class I PHA synthase (PhaC)

PHA synthases are important enzymes in catalysing the final enzymatic conversion of (*R*)-3-hydroxyacyl-CoA into PHA with the concurrent release of free CoA (Grage *et al.*, 2009). Currently, there are greater than 88 PHA synthases from at least 68 different bacteria. Although, extensive studies have been conducted around the synthesis mechanism and structure of these enzymes, still to date there is no resolved structural data available (Rehm, 2007). This project aimed to purify class I PHA synthase (PhaC) from *C. necator* from recombinant *E. coli*.

Significant amounts of the soluble PHA synthase enzyme, both the full length and truncated forms (93 amino acid deletion at the N-terminus) were obtained at greater than 90% purity (Figure 20). This was achieved by employing a polyHistidine affinity tag (9 or 10 histidine residues) in combination with a solubility enhancing tag (IgG binding ZZ or GB1 domain of protein A and G respectively) at the N-terminus of PhaC and purified by Immobilised Metal Affinity Chromatography (IMAC).

It is common to produce proteins in both full length and truncated forms and construction of plasmids encoding various fusion proteins increases the probability of generating soluble protein. Therefore, several different plasmids were designed utilising both the full length (64.3 kDa) and truncated (54.7 kDa) versions of the PHA synthase. The truncated form (Δ1-93C) of the class I PHA synthase was used primarily to help with protein solubility, as previously mentioned, the first 100 amino acids of the class I PHA synthase is highly variable and has been demonstrated to be dispensable (Rehm, 2003). However, the truncated version was suggested to have reduced activity. No indication of reduced activity in the truncated versions of the PHA synthase can be concluded in this study (Grage *et al.*, 2009). In addition to increasing solubility of the synthase, the truncated form should also allow for higher probability of crystallization occurring and easier determination of structure due to its reduced size.

Protein fusions to either the N- or C-terminus also need to be considered when making fusion proteins, as this can highly influence both protein solubility and protein production (Graslund *et al.*, 2008). The PHA synthase has been successfully demonstrated to tolerate a range of fusion to the variable N-terminus while still remaining functionally active *in vivo,* while fusions to the highly conserved and

hydrophobic C-terminal region proved difficult and resulted in the inactivation of the PHA synthase. Therefore, the N-terminal region of the PHA synthase is commonly targeted for protein fusions and protein fusion to the C-terminal region has only been recently demonstrated with the class I PHA synthase from *C. necator in vivo* (Grage *et al.*, 2009; Jahns & Rehm, 2009). The N-terminus region of the class I PHA synthase from *C. necator* was chosen as a first attempt in this study, as fusions of the positively charged polyHis-tag and hydrophilic IgG binding domain to the N-terminal is less likely to interfere with the normal activity of the PHA synthase as compared to fusions with the highly conserved and hydrophobic C-terminal region.

Protein production using the T7 promoter based system in an *E. coli* protein production host allowed for significant overproduction of our protein of interest (Figure 18). The majority of heterologous protein was seen to be overproduced only 2 hours post induction when induced with 1 mM IPTG. This significant overproduction of heterologous protein was due to the implementation of the strong T7-promotor in combination with the high activity of the T7 bacteriophage RNA polymerase (Lussier *et al.*, 2010). This allowed for a considerable reduction in the time required to obtain signification levels of heterologous protein. Although the protein was highly overproduced, a large fraction remained insoluble due to protein aggregation as a consequence of overproduction (Figure 18). The probability of obtaining soluble protein has been shown to decrease with proteins greater than 60 kDa (Graslund *et al.*, 2008). Plasmids $His_{10}ZZC$, $His_{10}GB1TEVD1-93C$, and $His_9ZZTEVD1-93C$ have fusion proteins of 81.86 kDa, 63.0 kDa, and 71.6 kDa respectively. In addition, large proteins in comparison to small proteins require more complex folding mechanisms, making them more likely to aggregate when associated with overproduction (Hammarstrom *et al.*, 2002).

It was observed by SDS-PAGE analysis that more heterologous protein was overproduced using *E. coli* BL21 (DE3) harbouring the pLysS plasmid compared to strains without the pLysS plasmid. The pLysS plasmid offered tighter regulation of the T7 RNA polymerase by preventing leaky gene expression as seen in BL21 (DE3) when cultured using an undefined medium e.g. Luria-Bertani (LB) medium (Figure 19). The pLysS plasmid encodes a bacteriophage T7 lysozyme which is known to inhibit the transcription of the T7 RNA polymerase (Stano & Patel, 2004).

Higher yields of soluble protein could be recovered by lowering post induction incubation temperature from 37°C to 25°C and only culturing for 2 hours post induction. Lowering of growth temperatures between 15 °C to 25 °C is commonly used for increasing yield of soluble protein. This allows for proper protein folding by slowing protein production (Baneyx, 1999). It was seen that when cultured for more than 2 hours post induction, the recombinant protein became increasingly insoluble, while no significant increases of protein formation was observed, resulting in less soluble protein (Figure 18). Formation of insoluble aggregates is thought to be related to two factors, rate of translation and rate of protein folding (Bucher *et al.*, 2002; Esposito & Chatterjee, 2006). However, in addition to lower temperatures, co-production of chaperons and modulators can also help increase the probability of obtaining soluble protein by providing an environment which promotes protein folding. Other commonly tested parameters include different protein production strains (Esposito & Chatterjee, 2006). Due to time limitations these other factors have yet to be explored.

A major known bottle neck with protein purification is the formation of insoluble protein aggregates, leading to poor recovery of soluble recombinant protein. Greater than 50% of all recombinantly produced protein in *E. coli* accumulates as insoluble aggregate (Waugh, 2005). The most common strategy for increasing protein solubility involves protein fusion with a known solubility enhancing proteins (Hammarstrom *et al.*, 2002). Currently, there is a large list of available solubility-enhancing fusion tags (protein which are known to have high solubility properties) and for this study the ZZ domain of protein A from *Staphylococcus aureus* and GB1 domain of protein G from *Streptococcus* group G. Other well known examples include maltose-binding protein, N-utilization substance A and more recently SUMO (Waugh, 2005). These are commonly employed as solubility enhancing fusion tags for heterologous protein production in recombinant *E. coli* and have been successfully used to purify a range of proteins (Esposito & Chatterjee, 2006; Zhou & Wagner, 2010). However, certain solubility-enhancing tags have been shown to be more successful than others and they do not provide a universal means for enhanced solubility (Terpe, 2003). In addition, solubility-enhancing tags are frequently used in conjunction with small affinity tags, such as polyHis-, polyarg- and FLAG- tags to aid purification (Terpe, 2003). His-tags are by far the most frequently used small affinity tag for recombinant protein purification by immobilisation metal affinity chromatography (IMAC). His-tags are

known to offer lower levels of protein solubility and enhanced protein production in comparison to other types of solubility tags (Hammarstrom *et al.*, 2002). For this study, several plasmids were designed involving dual tag fusions of a polyhis (9-10 histidines) and a IgG binding (ZZ or GB1) domain to the N-terminus of a full length or truncated PHA synthase (class I) from *C. necator*. Only the N-terminal ZZ domain fusion plus N-terminal polyhis fusion to the full length PHA synthase was used to assess the effects on solubility and protein production in comparison to wildtype (PhaC) PHA synthase in recombinant *E. coli* (Figure 17).

All *E. coli* BL21 (DE3) pLysS strains expressing their respective plasmids showed overproduction of their fusion protein after induction using 1 mM IPTG in early log phase and grown for 2 hours post-induction to maximise yield of soluble protein (Figure 17). In comparison to the wildtype (PhaC), both plasmids, either with the N-terminal ZZ domain or polyHis-tag, showed enhanced levels of protein production, with the latter being more effective as assessed by SDS-PAGE (Figure 17 A lanes 4-6). This is a result of the affinity/solubility tag, which is thought to provide a reliable context for translation initiation, leading to increased translation and resulting in more protein production (Waugh, 2005). In addition, increased protein production was seen to correlate with increased levels of protein aggregation as indicated in the low speed centrifugation fractions and insoluble fractions (Figure 17 A lanes 7-9 and B lanes 16-18).

The fusion of a ZZ domain of protein A to the PHA synthase led to significant increase in the level of protein solubility of the recombinant PHA synthase in comparison to wildtype (PhaC) without the solubility-enhancing tag (Figure 17 B, lanes 13-14). An approximately 3 fold increase in the level of protein in the soluble fraction compared to wildtype (PhaC) was observed with the fusion. This indicates the high solubility property of the ZZ domain confers a positive effect on solubility of the PHA synthase. However, the N-terminal polyhis showed poor protein solubility in comparison to the wildtype and can be considered to have a negative impact on protein solubility. This significant difference is a consequence of overproduction, leading to significant amounts of protein aggregation. However, a combination effect of the two tags may offer to be advantageous than the use of individual tags alone for protein solubility and protein production.

Enhanced solubility and protein production of the polyHis-tag, ZZ domain and GB1 domain have been extensively demonstrated as described in the literature (Bucher *et al.*, 2002; Hammarstrom *et al.*, 2002). It is important to note, protein solubility and yield is highly influenced by the type of tags employed (Hammarstrom *et al.*, 2002). It is therefore, advisable to optimise solubility and protein production for each system by screening a number of available affinity and/or solubility tags as each tag varies in its ability to express and solubilise protein (Esposito & Chatterjee, 2006). However, due to time restraints, other fusion tags have yet to be explored.

Potential drawbacks of affinity tags include interference with normal biological activity of target protein or its ability to crystallize (Bucher *et al.*, 2002). Therefore, fusion proteins with affinity/solubility tags are commonly designed to be removed by site specific proteases e.g. Tobacco Etch virus (TEV) (Graslund *et al.*, 2008). However, crystallization and NMR studies involving uncleaved polyHis-tagged proteins have successfully generated three-dimensional structures. In comparison to the cleaved versions, it has been demonstrated there is little to no difference between their resulting three-dimensional structures (Graslund *et al.*, 2008).

In this project it was demonstrated that the fusion partner can be successfully cleaved from fusion proteins $His_9ZZTEV\Delta1-93C$ and $His_{10}GB1TEV\Delta1-93C$ containing the site specific TEV recognition sequence (EXXYXQ(G/S)) when treated with TEV protease (Figure 21). SDS-PAGE analysis confirmed that both proteins were successfully cleaved from its fusion partner resulting in a ~54.7 kDa band which is consistent with theoretical molecular weight of $\Delta1-93C$. However, three prominent bands were seen for fusion protein $His_{10}GB1TEV\Delta1-93C$, with one identified as $\Delta1-93C$ and the 50 kDa band as TEV protease. A slightly smaller molecular weight band ~47 kDa was unexpected and has yet to be identified by Maldi-TOF/MS analysis as outlined in (2.13.3). The extra resulting band could either be a degradation product or even due to nonspecific proteolytic cleavage due to prolonged reaction times.

Cleavage of solubility tags in some cases has been shown to render the target protein insoluble (Esposito & Chatterjee, 2006). Solubility of the cleaved PHA synthase however, solubility of the cleaved product needs to be assessed before it can be used for crystal studies. Solubility can be demonstrated by removing the TEV protease after digestion by binding the protease and cleaved fusion partner with IMAC (Ni^{2+}-NTA),

then subjecting the cleaved fusion product to ultracentrifugation at 100,000 x g for 2 hours and assessing fractions by SDS-PAGE. However this has yet to be assessed.

Affinity purification utilizing immobilisation metal affinity chromatography (IMAC) and a small polyHistidine-tag is the most commonly employed method to purify recombinant protein (Terpe, 2003; Waugh, 2005). This is based on the strong interaction of the histidine residues with a transition metal ion (Ni^{2+}), forming dative covalent bonds between the histidine with the immobilised transition metal (Bucher *et al.*, 2002; Terpe, 2003). Due to this strong interaction, recombinant protein displaying consecutive histidine residues are effectively retained on the column. Nonspecific host proteins are typically removed by several mild washing steps containing low concentrations of imidazole. Elution of the bound recombinant protein can be achieved using high concentrations of imidazole (typically > 200 mM). It is important to note, however, presence of imidazole can also result in protein aggregation (Terpe., 2003). Purification efficiency is dependent on the length of the polyHistidine and the solvent used (Terpe, 2003). Several polyHistidine-tagged (9 - 10 histidines) N-terminally fused to either a truncated or full length phaC were successfully constructed in this study. SDS-PAGE analysis of protein fractions from affinity purification (Figure 20) of $His_{10}ZZC$, $His_9ZZTEV\Delta 1-93C$, and $His_{10}GB1TEV\Delta 1-93C$ showed that recombinant protein was successfully purified to greater than 90% purity by employing an N-terminal polyHistidine-tag and purification by IMAC. Various buffers and salt concentrations were altered to enhance protein solubility and reduce contaminants. These variables included buffers (KPO_4, PBS, HEPES) and salt concentration ($0 - 250$). Results on SDS-PAGE indicated no significant differences in terms of solubility or reduction in contaminants for the different buffers used (data not shown).

Gel filtration chromatography using an AKTA explorer 100 system with a Superdex 200 10/300 column was used to analyse and purify the His-tagged proteins prior to crystallisation studies. Chromatogram results for fusion protein $His_{10}ZZC$ (Figure 23) and $His_{10}GB1\Delta 1-93C$ (Figure 24) indicated the presence of protein oligomerisation (dimer or trimer). In addition, an equilibrium is seen between the monomer and oligomer states of the purified PHA synthase in a 2:1 ratio. To further substantiate this observation, the fraction for peak at 12.81 ml for $His_{10}ZZC$ gel filtration run (Figure 23 A) corresponding to the approximately 200 kDa protein complex was concentrated using a centrifuge concentrator with a 30 kDa cut-off, before being re-analysed using

gel filtration under the same running conditions (Figure 23 B). The resulting chromatogram was similar to that obtained earlier. This is consistent with reports in the literature whereby purified PHA synthases have been shown to exist in an equilibrium of monomeric and dimeric forms (Rehm, 2007). This also fits in with the recently proposed reaction mechanism model based on lipases belonging to the α/β-hydrolase superfamily, whereby active PHA synthase involves the formation of homodimers in class I when substrate is present (Rehm, 2003; Valappil *et al.*, 2007).

The preparation of high quality protein crystals for X-ray crystallography still remains a major obstacle (Benvenuti & Mangani, 2007). Crystal formation is a phase shift which occurs when an aqueous protein solution is brought into a state of supersaturation (Chayen, 2004). The process of obtaining suitable crystals is cumbersome despite advances in the theory and practice in the field of crystallisation. A protein purity of 90-95% should be achieved before attempting crystallization screening (Benvenuti & Mangani, 2007).

Significant quantities of PHA synthase were successfully purified to greater than 90% from plasmids $His_{10}ZZC$ and $His_{10}GB1\Delta1$-93C in the present study. In the first attempt at crystallisation, uncleaved form of the PHA synthase fusion protein was used for screening of crystallization conditions in a vapour diffusion setup. However, the likely hood of not obtaining a protein crystal is far greater than obtaining one (Chayen, 2004). To date, no protein crystals have been identified in any of the reactions set up so far (i.e. after 5 - 6 months). Buffers which contain phosphate (50 mM KPO_4) produced unwanted salt crystals in the crystal screens and therefore 50 mM HEPES buffer was used to replace KPO_4 buffer in subsequent screens. Significant amounts of precipitation were observed when initially setting up the screen, indicating high supersaturation. It was noted, samples which were incubated at 4 °C showed reduced amount of protein precipitation and indicates proteins are not as stable at room temperature.

There are many reasons why no protein crystals have been produced so far and the most likely reasons will be discussed below. Although, the protein was purified to greater than 90% purity, even very tiny amounts of contamination can inhibit protein crystallization by interfering with the nucleation process and protein concentrations of 95 - 99% may be required to successfully obtain protein crystals (Benvenuti & Mangani, 2007).

Concentration of a protein for crystallization can vary considerably, from as low as 2 mg/ml to as high as 100 mg/ml (McPherson, 2004). Therefore, concentration of the protein plays a very important role, as several states of supersaturation can occur (1): high supersaturation, resulting in precipitation; (2): moderate supersaturation, where spontaneous nucleation will occur; (3): metastable zone, where nucleation may occur; and (4) undersaturation where no nucleation will occur (Chayen, 2004). The metastable zone is the zone where protein crystal formation is more likely to occur (Benvenuti & Mangani, 2007).

A large library of protein crystal structures with uncleaved His-tags have been resolved and entered into the RCSB Protein Data Bank (PDB) (Bucher *et al.*, 2002). However as previously mentioned, effects of affinity tags are not universal and although small affinity tags such as the His-tag are less likely to interfere with crystallization, this may not always be the case (Bucher *et al.*, 2002; Terpe, 2003). Commonly used affinity tags are removed by site specific proteolytic digestion to avoid the negative effects of the fusion tag. The positive charge of the polyHis-tag may be interfering with normal protein crystallisation by causing the individual protein molecules to repel each other. In this study we have employed His-tags which have 9 to 10 consecutive histidine residues, while commonly hexahistidine tags (His_6) are used. In addition, the solubility tag (ZZ or GB1) may also interfere with protein crystalisation. However, cleavage of the solubility tag in some cases cause the passenger protein to become insoluble. The next logical step involves the crystalisation of the cleaved PHA synthase product. Solubility of the cleaved fusion product has yet to be determined.

It has also been suggested that the lack of structural homogeneity in a single invariant state may prevent crystallisation from occurring (Benvenuti & Mangani, 2007; McPherson, 2004). Gel filtration analysis has indicated that purified PHA synthase exists in a state of equilibrium between monomer and different oligomeric states in a ratio of 2:1 respectively (Figure 23). Addition of substrate or a substrate analogue prior to crystallization trials may help shift the oligomerization state to one predominant form and therefore increase the probability of crystallization occurring (Rehm, 2007).

In addition, other major contributing factors which need to be considered include temperature, buffer, pH, salt concentrations and contamination.

4.2 Production of PHA inclusions *in vivo*

A large number of proteins and enzymes have already been successfully immobilised on the surface of these polyester beads to produce functionalised micro beads (Grage *et al.*, 2009). In this project, N-terminal fusion of the polyHis-tag and IgG binding domain to the N-terminus of the truncated and full length PHA synthase does not inhibit its activity by expressing the respective plasmids in *E. coli* BL21 (DE3) under PHB accumulating conditions. Interestingly, it was observed that *E. coli* cells expressing plasmids encoding the polyHis-tag produced PHB *in vivo* which were extremely small, which were up to 60% smaller than there respective controls.

SDS-PAGE of isolated PHB beads confirmed the overproduction of the fusion protein displayed on the surface of these isolated beads when isolated from recombinant *E. coli* harbouring plasmids encoding proteins $His_9ZZTEVD1-93C$, $His_{10}ZZC$, and $His_{10}GB1TEVD1-93C$ using the T7 system in *E. coli* (Figure 28). Other prominent protein bands were also present and have been previously identified as ATPase, Elongation factor-Tu and outer-membrane proteins (OmpF and OmpA) which commonly are found to co-purify with PHA beads produced in *E. coli (*Backstrom *et al., 2007).*

Intracellular PHB accumulation *in vivo* was confirmed by positive fluorescence seen under fluorescence microscopy when stained with lipophilic dye Nile-red (Figure 29) and subsequently confirmed and quantified using GC/MS analysis (Table 11). This indicated both versions of the PHA synthase; truncated and full length was functionally active. The truncated form of the PHA synthase was suggested to have reduced activity in comparison to the full length (Rehm, 2003; Grage *et al.*, 2009). However, no significant difference in activity can be concluded between the full length and truncated forms of the PHA synthase based on GC/MS results.

Under fluorescence microscopy PHB inclusion bodies were observed to be extremely small when produced with a polyhistidine-tag. These beads were up to 60% smaller than there respective controls and indicates that the polyHis-tag may play a role in PHB inclusion size (Figure 29). This observation was further confirmed by Transmission Electron Microscopy (TEM) of cells harbouring plasmids encoding WT (PhaC) and $pET16b-His_{10}C$, $pET14b-ZZTEV\Delta1-93C$ and $pET14b-His_9ZZTEV\Delta1-93C$, respectively (Figure 30). TEM results shows that PHB beads isolated from *E. coli*

expressing plasmid pET16b-His$_{10}$C had a bead diameter of between 31 nm to 249 nm and an average diameter of 97 nm, which is 53 % smaller in comparison to nonHis-tagged WT (PhaC) beads which have an average diameter of 174 nm and range between 62 - 424 nm (Figure 31). Similarly, PHB beads isolated from cells harbouring plasmid pET14b-His$_9$ZZTEVΔ1-93C produced beads with a diameter ranging from 54 nm to 410 nm with an average diameter of 175 nm which were 61% smaller compared to nonHis-tagged ZZTEVΔ1-93C (51 - 933 nm with an average of 295 nm) (Figure 31). In both cases expression of plasmids producing PHA synthase with the N-terminal polyHis-tag, produced significantly smaller PHA beads compared to their respective controls. This observation is possibly the result of the strong positive charge of the histidine residues causing like charges to repel each other. This repulsion is likely preventing the PHA beads coalescing during early stages of PHB bead formation, and hence the nano sized PHB beads. This observation would be consistent to the current model of bead formation *in vivo*, whereby larger PHA beads occur by coalescence of smaller PHA beads (Thomson *et al.*, 2009). This observation is consistent with why protein crystallisation with the uncleaved polyHis-tag has not occurred. Therefore, addition of a polyHis-tag of varying sizes could possibly be used as a way to control PHA bead size *in vivo*. It is also interesting to note that PHA beads produced from the expression of pET14b-ZZTEVΔ1-93C were considerably larger on average than the WT (PhaC) (Figure 31). This suggests either the 93 amino acid truncation or the IgG binding domain, or a combination of both, may be affecting bead size.

Enzyme-linked immunosorbent assay (ELISA) and subsequently IgG purification assay were used to assess the functionality of the IgG binding domain fused to the N-terminal of the PHA synthase. ELISA results (Figure 31 and 32) confirmed the display of the IgG binding (ZZ or GB1) domain at the surface of the PHB beads. Functionality of the surface displaying IgG binding domain was confirmed using IgG purification assay (Figure 34). Results successfully demonstrate that PHB beads isolated from the expression of plasmids pET16b-His$_{10}$ZZC, pET14b-ZZTEVΔ1-93C, pET14b-His$_9$ZZTEVΔ1-93C, and pET14b-His$_{10}$GB1Δ1-93C mediated significant levels of purified IgG which is comparable to commercially available protein A sepharose beads (GE, USA). Positive actively of the IgG binding domain of the purified PHB beads and demonstrates correct protein folding of the surfaced displayed IgG binding domain. Proper folding of this domain is important when used as a tag to help solubilise PHA

synthase (Figure 17). The purity of the eluted IgG was checked by SDS-PAGE analysis (Figure 35). The purity of the eluted IgG from $His_{10}ZZC$, $ZZTEV\Delta1$-93C, $His_9ZZTEV\Delta1$-93C, and $His_{10}GB1\Delta1$-93C is comparable to the commercially available Protein A sepharose beads (GE, USA) and is similar work published by Brockelbank *et al.* (2006).

4.3 *L. lactis* as a production host for PHA beads displaying surface immobilised antigens

The majority of PHAs which are engineered to display surface immobilised proteins are produced in Gram-negative organisms, primarily in recombinant *E. coli* (Grage *et al.*, 2009; Parlane *et al.*, 2009). However, Gram-negative organisms contain lipopolysaccharides endotoxins which are known to co-purify with functionalised PHA beads and this is undesirable in medically relevant applications. Therefore, the production of endotoxin free PHA beads in Gram-positive organisms are favourable alternatives, in particular generally-regarded-as-safe *L. lactis.* Only recently the PHB biosynthetic pathway from *C. necator* was established in recombinant *L. lactis* NZ9000 by Mifune *et al.* (2009). In addition to establishing the PHB biosynthetic pathway, Mifune and co-workers had also demonstrated that functionalised PHB beads could be produced displaying the IgG binding ZZ domain of *Staphylococcus aureus* protein A. Much like the ZZ beads produced in Gram-negative *E. coli,* ZZ beads produced from *L. lactis* showed equivalent binding and elution of IgG from the beads. This paved the way for further studies involving immobilization of proteins, in particular medically relevant proteins on the surface of PHB beads produced in recombinant *L. lactis*.

In this project, medically relevant functionalised PHB beads displaying surface immobilised antigens were made in Gram-positive GRAS *L. lactis* (NZ9000) as a safe production system which is comparable to immobilised antigen beads made in *E. coli*. Influenza A virus (H2N2) Hemagglutinin (HA) and Hepatitis C virus core antigen (HepC) were chosen as candidates, as HA and HepC beads made in *E. coli* have been successfully produced and assessed by Natalie Parlane (Hopkirk Institute, AgResearch).

SDS-PAGE analysis of the purified PHB beads from *L. lactis,* HepC-PhaC and HA-PhaC showed only HepC-PhaC fusion protein was found to be successfully

overproduced at the surface of the PHB beads using the nisin-controlled gene expression system (NICE) for the production of heterologous protein in recombinant *L. lactis* (Figure 39). It is not clear why HA-PhaC was not expressed, however, this could be due to the weak production of HA protein under the NICE system and/or instability of the fusion leading to mis-folding and degradation. The HepC-phaC fusion was further confirmed by Maldi-TOF/MS (2.13.3). Results show sequence coverage of 50 % with ion scores > 100 on average (data not shown). In addition, the HepC-PhaC fusion protein gene has been successfully expressed in *E. coli* under the control of the T7 promoter. In comparison to HepC-PhaC made in *L. lactis*, significantly less fusion protein was seen on the surface of the PHB beads produced in *E. coli* (data not shown). Suggesting the NICE system may offer tighter regulation and high degree of induction (Mierau & Kleerebezem, 2005).

FM analysis of *L. lactis* expressing plasmids pNZ-HA*CAB* and pNZ-HepC*CAB* shows accumulation of PHB at very low levels, indicated by the positive fluorescence in only a few cells (Figure 40). In *L. lactis* it is possible using the NICE system to accumulate 50% of its total cellular protein in recombinant protein (Mierau & Kleerebezem, 2005). Since the NICE system for protein production is influenced by nisin-dose dependent gene expression, optimisation of the nisin concentration used during induction could result in higher production of the fusion protein of interest (Mierau & Kleerebezem, 2005). However Mifune *et al.* has shown that concentrations > 2.5ng/ml only gave minimal increase in PHB yield and concentrations > 10 nm/ml had an inhibitor effect on growth (Mifune *et al.*, 2009). It has also been suggested by Mifune *et al.* (2009) that more fundamental modification besides medium composition, growth and induction conditions may be required to increase PHB yield in *L. lactis*.

TEM analysis (2.12.5) was used to assess PHB inclusion body formation *in vivo* in *L. lactis* strain NZ9000 expressing plasmid pNZ-HepC*CAB*. These inclusion bodies appeared to form spherical intracellular inclusion bodies, which has an approximant diameter of 140 nm, similar to what's been observed previously by Mifune *et al* (2009) (Figure 41). These PHB beads appeared more uniformed in size than beads produced for other organisms such as *E. coli* (Grage *et al.*, 2009).

Functionality of the isolated surface displaying HepC antigen beads was done in collaboration with Natalie Parlane (Hopkirk Research Institute, AgResearch). A mouse

model was used to functionally assess the immune response specifically to the antigen being displayed and not a response to endotoxins. Results successfully demonstrated that PHB beads displaying HepC core antigen on it surface produced in *L. lactis* mediated a significant antigen-specific cell immune response in comparison to the controls or other groups in the trial. In addition, the immune response was comparable to other vaccinated groups/controls such as the HepC microbeads produced in Gram-negative *E. coli* and recombinant HepC produced in *E. coli*. However, the overproduction of HepC-PhaC fusion protein seen in recombinant *L. lactis* did not correlate to an immune response greater than that seen with beads isolated from recombinant *E. coli* which showed approximately 2 time less fusion protein on SDS-PAGE (data not shown).

This study has shown that PHB beads engineered to display Hepatitis C virus core antigen (HepC) can be produced in an endotoxin free Gram-positive host which can mediate a significant antigen-specific cell mediated immune response comparable to HepC-phaC beads produced in *E. coli*. Other examples of successfully immobilised antigen in recombinant *E. coli* which could be produced in a Gram-positive host include Antigen 85A (Ag85A) and early secreted antigenic target (ESAT-6) from *Mycobacterium tuberculosis* (Parlane *et al.*, 2009).

4.4 Characterisation of PHB biogenesis in LDH deficient *L. lactis* strains

The production of PHA in Gram-positive organisms such as *C. glutamicum* and *L. lactis* is relativity poor (22% and 6 %, CDW respectively) in comparison to their Gram-negative counterparts (Jo *et al.*, 2006; Mifune *et al.*, 2009). However, in a recent publication by Mifune *et al.* (2009), it was suggested PHB yield in *L. lactis* could be improved by looking at the organism's metabolic flux, in particular the pyruvate pool/flux in LDH deficient mutant strains of *L. lactis* NZ9000. To assess this hypothesis, two currently available mutant strains NZ9010 and NZ9020 were employed in this study. NZ9010 in a derivative of NZ9000 with a single *ldh* gene knockout, while NZ9020 is a derivative of NZ9010 with an additional lactate dehydrogenase gene (*ldhB*) knockout (Bongers *et al.*, 2003; Hoefnagel *et al.*, 2002). PHB production in the non-native host *L. lactis* was mediated by the transformation of plasmid pNZ-CAB, harbouring codon optimised genes (PHA operon) from *C. necator* (Figure 36).

Several parameters were assessed to characterise *L. lactis* mutant strains when growth under PHB accumulating growth condition over a 24 hour period, these include optical density, media pH, lactate and acetate. No differences were seen in the growth characteristics or media pH when *L. lactis* NZ strains (NZ9010, and NZ9020) grown in GM17 media harbouring plasmid pNZ-*CAB* or pNZ-8148 (Figure 43). This suggests PHB production does not impact on growth or pH. It was observed that both LDH deficient mutants NZ9010 and NZ9020 independent of plasmid expressed reached high cell densities in comparison to control NZ9000. Although, NZ9020 tends to have a much longer lag phase in comparison to both NZ9000 and NZ9010. This increase growth to high cell densities seen in mutant strains is most likely corresponding to the pH in the media, as lower pH seen in NZ9000 may be inhibitory to growth (Mifune *et al.*, 2009). Change in the media pH is primarily due to the synthesis of lactate acid as a product of fermentation (Hoefnagel *et al.*, 2002). pH levels measured in growth culture show LDH mutants NZ9010 and NZ9020 produce very little lactate in comparison to wildtype strain NZ9000 (Figure 43). Lactate analysis of culture medium confirms the LDH knockout phenotype for both NZ9010 and NZ9020, as insignificant levels of lactate (< 5mM) was produced in comparison to NZ9000 (34 -36 mM) in the 24 hour sample of the culture medium (Figure 44). The level of lactate produced correlates with what was observed with the change in pH in the culture medium (Figure 43).

After confirming the *L. lactis* LDH knockout phenotype in NZ9010 and NZ9020, a redistribution of the carbon flux from pyruvate which is normally directed to lactate production towards other products such as acetate or PHB biogenesis indirectly via increase in acetyl-CoA (Figure 5). Acetate analysis of the growth medium shows increase in the level of acetate produced in LDH deficient strains which is significantly higher than the control (NZ9000) (Figure 45), confirming what was expected and whats shown in literature (Hoefnagel *et al.*, 2002). However, it is interesting to note the level of acetate in strains harbouring plasmid pNZ-*CAB* under PHB accumulating condition is slightly higher than its corresponding strain harbouring plasmid pNZ-8148 (negative control). The formation of PHB was expected to decrease the level of available acetyl-CoA for acetate formation due to the increased distribution of acetyl-CoA towards PHB biogenesis.

GC/MS analysis showed that under aerobic PHB accumulating growth conditions, positive control NZ9000 harbouring pNZ-*CAB* showed an average yield of 3.57 % PHB

per mg/dry weight, which is in similar to that previously published by Mifune *et al.* (2009) for PHB accumulation under aerobic condition, with glucose as the carbon source and additive L-Arginine (Table 12). All negative controls were negative. However, very little to no PHB is present in NZ9010 and NZ9020 in comparison to NZ9000 harbouring plasmid pNZ-*CAB*. This result was unexpected and in addition, the higher level of acetate found in NZ9010 and NZ9020 harbouring plasmid pNZ-*CAB* may suggest the LDH knockout phenotype may have a negative impact on PHB biogenesis. However, under anaerobic PHB accumulating growth conditions, showed a considerable increase in levels of PHB produced in LDH deficient mutants in comparison to cultivation under aerobic conditions. *L. lactis* is a facultative aerobe, meaning the main metabolism is through the anaerobic pathway and this could explain the increase in PHB in *L. lactis* mutants grown under anerobic condition. Under these conditions an increase in lactate formation in normal wildtype *L. lactis* is expected when compared to growth under aerobic conditions. Since *L. lactis* LDH mutants are unavailable to produce significant amounts of lactate, we would see this correlating to an increase in PHB yield due to the indirect increase in available acetyl-CoA under anaerobic growth conditions. This hypothesis could be tested by quantifiying levels of lactate and acetate produced during anaerobic fermentation with wildtype and LDH mutants and comparing results to cultivation under aerobic conditions.

Acetate formation is seen to be dominant over PHB biogenesis and results in increase acetyl-CoA being directed towards acetate formation and not PHB. This may suggests why NZ9020 has much higher production of PHB in comparison to NZ9010. This is illustrated in Figure 45, where the production of acetate in NZ9020 is much slower than NZ9010 and has allowed more time for acetyl-CoA to be directed towards PHB biogenesis.

PHB production using LDH deficient mutants NZ9010 and NZ9020 did not mediate significant increases in PHB in comparison to NZ9000. Other means of increasing PHB yield could include knocking out the acetate pathway in the LDH deficient strains, therefore increasing levels of available acetyl-CoA. Another possibility mentioned by Mifune *et al.* (2009), involves the modification to gene expression of the *pha* genes. For example, typical modifications include gene dosage e.g. by increasing plasmid-copy-numbers; looking at maintaining plasmid stability; transcriptional elements e.g. strong promoter and induction factors.

Chapter 5: Conclusions and future work

Class I PHA synthase from *C. necator* in recombinant *E. coli* was successfully purified to greater than 90 % purity as assessed by SDS-PAGE. This was achieved by utilising duel tag fusions of an affinity tag (polyHis-tag) and solubility tag (IgG binding ZZ or GB1 domain of protein A and G respectively from *Staphylococcus aureus*) to the N-terminus of the PHA synthase and purified by IMAC.

However, our first attempts at protein crystallisation of the purified PHA synthase from two plasmids full length and truncated was unsuccessful. This could be due to a large range of possible reasons and the most likely reasons identified include protein concentration, affinity tag, lack of structural homology, and contamination. Although, crystallisation of the PHA synthase could be possible, another alternative to protein crystallisation is available. This is the use of NMR, as purified PHA synthase has been observed to be relatively stable at 4 °C and in a range of buffers for long periods of time. However, the structure of the PHA synthase still remains unknown.

Activity and functionality of recombinant proteins used for protein purification were confirmed *in vivo* in recombinant *E. coli*. PHB inclusion bodies were successfully produced and isolated from all plasmids used for protein purification. Both functionality of the PHA synthase and IgG binding (ZZ or GB1) domain was successfully demonstrated by FM, TEM, GC/MS, ELISA, and IgG purification assays. No differences between full length and truncated version of the PHA synthase could be concluded. However, *in vivo* assessment of the activity of the PHA synthase does not indicate if the PHA synthase remains functional when produced under non-PHB accumulating conditions. Therefore, an *in vitro* PHA synthase assay would be more suitable. In addition, an *in vitro* PHA synthase assay would allow us to determine effectiveness of protein purification or storage conditions among others. *In vitro* PHA synthase assays have been described in literature and typically contain the following: PHA synthase, substrate (*R*)-3-hydroxyaceyl-CoA), and 5,5'-dithiobis-2-nitrobenzoic acid (DTNB) (Qi *et al*., 2000; Normi *et al*., 2005; Sheu *et al*., 2009).

Interestingly, the polyHis-tag was found *in vivo* to effect size of the PHB inclusion bodies. In this study we have employed polyHis-tags which have 9 to 10 consecutive

histidine residues, while commonly hexahistidine tags (His_6) are used. This observation was likely due to the effects of the positive charge associated with the amino acid histidine, resulting in repulsion like effects, preventing individual PHA inclusions from coalescing. In addition, the effect of the polyHis-tag may be contributing to part of the reason why we were unsuccessfully at obtaining protein crystals using uncleaved purified PHA synthase thus far.

For functionalised PHB inclusion biogenesis in Gram-positive *L. lactis* (NZ9000, Only PHB beads displaying the Hepatitis C virus core antigen (HepC) was successfully overproduced and immobilised on its surface as confirmed by SDS-PAGE, Maldi-TOF/MS, FM, TEM, and GC/MS analysis. PHB beads displaying Influenza A virus (H2N2) Hemagglutinin (HA) however was unsuccessful. Functionality of the HepC displaying beads produced a significant cell mediated immune response in a mouse model as assessed by Natalie Parlane (Hopkirk Research Institute, AgResearch). Demonstrating antigens can be successfully immobilised on the surface of PHB beads in an endotoxin free Gram-positive production host for vaccine delivery. However, PHB production in *L. lactis* NZ9000 was poor and results were similar to that published by Mifune *et al.* (2009). It was suggested that PHB production can be improved by looking at the organism's metabolic flux, in particular the pyruvate pool/flux in LDH deficient mutant strains of *L. lactis* NZ9000.

Results however for the characterisation of LDH deficient strains for PHB biogenesis, did not mediate significant increases in PHB indirectly through the increase in acetyl-CoA from the redistribution of carbon towards Acetate production as confirmed by Acetate, and GC/MS analysis. This suggests LDH knockout phenotype may have a negative effect on PHB biogenesis, which is currently undetermined.

Future work for molecular characterisation of PHA synthase includes assessing the main reasons why we failed to generate protein crystals, such as removal of the fusion tag; generation of proteins in a single oligomeric state and other likely parameters such as temperature, buffer and protein concentration. In addition, identification of unknown 47 kDa protein from TEV digest of $His_{10}GB1\Delta1$-93C and an *in vitro* PHA synthase activity assay will be used to assess functionality of the PHA synthase in terms of

purification and storage conditions. If protein crystallisation is still unsuccessful, structural determination by NMR would provide another option.

In terms of antigen display on the surface of PHB beads produced *L. lactis*, other possible antigens for example, (Ag85A) and (ESAT-6) from *Mycobacterium tuberculosis* which has already been successfully produced and assessed in *E. coli* (Parlane *et al.*, 2009). PHB displaying these antigens can be produced in *L. lactis* and directly compared to those from *E. coli* to assess functionality. Although increase in PHB production in LDH deficient mutants were unsuccessful, several other possibilities can be looked at, such as knocking out the acetate pathway in the LDH mutants, leading to significant increase in the pool of available acetyl-CoA or modification of gene expression levels of the *pha* genes.

In summary, this study has successfully demonstrated the purification of a class I PHA synthase (PhaC) from *C. necator* in recombinant *E. coli*. Although currently unsuccessful at protein crystallisation of the PHA synthase, acquisition of a protein crystal with a quality high enough for x-ray diffraction studies, leading to a three-dimensional structure would be of tremendous importance. As a resolved three-dimensional structure will provide a valuable insight into its structure and function, leading to chemical and physical enhancement and the production of tailor made PHAs (McPherson, 2004).

The successful immobilisation of proteins to the surface of PHA beads in *L. lactis* is particularly relevant for medical applications requiring endotoxin free products. In addition, production of functionalised beads in Gram-positive organisms removes the need for tedious purification steps normally involved with Gram-negative organisms. However, to be truly competitive, PHB production in *L. lactis* needs to be seriously considered.

Chapter 6: References

Amara, A. A., & Rehm, B. H. A. (2003). Replacement of the catalytic nucleophile cysteine-296 by serine in class II polyhydroxyalkanoate synthase from *Pseudomonas aeruginosa*-mediated synthesis of a new polyester: identification of catalytic residues. *Biochemical journal* **347**, 413-421.

Arnau, J., Lauritzen, C., Petersen, G. E. & Pedersen, J. (2006). Current strategies for the use of affinity tags and tag removal for the purification of recombinant proteins. *Protein Expression and Purification* **48**, 1-13.

Atwood, J. A. & Rehm, B. H. A. (2009). Protein engineering towards biotechnological production of bifunctional polyester beads. *Biotechnology Letters* **31**, 131-137.

Bäckström, B. T., Brockelbank, J. A. & Rehm, B. H. A. (2007). Recombinant *Escherichia coli* produces tailor-made biopolyester beads for applications in fluorescence activated cell sorting: functional display of the mouse interleukin-2 and myelin oligodendrocyte glycoprotein. *Bmc Biotechnology* **7**.

Baneyx, F. (1999). Recombinant protein expression in Escherichia coli. *Current Opinion in Biotechnology* **10**, 411-421.

Banki, M. R., Gerngross, T. U. & Wood, D. W. (2005). Novel and economical purification of recombinant proteins: Intein-mediated protein purification using in vivo polyhydroxybutyrate (PHB) matrix association. *Protein Science* **14**, 1387-1395.

Barnard, G. C., McCool, J. D., Wood, D. W. & Gerngross, T. U. (2005). Integrated recombinant protein expression and purification platform based on *Ralstonia eutropha*. *Applied and Environmental Microbiology* **71**, 5735-5742.

Benvenuti, M. & Mangani, S. (2007). Crystallization of soluble proteins in vapor diffusion for x-ray crystallography. *Nature Protocols* **2**, 1633-1651.

Bermúdez-Humarán, L. G., Langella, P., Commissaire, J., Gilbert, S., Loir, Y. l., L'Haridon, R. & Corthier, G. (2003). Controlled intra- or extracellular production of staphylococcal nuclease and ovine ω interferon in *Lactococcus lactis*. *FEMS Microbiology Letters* **224**, 307-313.

Bolotin, A., Wincker, P., Mauger, S., Jaillon, O., Malarme, K., Weissenbach, J., Ehrlich, S. D. & Sorokin, A. (2001). The Complete Genome Sequence of the Lactic Acid Bacterium *Lactococcus lactis* ssp. *lactis* IL1403. *International Journal of Genome Research* **11**, 731-753.

Bongers, R. S., Hoefnagel, M. H. N., Starrenburg, M. J. C., Siemerink, M. A. J., Arends, J. G. A., Hugenholtz, J. & Meerebezem, M. (2003). IS*981*-mediated adaptive evolution recovers lactate production by ldhB transcription activation in a lactate dehydrogenase-deficient strain of *Lactococcus lactis*. *Journal of Bacteriology* **185**, 4499-4507.

Bornke, F. & Broer, I. (2010). Tailoring plant metabolism for the production of novel polymers and platform chemicals *Current Opinion in Plant Biology* **13**, 353-361.

Brockelbank, J. A., Peters, V. & Rehm, B. H. A. (2006). Recombinant *Escherichia coli* strain produces a ZZ domain displaying biopolyester beads suitable for immunoglobulin G purification. *Applied and Environmental Microbiology* **72**, 7394-7397.

Bucher, M. H., Evdokimov, A. G. & Waugh, D. S. (2002). Differential effects of short affinity tags on the crystallization of *Pyrococcus furiosus* maltodextrin-binding protein. *Acta Crystallographica Section D-Biological Crystallography* **58**, 392-397.

Carr, P. D. & Ollis, D. L. (2009). alpha/beta Hydrolase Fold: An Update. *Protein & Peptide Letters* **16**, 1137-1148.

Chayen, N. E. (2004). Turning protein crystallisation from an art into a science. *Current Opinion in Structural Biology* **14**, 577-583.

Esposito, D. & Chatterjee, D. K. (2006). Enhancement of soluble protein expression through the use of fusion tags. *Current Opinion in Biotechnology* **17**, 353-358.

Furrer, P., Panke, S. & Zinn, M. (2007). Efficient recovery of low endotoxin medium-chain-length poly([R]-3-hydroxyalkanoate) from bacterial biomass. *Journal of Microbiological Methods* **69**, 206-213.

Gerngross, T. U. & Martin, D. P. (1995). Enzyme-catalyzed synthesis of poly[(*R*)-(-)-3-hydroxybutyrate] - formation of macroscopic beads In-vitro. *Proceedings of the National Academy of Sciences of the United States of America* **92**, 6279-6283.

Ghosh, D., Erman, M., Sawicki, M. & other authors (1999). Determination of a protein structure by iodination: the structure of iodinated acetylxylan esterase. *Acta Crystallographica Section D-Biological Crystallogrphy* **55**, 779-784.

Grage, K., Jahns, A. C., Parlane, N., Palanisamy, R., Rasiah, I. A., Atwood, J. A. & Rehm, B. H. A. (2009). Bacterial Polyhydroxyalkanoate Beads: Biogenesis, Structure, and Potential Use as Nano-/Micro-Beads in Biotechnological and Biomedical Applications. *Biomacromolecules* **10**, 660-669.

Graslund, S., Nordlund, P., Weigelt, J. & other authors (2008). Protein production and purification. *Nature Methods* **5**, 135-146.

Hammarström, M., Hellgren, N., Van den Berg, S., Berglund, H. & Hard, T. (2002). Rapid screening for improved solubility of small human proteins produced as fusion proteins in *Escherichia coli*. *Protein Science* **11**, 313-321.

Han, X., Satoh, Y., Tajima, K., Matsushima, T. & Munekata, M. (2009). Chemo-enzymatic synthesis of polyhydroxyalkanoate by an improved two-phase reaction system (TPRS). *Journal of Bioscience and Bioengineering* **108**, 517-523.

Hanley, S. Z., Pappin, D. J. C., Rahman, D., White, A. J., Elborough, K. M. & Slabas, A. R. (1999). Re-evaluation of the primary structure of *Ralstonia eutropha* phasin and implications for polyhydroxyalkanoic acid bead binding. *FEBS Letters* **447**, 99-105.

Hazer, B. & Steinbüchel, A. (2007). Increased diversification of polyhydroxyalkanoates by modification reactions for industrial and medical applications. *Applied Microbiology and Biotechnology* **74**, 1-12.

Hoefnagel, M. H. N., Starrenburg, M. J. C., Martens, D. E., Hugenholtz, J., Kleerebezem, M., Van Swam, II, Bongers, R., Westerhoff, H. V. & Snoep, J. L. (2002). Metabolic engineering of lactic acid bacteria, the combined approach: kinetic modelling, metabolic control and experimental analysis. *Microbiology* **148**, 1003-1013.

Jahns, A. C., Haverkamp, R. G. & Rehm, B. H. A. (2008). Multifunctional Inorganic-Binding Beads Self-Assembled Inside Engineered Bacteria. *Bioconjugate Chemistry* **19**, 2072-2080.

Jahns, A. C. & Rehm, B. H. A. (2009). Tolerance of the *Ralstonia eutropha* Class I Polyhydroxyalkanoate Synthase for Translational Fusions to Its C Terminus Reveals a New Mode of Functional Display. *Applied and Environmental Microbiology* **75**, 5461-5466.

Jendrossek, D. (2005). Fluorescence microscopical investigation of poly(3-hydroxybutyrate) bead formation in bacteria. *Biomacromolecules* **6**, 598-603.

Jo, S. -J., Maeda, M., Ooi, T. & Taguchi, S. (2006). Production system for biodegradable polyester polyhydroxybutyrate by *Corynebacterium glutamicum*. *Journal of Bioscience and Bioengineering* **102**, 233-236.

Jossek, R., Reichelt, R. & Steinbüchel, A. (1998). *In vitro* biosynthesis of poly(3-hydroxybutyric acid) by using purified poly(hydroxyalkanoic acid) synthase of *Chromatium vinosum*. *Applied Microbiology and Biotechnology* **49**, 258-266.

Jossek, R. & Steinbuchel, A. (1998). In vitro synthesis of poly(3-hydroxybutyric acid) by using an enzymatic coenzyme A recycling system. *Fems Microbiology Letters* **168**, 319-324.

Keshavarz, T. & Roy, I. (2010). Polyhydroxyalkanoates: bioplastics with a green agenda. *Current Opinion in Microbiology* **13**, 321-326.

Kim, H. N., Lee, J., Kim, H. Y. & Kim, Y. -R. (2009). Enzymatic synthesis of a drug delivery system based on polyhydroxyalkanoate-protein block copolymers. *Chemical Communications*, 7104-7106.

Koller, M., Salerno, A., Dias, M., Reiterer, A. & Braunegg, G. (2010). Modern Biotechnological Polymer Synthesis: A Review. *Food Technology and Biotechnology* **48**, 255-269.

Lee, S. Y. & Lee, Y. (2003). Metabolic engineering of *Escherichia coli* for production of enantiomerically pure (*R*)-(-)-hydroxycarboxylic acids. *Applied and Environmental Microbiology* **69**, 3421-3426.

Legat, A., Gruber, C., Zangger, K., Wanner, G. & Stan-Lotter, H. (2010). Identification of polyhydroxyalkanoates in Halococcus and other haloarchaeal species. *Applied Microbiology and Biotechnology* **87**.

Lewis, J. G. & Rehm, B. H. A. (2009). ZZ polyester beads: An efficient and simple method for purifying IgG from mouse hybridoma supernatants. *Journal of Immunological Methods* **346**, 71-74.

Loir, Y. L., Azevedo, V., Oliveira, S. C. & other authors (2005). Protein secretion in *Lactococcus lactis* : an efficient way to increase the overall heterologous protein production. *Microbial Cell Factories* **4**, 1-13.

Lu, J., Tappel, R. C. & Nomura, C. T. (2009). Mini-Review: Biosynthesis of Poly(hydroxyalkanoates). *Polymer Reviews* **49**, 226-248.

Lussier, F. X., Denis, F. & Shareck, F. (2010). Adaptation of the Highly Productive T7 Expression System to Streptomyces lividans. *Applied and Environmental Microbiology* **76**, 967-970.

Lutke-Eversloh, T., Kawada, J., Marchessault, R. H. & Steinbuchel, A. (2002). Characterization of microbial polythioesters: Physical properties of novel copolymers synthesized by *Ralstonia eutropha*. *Biomacromolecules* **3**, 159-166.

Madison, L. L. & Huisman, G. W. (1999). Metabolic engineering of poly(3-hydroxyalkanoates): From DNA to plastic. *Microbiology and Molecular Biology Reviews* **63**, 21-53.

Magalhães, P. O., Lopes, A. M., Mazzola, P. G., Rangel-Yagui, C., Penna, T. C. V. & Pessoa, A. (2007). Methods of endotoxin removal from biological preparations: a review. *Journal of Pharmacy and Pharmaceutical Sciences* **10**, 388-404.

McPherson, A. (2004). Introduction to protein crystallization. *Methods* **34**, 254-265.

Mierau, I. & Kleerebezem, M. (2005). 10 years of the nisin-controlled gene expression system (NICE) in *Lactococcus lactis*. *Applied Microbiology and Biotechnology* **68**, 705-717.

Mifune, J., Grage, K. & Rehm, B. H. A. (2009). Production of Functionalized Biopolyester Beads by Recombinant *Lactococcus lactis*. *Applied and Environmental Microbiology* **75**, 4668-4675.

Mullaney, J. A. & Rehm, B. H. A. (2010). Design of a single-chain multi-enzyme fusion protein establishing the polyhydroxybutyrate biosynthesis pathway. *Journal of Biotechnology* **147**, 31-36.

Nardini, M. & Dijkstra, B. W. (1999). α/β hydrolase fold enzymes: the family keeps growing. *Current Opinion in Structural Biology* **9**, 732-737.

Normi, Y. M., Hiraishi, T., Taguchi, S., Abe, H., Sudesh, K., Najimudin, N. & Doi, Y. (2005). Characterization and properties of G4X mutants of *Ralstonia eutropha* PHA synthase for poly (3-hydroxybutyrate) biosynthesis in *Escherichia coli*. *Macromolecular Bioscience* **5**, 197-206.

Ollis, D. L., Cheah, E., Cygler, M. & other authors (1992). The α/β hydrolase fold *Protein Engineering* **5**, 197-211.

Parlane, N. A., Wedlock, D. N., Buddle, B. M. & Rehm, B. H. A. (2009). Bacterial Polyester Inclusions Engineered To Display Vaccine Candidate Antigens for Use as a Novel Class of Safe and Efficient Vaccine Delivery Agents. *Applied and Environmental Microbiology* **75**, 7739-7744.

Peters, V. & Rehm, B. H. A. (2005). *In vivo* monitoring of PHA bead formation using GFP-labeled PHA synthases. *FEMS Microbiology Letters* **248**, 93-100.

Peters, V. & Rehm, B. H. A. (2008). Protein engineering of streptavidin for *in vivo* assembly of streptavidin beads. *Journal of Biotechnology* **134**, 266-274.

Philip, S., Keshavarz, T. & Roy, I. (2007). Polyhydroxyalkanoates: biodegradable polymers with a range of applications. *Journal of Chemical Technology and Biotechnology* **82**, 233-247.

Pötter, M., Madkour, M. H., Mayer, F. & Steinbuchel, A. (2002). Regulation of phasin expression and polyhydroxyalkanoate (PHA) bead formation in *Ralstonia eutropha* H16. *Microbiology-(UK)* **148**, 2413-2426.

Pötter, M. & Steinbüchel, A. (2005). Poly(3-hydroxybutyrate) bead-associated proteins: Impacts on poly(3-hydroxybutyrate) synthesis and degradation. *Biomacromolecules* **6**, 552-560.

Qi, Q., Steinbuchel, A. & Rehm, B. H. A. (2000). *In vitro* synthesis of poly(3-hydroxydecanoate): purification and enzymatic characterization of type II polyhydroxyalkanoate synthases PhaC1 and PhaC2 from *Pseudomonas aeruginosa*. *Applied Microbiology and Biotechnology* **54**, 37-43.

Rasiah, I. A. & Rehm, B. H. A. (2009). One-Step Production of Immobilized α-Amylase in Recombinant *Escherichia coli*. *Applied and Environmental Microbiology* **75**, 2012-2016.

Rasiah, I. A., Parlane, N., Grage, K., Palanisamy, R., Jahns, A. C., Atwood, J. A. & Rehm, B. H. A. (2010). Biopolyester particles: preparation and applications. *Encyclopedia of Industrial Biotechnology*, 1-16.

Rehm, B. H. A. & Steinbuchel, A. (1999). Biochemical and genetic analysis of PHA synthases and other proteins required for PHA synthesis. *International Journal of Biological Macromolecules* **25**, 3-19.

Rehm, B. H. A. (2003). PHA synthases: natural catalysts for plastics. *Biochemical Journal* **376**, 15-33.

Rehm, B. H. A. (2006). Genetics and biochemistry of polyhydroxyalkanoate bead self-assembly: The key role of PHA synthases. *Biotechnology Letters* **28**, 207-213.

Rehm, B. H. A. (2007). Biogenesis of microbial polyhydroxyalkanoate beads: a platform technology for the production of tailor-made bioparticles. *Current Issues in Molecular Biology* **9**, 41-62.

Rehm, B. H. A. (2010). Bacterial polymers: biosynthesis, modifications and applications. *Nature Reviews Microbiology* **8**, 578-592.

Rey, D. A., Strickland, A. D., Kirui, D., Niamsiri, N. & Batt, C. A. (2010). *In vitro* Self-Assembly of Gold Nanoparticle-Coated Poly(3-hydroxybutyrate) Beads Exhibiting Plasmon-Induced Thermo-Optical Enhancements. *Acs Applied Materials & Interfaces* **2**, 1804-1810.

Saegusa, H., Shiraki, M., Kanai, C. & Saito, T. (2001). Cloning of an intracellular poly[D(-)-3-hydroxybutyrate] depolymerase gene from *Ralstonia eutropha* H16 and characterization of the gene product. *Journal of Bacteriology* **183**, 94-100.

Satoh, Y., Tajima, K., Tannai, H. & Munekata, M. (2003). Enzyme-Catalyzed poly(3-Hydroxybutyrate) synthesis from acetate with CoA recycling and NADPH regeneration *in vitro*. *Bioscience and Bioengineering* **95**, 335-341.

Sheu, D. S., Lai, Y. W., Chang, R. C. & Chen, W. M. (2009). Detection of polyhydroxyalkanoate synthase activity on a polyacrylamide gel. *Analytical Biochemistry* **393**, 62-66.

Spiekermann, P., B. H. A. Rehm, R. Kalscheuer, D. Baumeister & A. Steinbuchel. (1999). A sensitive, viable-colony staining method using Nile red for direct screening of bacteria that accumulate polyhydroxyalkanoic acids and other lipid storage compounds. *Archives of Microbiology* **171**, 73-80.

Stano, N. M. & Patel, S. S. (2004). T7 lysozyme represses T7 RNA polymerase transcription by destabilizing the open complex during initiation. *J Biol Chem* **279**, 16136-16143.

Steinmann, B., Christmann, A., Heiseler, T., Fritz, J. & Kolmar, H. (2010). *In Vivo* Enzyme Immobilization by Inclusion Body Display. *Applied and Environmental Microbiology* **76**, 5563-5569.

Taguchi, S., A. Maehara, K. Takase, M. Nakahara, H. Nakamura & Y. Doi. (2001). Analysis of mutational effects of a polyhydroxybutyrate (PHB) polymerase on bacterial PHB accumulation using an *in vivo* assay system. *Fems Microbiology Letters* **198**, 65-71.

Terpe, K. (2003). Overview of tag protein fusions: from molecular and biochemical fundamentals to commercial systems. *Applied Microbiology and Biotechnology* **60**, 523-533.

Thomson, N., Roy, I., Summers, D. & Sivaniah, E. (2009). *In vitro* production of polyhydroxyalkanoates: achievements and applications. *Journal of Chemical Technology and Biotechnology* **85**, 760-767.

Thomson, N., Summers, D. & Sivaniah, E. (2010). Synthesis, properties and uses of bacterial storage lipid beads as naturally occurring nanoparticles. *Soft Matter* **6**, 4045-4057.

Tian, J. M., Sinskey, A. J. & Stubbe, J. (2005). Kinetic studies of polyhydroxybutyrate bead formation in *Wautersia eutropha* H16 by transmission electron microscopy. *Journal of Bacteriology* **187**, 3814-3824.

Valappil, S. P., Boccaccini, A. R., Bucke, C. & Roy, I. (2007). Polyhydroxyalkanoates in Gram-positive bacteria: insights from the genera *Bacillus* and *Streptomyces*. *Antonie Van Leeuwenhoek International Journal of General and Molecular Microbiology* **91**, 1-17.

van Hylckama Vlieg, J. E. T., Rademaker, J. L. W., Bachmann, H., Molenaar, D., Kelly, W. J. & Siezen, R. J. (2006). Natural diversity and adaptive responses of *Lactococcus lactis*. *Current Opinion in Biotechnology* **17**, 183-190.

Vantilbeurgh, H., Egloff, M. P., Martinez, C., Rugani, N., Verger, R. & Cambillau, C. (1993). Interfacial activation of the lipase procolipase complex by mixed micelles revealed by x-ray crystallography. *Nature* **362**, 814-820.

Wang, Z. H., Wu, H. N., Chen, J., Zhang, J., Yao, Y. C. & Chen, G. Q. (2008). A novel self-cleaving phasin tag for purification of recombinant proteins based on hydrophobic polyhydroxyalkanoate nanoparticles. *Lab on a Chip* **8**, 1957-1962.

Waugh, D. S. (2005). Making the most of affinity tags. *Trends in Biotechnology* **23**, 316-320.

Wei, Y. Y., Swenson, L., Castro, C. & other authors (1998). Structure of a microbial homologue of mammalian platelet-activating factor acetylhydrolases: *Streptomyces exfoliatus* lipase at 1.9 angstrom resolution. *Struct Fold Des* **6**, 511-519.

Wieczorek, R., Pries, A., Steinbüchel, A. & Mayer, F. (1995). Analysis of a 24-kilodalton protein associated with the polyhydroxyalkanoic acid beads in *Alcaligenes-eutrophus*. *Journal of Bacteriology* **177**, 2425-2435.

Yu, H. -H., Nakase, I., Pujals, S., Hirose, H., Tanaka, G., Katayama, S., Imanishi, M. & Futaki, S. (2010). Expressed protein ligation for the preparation of fusion proteins with cell penetrating peptides for endotoxin removal and intracellular delivery. *Biochimica Et Biophysica Acta-Biomembranes* **1798**, 2249-2257.

Zhang, S., Wang, Z. H. & Chen, G. Q. (2010). Microbial polyhydroxyalkanote synthesis repression protein PhaR as an affinity tag for recombinant protein purification. *Microbial Cell Factories* **9**.

Zhou, P. & Wagner, G. (2010). Overcoming the solubility limit with solubility-enhancement tags: successful applications in biomolecular NMR studies. *Journal of Biomolecular Nmr* **46**, 23-31.

Zinn, M., Witholt, B. & Egli, T. (2001). Occurrence, synthesis and medical application of bacterial polyhydroxyalkanoate. *Advanced Drug Delivery Reviews* **53**, 5-21.